

**The Spreading Behaviour of Stainless Steel Powders for
Additive Manufacturing**

Zobaideh Haydari

**Submitted in accordance with the requirements for the degree of
Master of Research**

The University of Leeds

School of Chemical and Process Engineering

July 2021

Acknowledgements

I would like to express my sincerest gratitude to my supervisors Dr Ali Hassanpour and Professor Andrew Bayly for their advice and assistance throughout this project.

Special thanks to Dr Jabbar Gardy for his continuous help, building the rig and sharing his valuable data regarding powder characterisation of samples during the pandemic as working in the laboratories was very difficult.

I would also like to thank my colleagues at the University of Leeds in the School of Chemical and Process Engineering for their kindness and care.

Very special thanks to my husband and son for being very supportive through all ups and downs.

Abstract

Additive manufacturing (AM) is a rapidly developing technology that transforms the manufacturing toolbox and operation of industrial companies. In this technology, material is selectively added layer-by-layer in order to create a complex part that is not easy to be produced in subtractive methods. Physical and chemical behaviour of powders used in additive manufacturing is a key element in industrial applications. Hence, it is necessary to accurately control and optimise the processing techniques with precise powder characterisation. There has been a considerable attention to the bulk powder behaviour in different fields of powder technology, but there is a lack of extensive research on the spreadability of powders in additive manufacturing (AM). To date, no prediction in spreadability of AM feedstock has been established hence no feasible powder spreadability metrics is achieved so far. While quantifying powder spreadability is a vital step for AM, there is no standard strategy for this purpose. Lack of a generally agreed definition for spreadability in AM might be related to the heterogenous nature of the powders which may differ by powders types, method of AM application and processes conditions. Therefore, precise monitoring of the spread behaviour of powders seems to be very challenging since powders may change their spreading dynamics at any period of time during the experiments and results to uncertainty. In other words, one spreadability metric may perfectly fit with a specific type of powder or process condition, while for a different choice of material or application it may not be relevant. Hence a parallel investigation on powder properties and processes parameters may be a suitable approach to develop the understandings in powders spreadability.

However, expanding of the current understandings regarding the spread behaviour of powders may help to establish a standard measurement method for spreadability.

In this project the combined effect of powder characterisations and processes parameters such as gap size, spread velocity and environmental conditions on the spreadability of stainless steel powders has been investigated. The samples are two different batches of 316L stainless steel and their particle size distributions are both in the range of 15-105 μm . Series of experiments are conducted through using an in-house spreading rig to quantify the spreading behaviour of two different samples. This work investigates the spread quality of powders through obtaining the bulk density of spread layer on the build plate and form a comparison to the initial bulk density of the respective powders.

Table of Contents

Acknowledgements	i
Abstract.....	ii
List of Figures.....	v
List of Tables	vi
Abbreviations	vii
Chapter 1. Introduction	1
1.1 Aims and Objectives	2
1.2 Structure of Thesis.....	5
.....	7
.....	7
Chapter 2. Review of Literature.....	8
2.1 Types of Additive Manufacturing	8
2.1.1 VAT Photo Polymerisation.....	8
2.1.2 Material Jetting	9
2.1.3 Binder Jetting.....	9
2.1.4 Material Extrusion	9
2.1.5 Powder Bed Fusion (PBF).....	9
2.1.6 Directed Energy Deposition (DED).....	10
2.1.7 Sheet Lamination	10
2.2 Types of Powder Production Methods in Additive Manufacturing.....	12
2.2.1 Water Atomisation (WA)	12
2.2.2 Plasma Atomisation (PA)	12
.....	13
2.2.3 Plasma Rotating Electrode Process (PREP)	13
2.2.4 Gas Atomisation (GA).....	13
2.2.5 Production of Steel Powders.....	15
2.3 Types of Powder Characterisation in Additive Manufacturing.....	18
2.3.1 Powder Flowability.....	18
2.3.1.1 Angle of Repose (AOR).....	20
2.3.1.2 Hall Flowmeter	21
2.3.1.3 FT4 Powder Rheometer	22
2.3.1.4 Avalanche Tester	23
2.3.1.5 Dimensionless Shear Rate.....	23
2.3.1.6 Effect of Powder Flowability on the Final Part in AM.....	24
2.3.2 Bulk and Tapped Density	26
2.3.2.1 Effect of Bulk and Tapped Density on the Final Part in AM	27
2.3.3 Particle Size and Size Distribution	28
2.3.3.1 Effect of Particle Size and Size Distribution on the Final Part in AM	29

2.3.4 Powder Morphology.....	31
2.3.4.1 Effect of Morphology on The Final Part in AM.....	32
2.3.5 Surface Properties.....	33
2.3.5.1 Effect of Surface Properties on the Quality of Final Part	34
2.4 Effect of Spreading Process on the Quality of Final Part	36
2.4.1 Gap Size (Layer Thickness)	36
2.4.2 Spreading Velocity.....	37
2.4.3 Spreader Type and Design.....	38
2.4.4 Humidity.....	40
2.5 Definition of Spreadability Within the Literature	41
2.6 Knowledge Gap Regarding the Spreadability of Powders Within the Literature	45
2.7 Summary of Chapter	46
Chapter 3. Material and Methodology.....	50
3.1 Size and Morphological Properties of Samples.....	50
3.2 Measurement of Flowability of Samples	54
3.2.1 Angle of repose	54
3.2.2 Hall flowmeter.....	54
3.4 Summary of Chapter	59
Chapter 4. Effect of Processes Parameters on the Spread Layer of Stainless steel	
(Velocity, Gap Size, Humidity).....	61
4.1 Spreading Profiles.....	61
4.2 Percentage of Spread	68
4.3 Mass Per Area(g/cm²)	69
4.4 Bulk Layer Density	72
4.5 Ratio of Layer Bulk Density to Initial Bulk Density	75
4.6 Dimensionless shear rate.....	78
4.7 Effect of Humidity on the Spread Layer (Conditioning)	81
4.8 Summary of Chapter	83
.....	85
Chapter 5. Conclusions	86
Chapter 6. Future Work	91
Chapter 7. References	94
Appendix	109

List of Figures

Figure 1: (a) Vat photo-polymerisation, (b) material jetting, (c) material extrusion, (d) power bed fusion, (e) binder jetting, (f) sheet lamination, (g) direct energy deposition [5].....	8
Figure 2:WA process [17].....	12
Figure 3:PA process [22].	12
Figure 4:PREP process [22].....	13
Figure 5:GA process [22].....	13
Figure 6:Schaeffler diagram (A-austenite; M–martensite; F–ferrite) [26].	15
Figure 7:Binary phase diagram for a eutectic [27].	16
Figure 8: (a)Angle of Repose [60].	20
Figure 9: Hall Flowmeter.....	21
Figure 10: (a)Rt-hole, (b)Arching, (c)Clinging, (d)Bridging [64].....	21
Figure 11: FT4 Powder Rheometer [66].	22
Figure 12: Revolution Powder Analyzer principle [71].	23
Figure 13: Classification of flow regime according to Tardos et al. [74,75].....	24
Figure 14: (a) Volume- based particle size distribution and (b) cumulative volume-based particle size distribution.....	52
Figure 15: SEM Images of sample 1 and sample 2.	53
Figure 16: Angle of repose.	54
Figure 17: Hall flowmeter.....	54
Figure 18: (a) Side view of ratholing, (b) Ratholing in sample 1, (c) Free flow in Sample 2. 55	
Figure 19: AOR of the powder bed at ambient condition.....	55
Figure 20: Front view of the rig.....	56
Figure 21: (a) Top view of spreading rig, (b) rectangular feeder, (c) Deposited Heap in front of the bevelled blade.	57
Figure 22: (a) Feeding the powder, (b) Initial powder heap- side view.	57
Figure 23 : Spreading profile of gap size 51 μm (sample 1)	62
Figure 24: Area of Spread layer through ImageJ.....	69
Figure 25: Graph of Speed (mm/s) Against Mass Per Area for Gap size 318 μm	70
Figure 26: Graph of Speed (mm/s) Against Mass Per Area for Gap size 191 μm	71
Figure 27: Graph of Speed (mm/s) Against Mass Per Area for Gap size 102 μm	71
Figure 28: Graph of Speed (mm/s) Against Layer Density for Gap size 318 μm	72
Figure 29: Graph of Speed (mm/s) Against Layer Density for Gap size 191 μm	73
Figure 30: Graph of Speed (mm/s) Against Layer Density for Gap size 102 μm	73
Figure 31: Graph of Layer Bulk Density/Initial Bulk Density against speed for Gap size 318 μm	77
Figure 32: Graph of Layer Bulk Density/Initial Bulk Density against Speed for Gap size 191 μm	77
Figure 33: Graph of Layer Bulk Density /Initial Bulk Density against Speed for Gap size 102 μm	78
Figure 34: Dimensionless shear rate against bulk layer density of Sample1.....	80
Figure 35: Dimensionless shear rate against bulk layer density of Sample 2.....	80
Figure 36: Comparison of Bulk Layer Density for Gap Size 318 μm With Change in Humidity.	82
Figure 37: Comparison of Bulk Layer Density/Initial Density for Gap Size 318 μm With Change in Humidity.....	83

List of Tables

Table 1: Advantages and disadvantages of different powder production types.	14
Table 2: Jenike, 1964 Classification of flowability [49].....	19
Table 3: Carr classification of flowability [61].....	20
Table 4: Scale of flowability based on CI and HR [61].....	26
Table 5: Material Properties.....	50
Table 6: Morphological characteristics of the two samples (v and n denote volume and number based, respectively). (Dr Jabbar Gardy)	51
Table 7: Scales of flowability for 200 g of powders.....	55
Table 8: Angle of repose of 7g powder bed.....	56
Table 9: Mass of powder in spreading test for sample 1 and sample 2.	61
Table 10: Ratio of Gap Size to $D[v,0.9]$ for Sample 1.	62
Table 11: Ratio of Gap Size to $D[v,0.9]$ for Sample 2.	62
Table 12: Spreading profiles of sample 1	63
Table 13: Spreading profiles of sample 2	64
Table 14: Spreading profiles of sample 1&2 stored under 73%humidity	67
Table 15: Percentage of Spread for Sample 1.....	68
Table 16: Percentage of Spread for Sample 2.....	68
Table 17: Dimensionless shear rate for sample 1.	79
Table 18: Dimensionless shear rate for Sample 2.....	79

Abbreviations

AM	Additive Manufacturing
PSD	Particle Size Distribution
DEM	Discrete Element Method
FDM	Fuse Deposition Modelling
PBF	Powder Bed Fusion
LBM	Laser Beam Melting
LMD	Laser Metal Deposition
SLM	Selective Laser Melting
DMLS	Direct Metal Laser Sintering
EBM	Electron Beam Melting
SHS	Selective heat sintering
SLS	Selective laser sintering
DED	Directed Energy Deposition
UAM	Ultrasonic Additive Manufacturing
LOM	Laminated Object Manufacturing
LOF	Lack of Fusion
WA	Water Atomisation
PA	Plasma Atomisation
PREP	Plasma Rotation Electrode Process
GA	Gas Atomisation
EIGA	Electrode Induction Melting Gas Atomisation
ASTM	American Society for Testing and Materials
ISO	International Organization for Standardization
AOR	Angle of repose
HR	Hausner Ratio
CI	Compressibility Index
LBD	Layer Bulk Density
IBD	Initial Bulk Density

CHAPTER ONE

Introduction

1.1 Aims and Objectives

1.2 Structure of Thesis

Chapter 1. Introduction

Additive Manufacturing (AM) is a novel technology that due to its ability to produce complex geometrical parts, raises attention in current manufacturing industries. Unlike the conventional subtractive method of manufacturing that creates the part from a continuous piece, additive manufacturing technology produces optimised components through production of successive layers. The three-dimensional part is manufactured directly from a computer aided design (CAD) model that can significantly reduce the time, cost and material waste mainly because post modification process is not necessarily required in AM parts compared to conventional method of manufacturing [1]. Vat photo-polymerisation (VAT), material jetting, material extrusion, power bed fusion (PBF), binder jetting (BJ), sheet lamination and direct energy deposition (DED) are 7 types of additive manufacturing. Powder bed fusion is a common method of AM in which a desirable powder layer is deposited and spread on the build plate and afterwards the build plate containing the powder layer is lowered down to a pre-allocated height to create a gap for next deposition of the new layer. Therefore, an explicit understanding of powder characteristics and properties of recoating systems such as build plate, spreader, gap size and velocity of the spreading machine is necessary to enhance the spread quality. While separate investigation of the powder quality and process parameters are the key factors for quality control, the combined effect of both parameter on the spread layer and subsequently the final product is very crucial in AM. Therefore, a thorough study of process parameters during spreading of powders and their impact on the spread quality that is commonly known as “spreadability” is required in AM technology [2]. Spreadability is generally referred to spread uniformity of highly packed powders without formation of empty patches [3].

In spread based additive manufacturing and particularly in powder bed fusion methods, creating a very thin layer of powder is essential. Utilising fine powders is inevitable for generating thin layers, while this may increase the powders cohesiveness that reduces the flowability of powders, which consequently decreases the homogeneity of the layers. However it is important to note that although flowability is a useful index to predict the powder quality but it is not a sufficient metric to measure spreadability [3].

The quality of spread layer is not only affected by flowability but is significantly related to processes parameters and environmental conditions. The processes parameters such as gap size and spread velocity has direct influence on layer consistency. Consistent thickness, surface roughness and uniformity of individual layers are key factors for spread layer quality and ultimately final product. While spreadability of powders is a fundamental aspect of powder bed fusion manufacturing method, an accepted standard measure for spreadability is not yet available.

Although, some studies attempt to define a standard metric for spreadability through experimental and numerical approaches, a solid agreement regarding the definition of spreadability still lacks. Thus, an optimised measure of layer uniformity as well as spread quality and their correlation to characterisation of stainless steel powders is the main interest on this research.

Laser or other common energy resources for melting or sintering of spread layers is also a very important factor to create defect free layers within AM production but has not been addressed in this project.

1.1 Aims and Objectives

The exponential growth of additive manufacturing (AM) is mainly due to its enormous potential in a wide range of markets such as medical, electrical, clothing and building constructions. The advantage of producing complex near-net-shapes that has been offered by additive manufacturing is the major ambition for further researches towards the development of this novel technology.

The impact of feed powder properties on the manufacturing process and end product quality has been the main focus of previous researches, which has been aiming at developing a standard method for powder characterisation in AM. The complex interaction between powder properties, bulk powder behaviour, in-process performance and product quality is the major interest of existing studies. However, despite of numerous studies on correlating powder properties with bulk powder behaviour, there is still a considerable lack of investigations in powder spreading behaviour under AM process conditions. Therefore, the aim of this research is to contribute in establishing a correlation between properties of stainless steel powders,

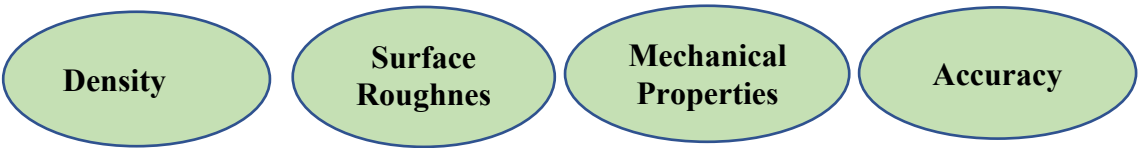
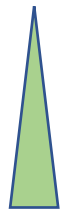
common AM process parameters and powder behaviour by devising appropriate test methods to achieve optimised outcomes. The evaluation of the outcomes is based on the value of bulk layer density accompanied with qualitative assessment of the spread layer.

Firstly, it has been attempted to identify the factors which may affect the spread quality of powders and consequently final part within the current literature and conduct series of experiments to investigate the effects of these factors. It has been gathered from the literature that powder parameters such as size, shape and bulk properties along with the process parameters such as gap size, spread velocity, spreader type and environmental conditions are the key factors influencing the spread behaviour of powders.

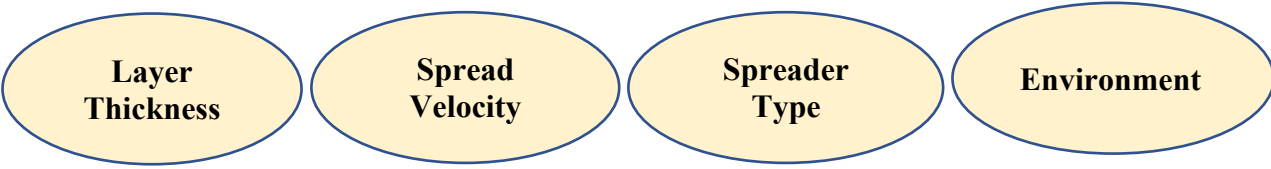
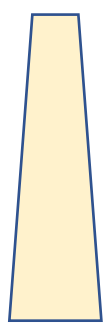
Flowability as a bulk parameter is a description of complex behaviour of powder when it is mobilised or subjected to stress. Therefore, correlation between single powder properties and bulk flow behaviour of the powder is a key term in this application. The impacts of mechanical, physical and chemical properties of powder on the flowability, layering and spreading process, highly affects the performance of the powder in additively manufactured products. Thus, discovering a suitable test method associated with the powder flow properties that impacts the quality of the layer is a critical objective to achieve in this project.

In this project, powder properties and their bulk flow behaviour will be characterised through using standard methods within the literature. Investigation on the spreading behaviour of powders by using an in-house spreading rig that imitates the actual AM process is also an objective in this research. The spreading process will be examined while considering different set of parameters such as gap thickness, spreader blade speed and mass of feed powder. In order to experimentally conduct the proposed case, one parameter such as speed will be considered as the variable and other parameters will remain constant and the effects of these parameters on the process condition will be investigated. Furthermore, the influence of humidity as an environmental factor has also been investigated as an objective in this project. Different steps to produce a final part with desirable quality in AM is shown in the map below;

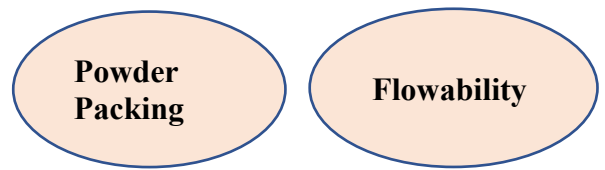
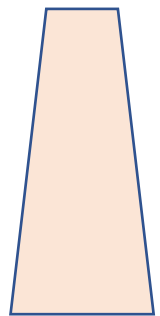
Final part properties



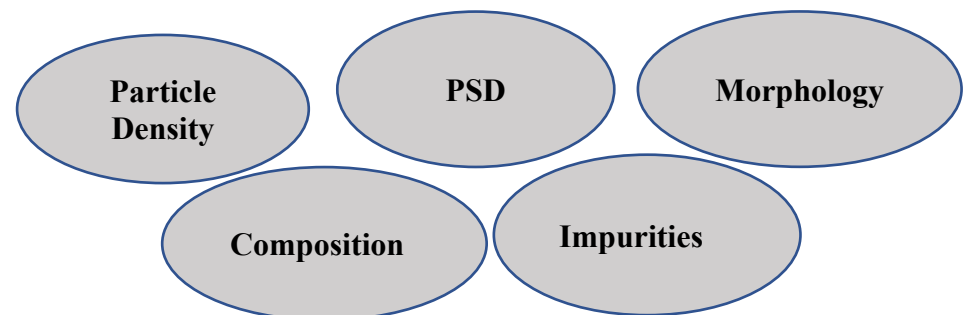
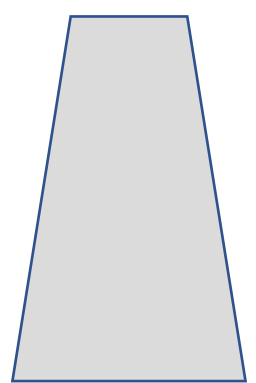
In-process properties



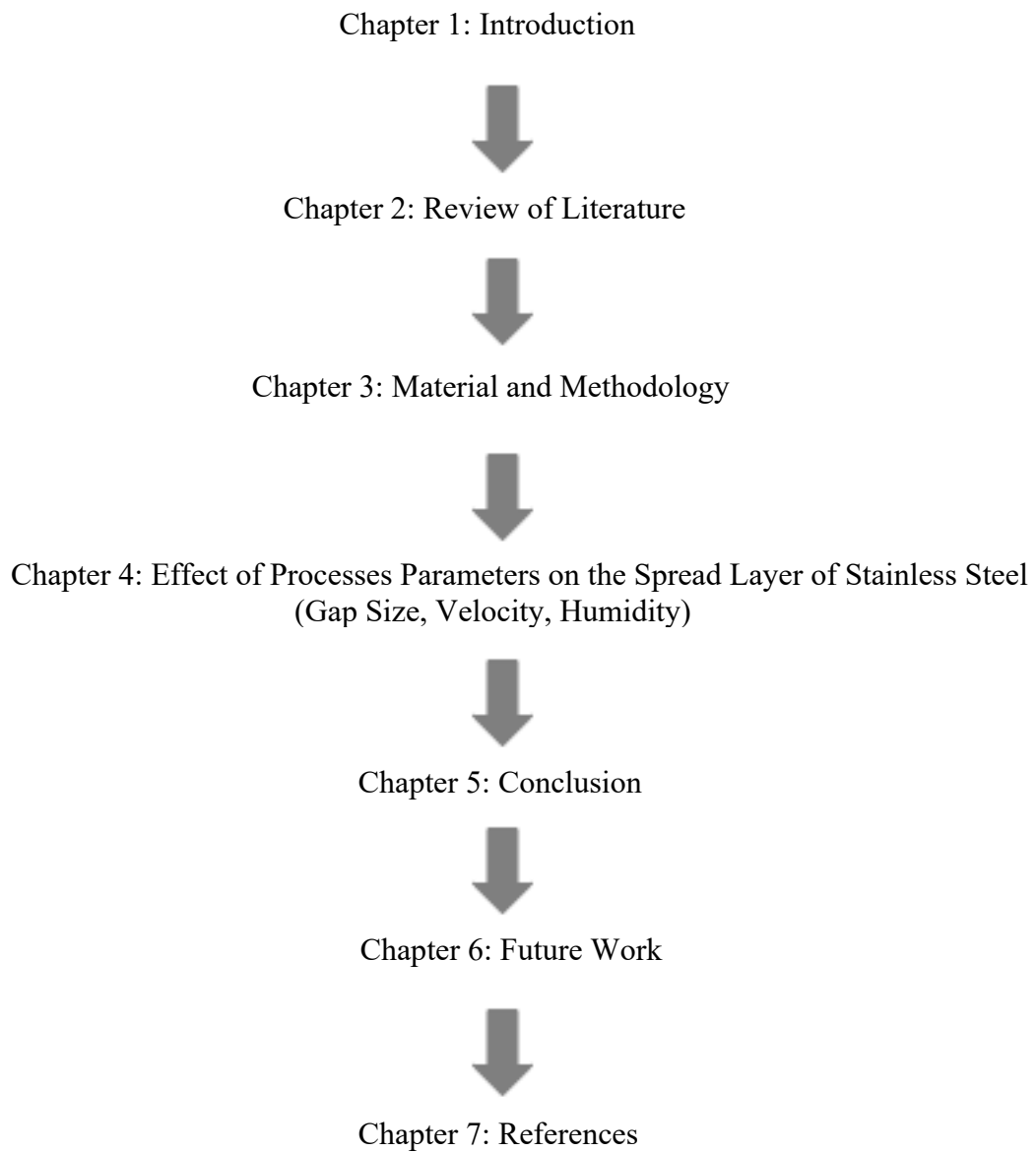
Bulk powder properties



Powder properties



1.2 Structure of Thesis



This thesis consists of 7 chapters that is briefly described as follows:

- Chapter 1 presents the introduction which consists of a relevant background of the research and an overview of the structure for this work. The aims and objectives of this project has been presented in this section.
- Chapter 2 consists of related studies that is available within the literature. The effect of powder characterisation and spreading processes on the final part is also gathered from the literature in this section. Definition and the knowledge gap of the term “spreadability” in additive manufacturing has been highlighted in this section.
- Chapter 3 provides information regarding the material and methods utilised in this project.
- Chapter 4 presents the effect of velocity and gap size as processes parameters on the spread layer of 316L stainless steel. Qualitative and quantitative analysis of these effects is carried out in this section. Furthermore, effect of humidity as an environmental factor on the spread layer of 316L stainless steel has been analysed in this chapter.
- Chapter 5 concludes the findings of this work where the results are illustrated in the form of matrices obtained through the experiments.
- Chapter 6 serves the future works and recommendation that may improve the accuracy of the results.
- Chapter 7 covers the list of references that has been used for the creation of this thesis.

CHAPTER TWO

Review of Literature

2.1 Type of Additive Manufacturing

2.2 Type of Powder Production Method in Additive Manufacturing

2.3 Type of Powder Characterisation in Additive Manufacturing

2.4 Effect of Spreading Processes on the Final Part

2.5 Definition of Spreadability Within the Literature

2.6 Knowledge Gap Regarding the Spreadability of Powders within the Literature

2.7 Summary of Chapter

Chapter 2. Review of Literature

2.1 Types of Additive Manufacturing

Additive Manufacturing processes is categorized into 7 groups by American Society for Testing and Materials (ASTM) group “ASTM F42” which has been listed in the Standard Terminology for Additive Manufacturing Technologies. These categories has been classified mainly based on the material used and machine technology [4].

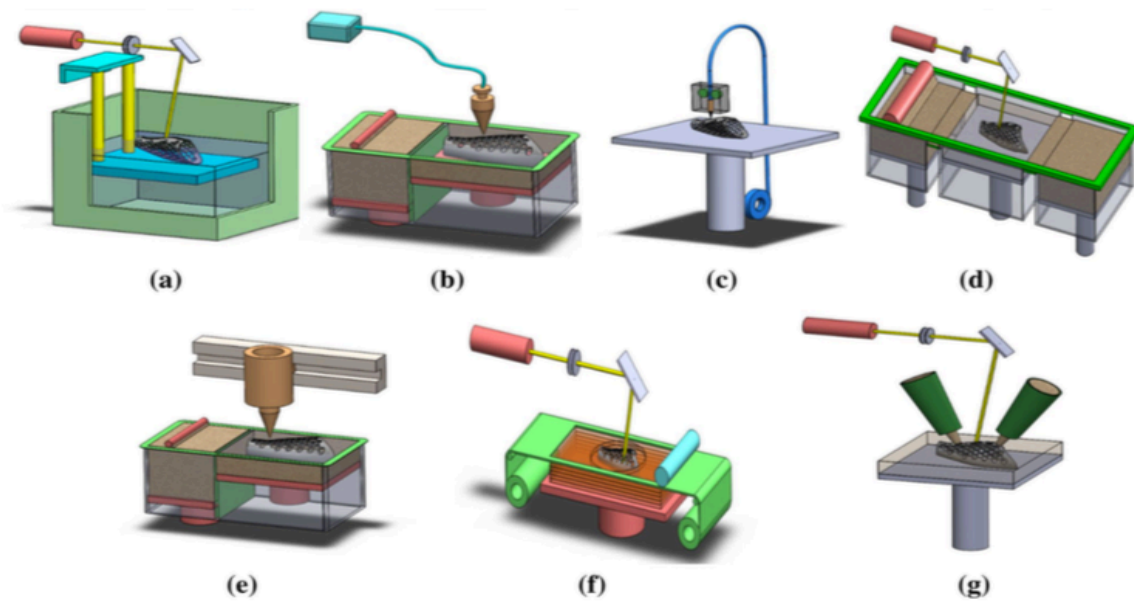


Figure 1: (a) Vat photo-polymerisation, (b) material jetting, (c) material extrusion, (d) power bed fusion, (e) binder jetting, (f) sheet lamination, (g) direct energy deposition [5].

2.1.1 VAT Photo Polymerisation

Vat polymerisation is a type of AM method which uses radiation to solidify layers of liquid photopolymer resin. Normally, an ultraviolet (UV) light is used to cure and form the 3D model layer-by-layer. Vat polymerisation method utilises liquid material to form the model therefore, a structural support is required to hold it. In some cases, the surface of each layer is smoothed by a blade to reduce the roughness of the resin base layer [5].

Fast production, ability of creating large objects with high quality are the benefits of this method but utilising resin as the build material results into creation of objects with less strength, durability and stability.

2.1.2 Material Jetting

Material jetting method works similar to inkjet printer but instead of ink deposition, droplets of material deposits from the nozzle onto the build plate and solidifies layer-by-layer. Layers are hardened by either self-cooling or cured through use of ultraviolet (UV) light. Polymer and casting wax are commonly used as feeding materials which are not mechanically strong and produced parts are structurally weak and may require support material. High dimensional accuracy, surface quality, homogeneity and low wastage of materials are the advantage of material jetting [5].

2.1.3 Binder Jetting

Two types of materials which is used for binder jetting process are commonly powder based material and the binder agent. The binder that mostly is liquid works as an adhesive on powders. Liquid binder is injected on the build material by the axially moving print head. Subsequently build platform is lowered to a specific height to create a space for the next layer and this process repeats for each layer. This method is capable of producing large objects with high production rate and different types of material such as metal, sands and ceramic can be used as build material. However, the production method is relatively expensive and due to use of binder the created parts are not structurally strong [5].

2.1.4 Material Extrusion

In extrusion based additive manufacturing process or fuse deposition modelling (FDM) material is deposited through an axially moving heated nozzle. High accuracy of final product in this method is mainly due to the constant pressure and speed of material deposition. It is very essential to consider a suitable flow rate when the new layer is plotted, because when the nozzle changes the direction, excess material might be deposited at the corners and causes inaccuracy within the layers. Polymer and plastics are used, and layers may be fused together or bonded by utilising a chemical agent. The production process is less expensive compare to other methods and built material are accessible [5, 6].

2.1.5 Powder Bed Fusion (PBF)

The powder bed fusion generally is subdivided to; direct metal laser sintering (DMLS), selective laser melting (SLM), electron beam melting (EBM), selective heat sintering (SHS), and selective laser sintering (SLS). In all types of PBF method, a layer of powder is deposited and

spread by a roller or blade. The deposited layer is then melted and sintered by laser or electron beam. The same process is carried out after lowering down the build plate and creating a new layer. Variety of materials, inexpensive process, dimensional accuracy of final part, mechanical strength of sintered objects and simplicity of application are the main benefits of this method while the production rate is relatively slow, high mass of powders is required for spreading and quality of final part is significantly related to powder properties and process conditions [5].

2.1.6 Directed Energy Deposition (DED)

Directed energy deposition (DED) is a type of AM that is commonly used to repair the existing object or add parts to the previously built section. Laser engineered net shaping, directed light fabrication, direct metal deposition and 3D laser cladding are categorised under DED processes. In this method a focused thermal energy such as laser or electron melt the material while it is deposited through number of moving nozzles simultaneously. This method has many advantages such as fast production rate, low wastage of material, high strength of final part, near net shape, repairing of existing parts and production of large objects. However, capital cost of manufacturing is very expensive while surface quality of created objects are not desirably high and may need post processing to improve the surface quality of built object [5].

2.1.7 Sheet Lamination

Ultrasonic additive manufacturing (UAM) and laminated object manufacturing (LOM) are two types of sheet lamination methods in additive manufacturing. Metal sheets or ribbons are welded by ultrasonic welding in the UAM process. The process uses high frequency vibratory energy to soften the metal sheets, which are then joined layer-by-layer. The stacked sheets are welded together to create a 3D object. The LOM process uses the same techniques but instead of metal, paper is used by applying adhesive between the layers in order to bond the paper sheets. High speed of production, lower cost and availability of build material are the benefits of this method, but surface finish of final part may require post processing and removing of excess material is time consuming and generates waste materials. Moreover, strength of final part may be reduced if the adhesives for bonding are not sufficient [5].

To date, majority of researches that cover steel powder application in AM are mostly limited to powder bed fusion, direct energy deposition and binder jetting method [7]. PBF is mainly applied to produce light weight engineering parts, architectural design and high-end applications. The main drawbacks of PBF method are low production rates and the necessity to continuously clean the un-melted powder [7]. Porosity and lack of fusion (LOF) through the layers are common imperfections of PBF method [8, 9]. Therefore, using regular spherical shape powders is recommended to reduce possible defects [10]. DED method is commonly used to fabricate defect-free, near-net shape products of high density [11]. However, due to complexity of process parameters in DED, the properties of final part is unpredictable in this method [7]. It is also reported that in the absence of continuous inert gas in DED method, formation of oxide layers is likely to occur. This defect can be amended by applying a shield layer such as chromium oxide on the surface of steel layer to avoid porosity on both the spread layer and final part [12, 13]. Rapid heating or cooling of melt pool is not involved in binder jetting method, therefore the occurrence of residual stress in the final part is prohibited. However, low density of final part is a considerable disadvantage of this method. Moreover, this method is not easily applicable with utilising ultra-fine and loosely packed particles [14-16].

2.2 Types of Powder Production Methods in Additive Manufacturing

Powders are the main feedstock of AM products hence the process of powder production has a significant influence on the quality of manufactured product. However, the production of feedstock in additive manufacturing is of even more prominence since application of powder in additive manufacturing requires a precise characterisation. Production method of metal powders are diverse but, gas atomisation (GA), water atomisation (WA), plasma rotating electrode process (PREP) are the most common powder production methods in AM.

2.2.1 Water Atomisation (WA)

Water atomisation process is the process of producing fine metal powders where the molten metal is atomised by a water jet. The feedstock is melted in a furnace and then deposited into a crucible that is called tundish. The tundish is used to control the flow rate of the liquid metal when it enters the atomisation chamber and flows through the gravity. High pressure water collides against the free-fall molten metal to atomise and solidify the particles and results into the production of fine powders. Furthermore, particles are collected and dried before post processing and packaging. However, it is notable that powder produced with this method is commonly categorised as irregular shaped particles [17, 18].

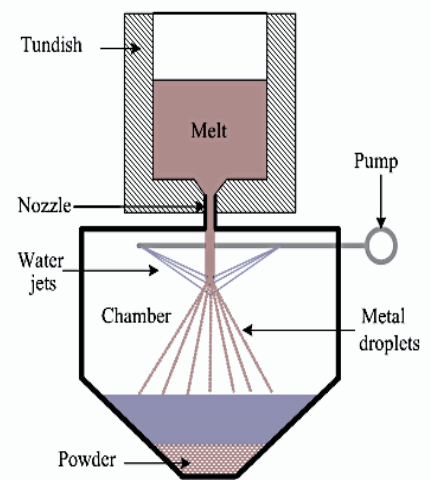


Figure 2:WA process [17].

2.2.2 Plasma Atomisation (PA)

Plasma atomisation (PA) is a powder production method that is developed by Pyro-Genesis and Hydro-Quebec (LTEE) [19-21] to produce different size of titanium powders with high sphericity and consequently good flowability. This process is also beneficial for recycling used powders. In this method the feedstock which is either in the form of wire or powder, feeds into the atomisation chamber. Afterwards, the input feedstock is melted by a heat source of plasma arc that produces high velocity hot zone to create high-purity spherical powders [18, 19, 22].

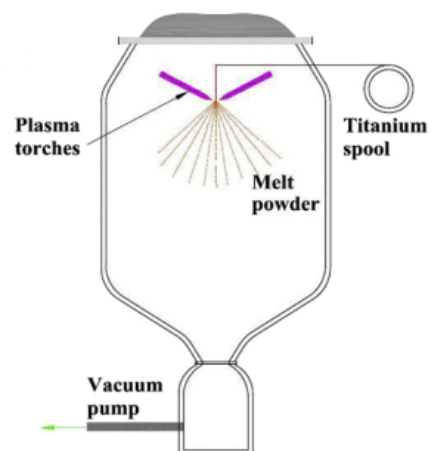


Figure 3:PA process [22].

2.2.3 Plasma Rotating Electrode Process (PREP)

Plasma rotating electrode process is similar to plasma atomisation, however, in PREP the end of the metal bar is melted by the plasma arc while it is being rapidly rotated in the chamber. Then the molten metal is spun off by the centrifugal force and subsequently solidified into spherical form. The uniformity and purity of produced powders improves further as particles are melted and solidified in a chamber that is filled with an inert gas jet [18].

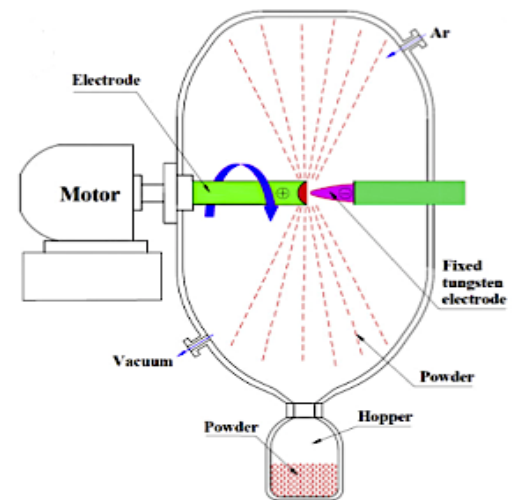


Figure 4:PREP process [22].

2.2.4 Gas Atomisation (GA)

Gas atomization process involves two factors known as, interaction of the melt and an atomising gas. In this method the melted metal from the top chamber is spherodised by a high-pressure atomizing gas. Air or inert gas is used to transfers a kinetic energy to the liquid metal. To prevent oxidization and contamination of the metal powder, nitrogen, argon, or helium are mostly used. To control the powder purity in manufacturing of complex designed products, electrode induction melting gas atomization (EIGA) and vacuum induction melting (VIM) is used.

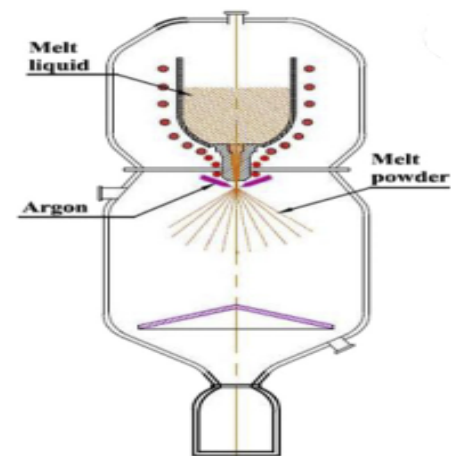


Figure 5:GA process [22].

Electrode induction melting gas atomisation (EIGA) is a method that controls contamination through heating and continuous melting of the feedstock rod. The free fall molten is solidified without contacting crucibles which prevents the contamination [18].

VIM uses electric currents that pass through a set of induction coils to melt the metal under vacuum condition. In this method, the melted metal is directly discharged into the atomisation chamber from the furnace instead of utilising a tundish[18].

Table 1 provides a summary for different types of powder production and their application in AM industry [23, 24].

Table 1: Advantages and disadvantages of different powder production types.		
Manufacturing process	Advantages	Disadvantages
Water Atomisation (WA)	<ul style="list-style-type: none"> • High throughput • Low cost • Wide range of particle size 	<ul style="list-style-type: none"> • Post processing to remove excess water • Irregular particles • Satellite present • Wide PSD • Low yield of powder
Gas Atomisation (GA)	<ul style="list-style-type: none"> • Excellent metallurgical quality • High powder flow rate due to high sphericity • Wide range of alloys available • Suitable for reactive alloys • Relatively low cost in high volume production • Large supply base 	<ul style="list-style-type: none"> • Satellite present • Wide PSD • Low yield of powder
Plasma Atomisation (PA)	<ul style="list-style-type: none"> • Excellent metallurgical quality • Very high flow rate due to high sphericity • Reactive and high melting point alloyed can be made 	<ul style="list-style-type: none"> • High cost • Limited supply base • Specific requirement of feedstock in the form of wire or powder
Plasma Rotation Electrode Process (PREP)	<ul style="list-style-type: none"> • Excellent metallurgical quality • Very high flow rate due to High sphericity • High purity • Reactive and high melting point alloyed can be made 	<ul style="list-style-type: none"> • High cost • Low productivity • Limited supply base • High quality bar needed as starting material
Electrode Induction Melting Gas Atomisation (EIGA)	<ul style="list-style-type: none"> • Excellent metallurgical quality • High flow rate • Reactive and high melting point alloyed can be made • High production rate 	<ul style="list-style-type: none"> • High cost • Limited supply base • Only alloy bar can be used as the starting material

2.2.5 Production of Steel Powders

Powder production type (e.g. processing of molten metals and the cooling rate) and the compositional elements of molten metal may impact the microstructure, surface properties, shape and size of solidified powders. All these properties will influence the powder spreading and final parts manufactured by AM.

Steel powders mainly consist of iron and carbons and when they resist corrosion they are known as stainless steel. The corrosion and oxidation resistance of stainless steel is mainly due to the chromium content. Stainless steel is produced when chromium content is sufficient to create a protective oxide film on the surface of the steel and the greater the amount of chromium the higher the corrosion resistance of stainless steel. Austenitic, ferritic, martensitic, duplex and precipitation are the five classes of stainless steel that is characterised based on crystalline structure and each of these five categories lay on different position of the Schaeffler diagram. The 300 series of stainless steel are chromium-nickel alloys and are categorised as austenitic [25].

Nickel, carbon, manganese and nitrogen are the main components to create an austenite form while chromium, silicon, molybdenum and niobium are essential elements for ferrite form of stainless steel. Figure 6 shows the diagram that is established by Anton Schaeffler in 1949 in which the low carbon stainless steel 316L is positioned in the dominantly austenite region with 3 to 10 percent of ferrite. The chromium and nickel content of 316L may vary between 16-18 % and 11-14 %, respectively. The position of 316L on the Schaeffler diagram is mainly based on the percentage of chemical composition of stainless-steel alloy [26].

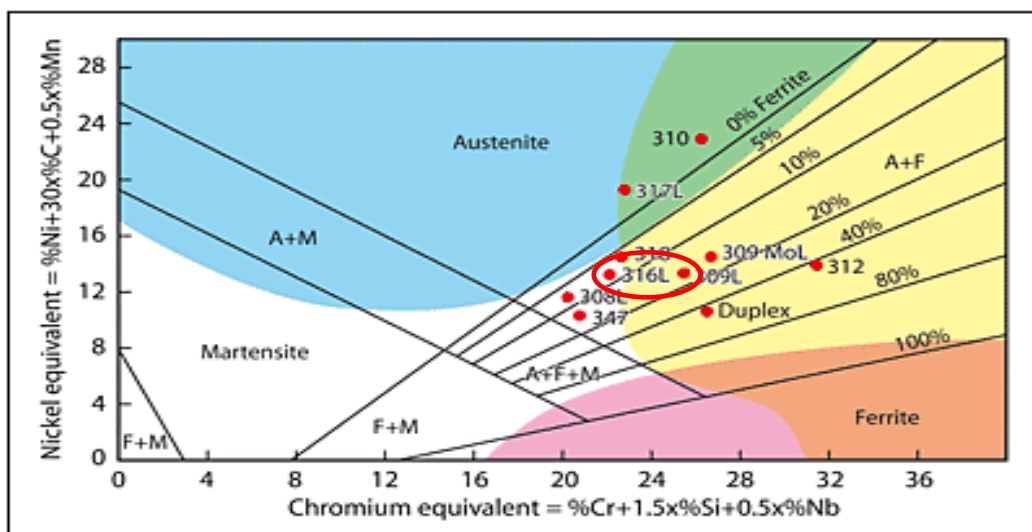


Figure 6: Schaeffler diagram (A-austenite; M-martensite; F-ferrite) [26].

Moreover, phase diagram indicates the position of the alloy based on its composition and the temperature in which it is either entirely liquid or solid. For instance, an alloy with a mixture of elements A and B may lie on the right or left side of the phase diagram which are known as hyper-eutectic and hypo-eutectic, respectively. Eutectic composition is a point in which the mixture solidifies at a temperature lower than any other composition.

As it shown in the Figure 7 the vertical axis of the diagram indicates the correct temperature based on the cooling rate of the mixture and the horizontal axis represents the composition changing from pure A to Pure B. Whereas; T_A and T_B are the melting temperatures of the pure substances and T_E is the unique eutectic temperature. α and β are the distinct solid phases and L denotes the liquid phase [27].

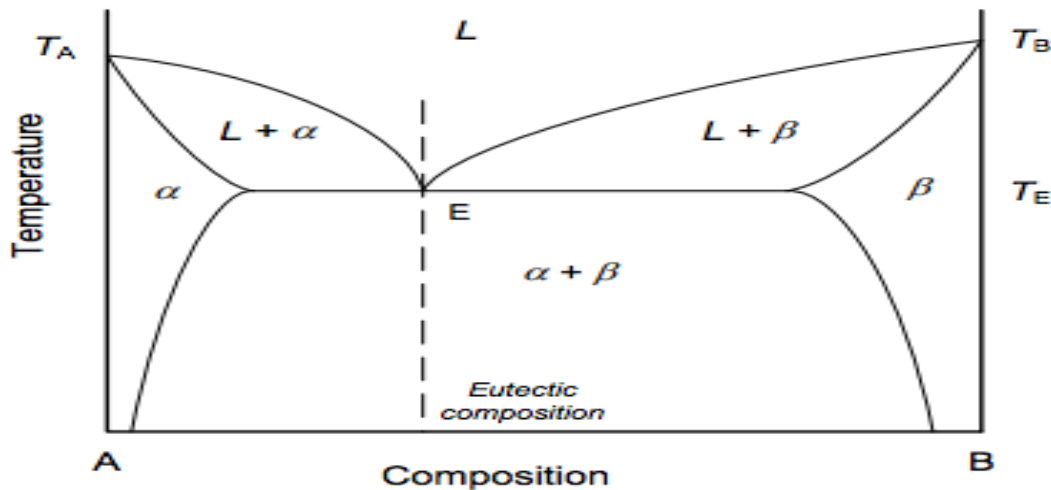


Figure 7: Binary phase diagram for a eutectic [27].

It is also important to note that the duration of time that austenitic steels exposed to high temperature is an influential factor of microstructural changes of steel powder [28].

Gas atomisation of metal powders is currently the most popular method of AM powder production and in particular spherical steel powder production as it gives a dry collection of highly spherical powders and it is relatively low cost in high volume production. The amount of oxidation in gas atomised powders is limited as the melting processes is taking place in a vacuum atmosphere or a protective environment. Moreover, this method is suitable for reactive alloys and wide range of alloys are available with this method [29]. However, even though powders are produced in low oxygen environment at inert gas conditions, the surface of the powders are still enriched with very thin layer of oxygen-affinity [29, 30]. The cooling rate was “defined as the time over which primarily crystallization occur” [31, 32]. Gas atomised

316L steel powders has lower rate of cooling compared to powders produced by water atomisation, which results in production of more spherical powders. However, irregularities of water atomised powders can be improved by altering the water jetting pressure and jet angle in water atomisation [29, 33, 34]. The morphology of solidified microstructure highly depends on the cooling rate of molten metal with respect to heat extraction during the transition from liquid phase to a solid [35, 36]. In order to have finer particles with enhanced chemical homogeneity, a high cooling rate is required, while a coarse microstructure is suggestive of low cooling rate during solidification [32, 36]. Size of the droplets and gas composition in the chamber has a significant impact on the cooling rate. Such that smaller droplets at 100% helium produce higher cooling rate and less solidification time since heat transfer is faster in these situations [37]. Particles atomised in lower cooling rate exhibit higher crystalline fraction and on the other hand particle atomised in a higher cooling rate show a higher amorphous fraction [31]. Amorphous metals exhibit excellent mechanical properties and have greater wear and corrosion resistance due to the absence of grain boundaries compare to crystalline materials [38-40]. Metal Cooling rate also has influence on the coating properties of powders such that increased cooling rates improves the coating properties of powder batch [41]. It has been found by Raza et al. that increased cooling rate, minimised the shrinkage of sintered gas atomised 316L stainless steel powders while its reduction resulted to lower density, mechanical properties and corrosion resistance of the powders [42].

Powder characterisation such as particle size distribution, morphology and chemical composition of GA powders is generally required following the production process, however, there is still some complications that prevent high quality metal powders to be produced. For instance, irregularity and satellite formation on the surface of particles are the common defects of gas atomised production method. These defects certainly have negative impact on the flowability and packing behaviour of the powders and accordingly reduces the quality of the final sintered product. However, an enhanced design of devices and chamber modification in GA processes reduces these defects within processing [43]. Moreover, hollow formation of particles is another defect that occurs when the gas atomised particle is surrounded by the molten droplets. Formation of hollow particles increases the inhomogeneity of layers, decreases the density of the powder and increases the possibility of pore formation in the final sintered part [10, 44, 45]. However, a novel gas atomisation method is developed by Neue Materialien Bayreuth GmbH along with bkl Lasertechnik and MBFZ tool craft in order to prevent these complications. This method is based on arc spraying process and it is reported by Chen et al. that the produced particles have higher sphericity, smoother surface and less

satellite formation. It is also stated that unlike the conventional gas atomisation method, the novel arc spraying method is capable of producing powders with much narrower particle size distribution which may be a desirable choice in additive manufacturing upon appropriate application [10].

2.3 Types of Powder Characterisation in Additive Manufacturing

To date, powder characterisation techniques for additive manufacturing are generally based on the earlier standards of powder characterisation in powder metallurgy (PM). However, challenges regarding powder characterisations in additive manufacturing requires in-depth standards that are specifically designed for AM industry. Standard guide of powder characterisation that is currently addressed by ASTM and ISO needs to be adjusted within AM industry [46]. It is important to note that powder characterisation covers the specific (individual) and bulk characterisation techniques. Specific characterisation techniques such as particle size, morphology, density, surface, chemistry and specific density generally measure the specific properties of one individual particle. On the other hand, bulk characterisation techniques such as Hall flowmeter and angle of repose mainly measure the collective effect of all powders in a batch [2].

2.3.1 Powder Flowability

Characterisation of bulk powder behaviour such as flowability is a common point of interest among previous studies. It has been frequently suggested within literature that flowability clearly impacts the process conditions in additive manufacturing. The flow behaviour of powders is directly influenced by the method of powder production. For instance, powder produced by gas atomisation method exhibits better flow behaviour compared to water atomised powders due to enhanced morphological quality [23, 24]. However, it is important to note that sometimes powders produced with the same production method may show different flow behaviour in spreading process due to differences in other parameters [47].

Powder flowability is defined as the “ability of powder to flow” [48]. True description of powder flow behaviour in experimental tests seems to be a multi-dimensional property rather than a single value which also depends on other characteristics of powders. Flowability is directly influenced by the physical properties of the powder aligned with other factors such as handling, storing, or measuring process; thus, it should be quantified as a multivariable

characteristic. Therefore, a comprehensive definition of flowability is stated as “the ability of powder to flow in a desired manner in a specific piece of equipment” [48].

In order to assess the flow behaviour of powders, a precise measurement of flow properties such as flow function, internal friction and wall friction is required. Flow function is obtained as a ratio of the major principle axis (σ_1) to the unconfined yield strength (σ_c) from Mohr’s circle, where the slope of the graph provides a descriptor for flowability [49]. Flow behaviour of powders is classified with the value of flow function as shown in the table below:

$$ff_c = \frac{\sigma_1}{\sigma_c} \quad \text{Equation 1}$$

where, σ_1 is the major consolidation stress and σ_c is the unconfined yield strength.

Table 2: Jenike,1964 Classification of flowability [49].	
Description	Flow function value
Very cohesive	< 2
Cohesive	2 to 4
Easy flowing	4 to 10
Free flowing	> 10

Internal friction is a parameter associated with failure properties of the bulk powder under stress and is obtained by measuring the stable value of shear stress depending on the normal load. Internal friction is measured as an indicator of flow and packing behaviour of the powders and occurs when particles move against each other. It is also defined as the rate of loss of work in the flow of powders [50]. It has been identified that particle shape has a great influence on the angle of internal friction such that increase in angularity of particles increases the angle of friction [51, 52]. Internal friction is mainly affected by size distribution, initial voids, loadings and surface properties of the particle [53]. Decrease in particle size will increase the internal friction [52, 54, 55]. The angle of internal friction is obtained by the Mohr-Coulomb yield standard and the formula is provided as; $\tau = \sigma \tan\theta + c$ where τ is the shear strength, σ is the normal stress, θ is the angle of friction and c is the cohesion [54].

Wall friction as an external friction is the angle of slide against the wall surface. In order to obtain the value of internal and external friction, the Jenike shear cell is commonly used to

measure the friction between the bulk material and wall of the container. The result shows whether the material will slide on the wall or adhere to it and is used to govern the mass flow or funnel flow behaviour in the container. The higher the angle of wall friction, the steeper the container wall needs to be for powder to flow. When the pressure from normal stress on to the powder increases, the effective angle of friction decreases, and wall friction also decreases. Friction between the powders and container wall increases when stored in a static situation for a period of time. It is also indicated in the book that fine particles with wide PSD exhibit more friction compared to that of larger particles with narrow PSD [56].

Hall and Carney Flowmeters, apparent and tapped density, angle of repose, laser diffraction particle sizing and scanning electron microscopy are the standard powder characterisation techniques that is reviewed in ASTM F3049. However, some novel powder characterisation techniques such as avalanche tester, powder rheometry and image analysis are commercially available [2].

2.3.1.1 Angle of Repose (AOR)

The angle of repose is defined by ISO-4490 [57] /ASTM B213 [58] as a flowability measurement for powders. In this method as it shown in Figure 8 powders are deposited through a funnel and settled onto a flat base plate. The slope angle of the created heap is known as angle of repose which measures the flowability as a level of friction within the powders [2, 59]. Other properties of powders such as shape, size and bulk density may affect the measured angle and commonly it is recommended that the steeper the angle, the more cohesive the powder is [60].

Table 3 represents the Carr classification of flowability for powdered particles based on the angle of repose [61].

Table 3: Carr classification of flowability [61].	
Description	Repose Angle
Very free flowing	<30°
Free flowing	30-38°
Fair to passable flow	38-45°
Cohesive	45-55°
Very cohesive (non-flowing)	>55°

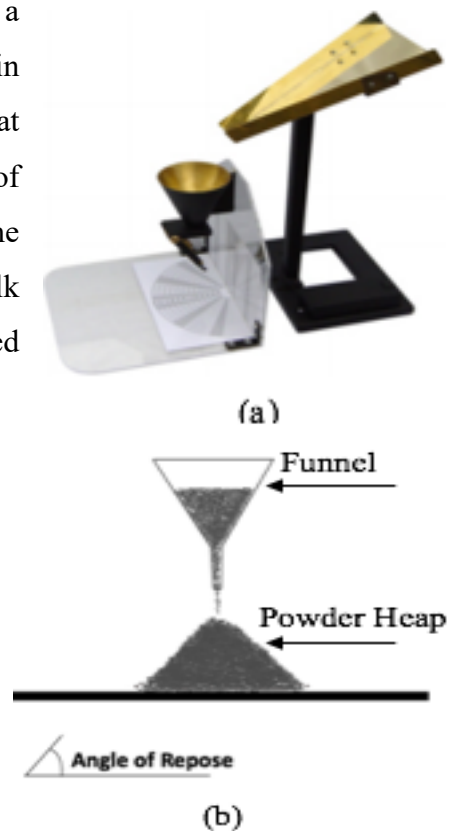


Figure 8: (a)Angle of Repose [60].
(b)Schematic Angle of Repose.

2.3.1.2 Hall Flowmeter

The Hall Flowmeter test is one of the ASTM standard method for measuring the flow rate of freely flowing powders such as metal. However, it is also used to measure other powder characteristics such as; apparent density, tapped density and angle of repose. Specific amount of powders is deposited through a closed orifice until all powders are settled. Figure 9 illustrates the apparatus used for this test and different size of orifice diameter may be used for this test. The tip of the orifice is then opened and consequently powders flow from the opening of the orifice. The required time for powders to completely flow is precisely measured. This procedure is repeated for several times to mitigate the human error.

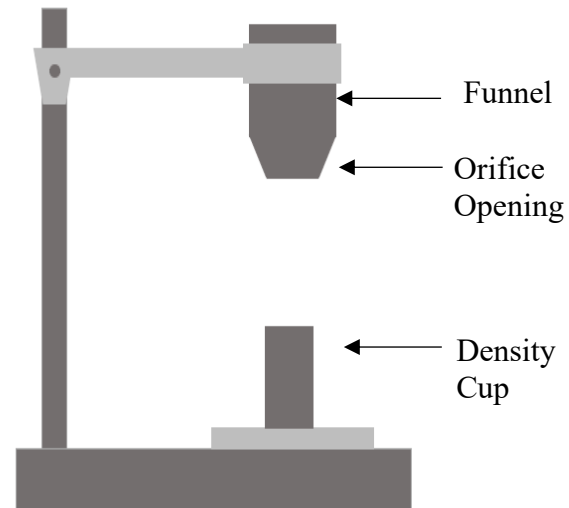


Figure 9: Hall Flowmeter.

However, it is important to note that flow behaviour of powders may vary when it passes through the air, hence the flow rate is not a consistent quantity but rather a simple comparative measure [62]. Hall flowmeter test is mainly suitable for free flowing specimens, hence it is not applicable for cohesive powders [63]. Inter-particle force is the most influential factor in powder flow which directly impacts the procedure in Hall flowmeter test. Difficulty in quantitative assessment of this test is mainly due to the large amount AM powder that passes through a small opening of orifice. Additionally, the stress state of the powder in real AM processing is different compared to that of the laboratory scale [59]. In addition, when free flowing powders are not completely dry, they are prone to rat-holing, arching, clinging and bridging in this test which is shown in the Figure 10 [62, 64].

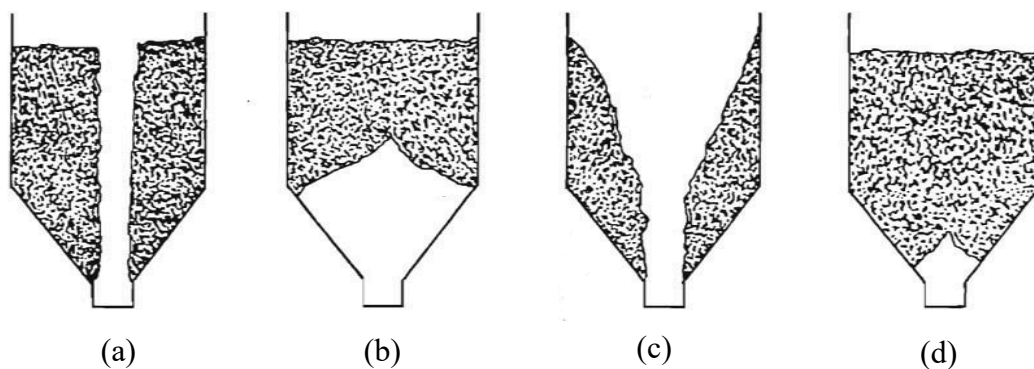


Figure 10: (a)Rat-hole, (b) Arching, (c) Clinging, (d) Bridging [64].

2.3.1.3 FT4 Powder Rheometer

FT4 powder rheometer[®] is the most common testing tool that is used to measure the dynamic flow resistance of powders [65]. While other standard characterisation techniques focus on the flowability of powders under the influence of gravity, FT4 powder rheometer aims to measure the dynamic shear load. Since shear is an indicative force during the spreading process of PBF, the FT4 tester is an interesting topic of investigation in AM researches [2]. It is a universal flow tester that has been designed by Freeman Technology and provides four categories of bulk, dynamic flow, shear and process in testing methodologies. Density, compressibility and permeability is measured under bulk category of tester. Basic flowability, aeration, consolidation, flow rate and specific energy is tested under dynamic flow criteria. Furthermore, shear cell and wall friction are analysed under shear methodology. Moreover, segregation, attrition, caking, electrostatic moisture and agglomeration tests is covered under process category [66]. It is designed to test the powders under a condition that resembles the true behaviour of powder in AM machines. It has been proven that testing the powders with this apparatus is very beneficial for powder optimisation, particularly when working with used and re-used metal powders [67]. The flow resistance of dynamic powders is measured by utilising a precision ‘blade’ [66]. The rotating blade driven downward or moving upwards into the bulk assembly to simulate the interaction and flow between the powders. The required energy by the rotating blade is considered as flowability [68]. The definition of an unconfined test (i.e. upward motion) clockwise motion is specific energy (SE) and the definition of a confined test (i.e. downward motion) is basic flowability energy (BFE) [69]. Change in flowability with FT4 rheometer appears to show promising results while testing with shear cell may not be able to fully detect those changes [69]. However, distribution of the stress inside the powder bed is not yet fully understand ,hence it is suggested that the results from the FT4 rheometer is generally reliable as a comparative data rather than design data [70].

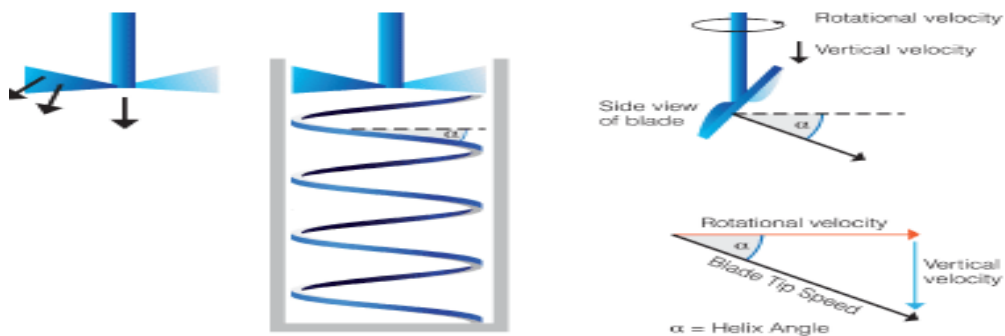


Figure 11: FT4 Powder Rheometer [66].

2.3.1.4 Avalanche Tester

REVOLUTION powder analyser is an avalanche tester that unlike some other standard flow test (i.e. Hall flowmeter and angle of repose), is not only based on gravity forces but rather imitates the dynamic behaviour of powder during the spreading processes. This device uses a rotating drum that rotates at a controlled velocity. The gravity and friction to the wall are influential factors to form the wave in the loaded powder until avalanche occurs [2]. Special camera in front of a backlight is operated to record the images from the surface and cross-sectional area of the powder that illustrates the exact motion of the powder in the drum. The occupied area of drum and the avalanche of the powders is shown as a black-and -white picture [71]. The Dynamic flow testing, packing analysis and multi-flow test can be conducted through the use of Revolution Powder Analyser [72].

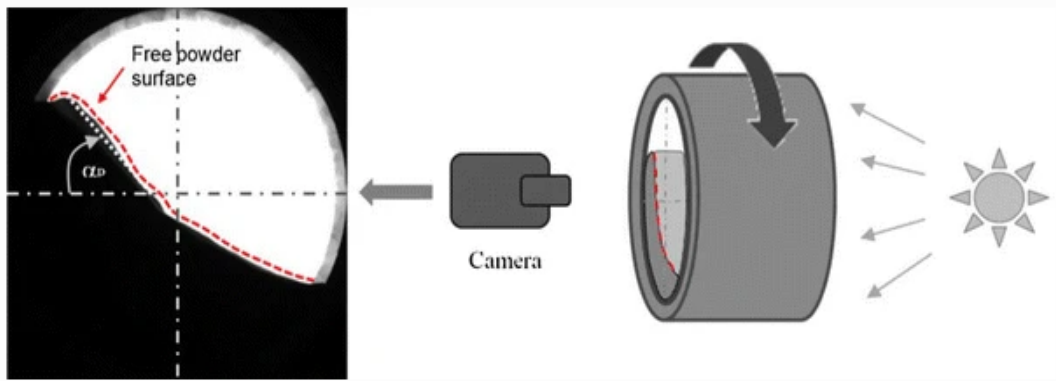


Figure 12: Revolution Powder Analyzer principle [71].

2.3.1.5 Dimensionless Shear Rate

Analysis of powders flow behaviour as a function of the shear rate is a useful measure due to dynamic nature of powders during the processes of manufacturing parts [73]. The dimensionless shear rate by Tardos et al. has been used to draw a classification for the flow regimes of powders which is presented by Equation 2.

$$\gamma^{o*} = \gamma^o [d_p / g]^{1/2} \quad \text{Equation 2}$$

where d_p is the mean particle diameter, g is the gravitational acceleration and γ^o is the shear strain rate. Shear strain rate is calculated as a ratio of spreading speed and depth of shear zone (gap size in powder bed spreading processes) [74, 75]. Based on the value of dimensionless shear rate the classification of the flow regimes according to Tardos has been presented in Figure 13.

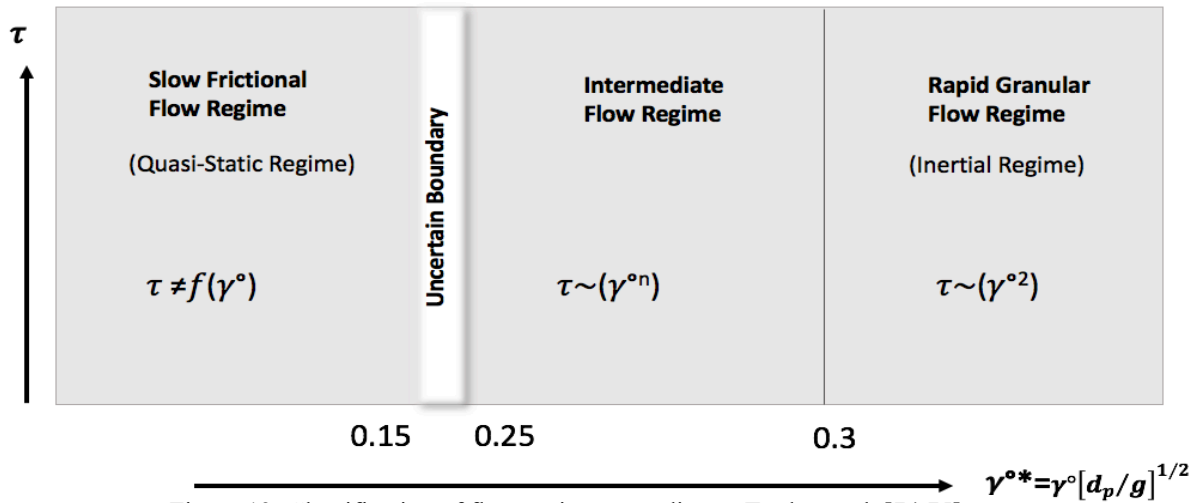


Figure 13: Classification of flow regime according to Tardos et al. [74,75].

The region on the left side of the classification diagram covers the boundary of low dimensionless shear rate (< 0.2) in which friction is the predominant force and is considered as the quasi-static regime. On the other hand, the dynamic regime of flow on the right side of the diagram is the region that collision between the particles overcomes the frictional force where the dimensionless shear rate is higher than 0.3 and the shear stress is double the magnitude of the shear strain rate. However, the intermediate regime with the dimensionless shear strain rate between 0.25 and 0.3 covers the region in which the collisional and frictional force between the particles are equally influential [74].

2.3.1.6 Effect of Powder Flowability on the Final Part in AM

Flowability is an effective parameter in additive manufacturing process and is considered as an indicator of powder behaviour during the spreading process [65, 67]. Powder flowability in correlation with other powder properties, influences the quality of final part in additive manufacturing [59]. This is mainly because flowability of powders may impact the movement of powders and consequently the arrangement of particles. Furthermore, if packing is disturbed by the flowability, the sintering may be negatively impacted which increases the porosity, surface roughness and reduces the density of final part. For instance, the use of near spherically shaped powders results into higher flowability and consequently produces homogeneous microstructure [76]. In-depth assessment of flowability is required since powders need a sufficient flow during the additive processing in AM. Flowability is a parameter that effects the process efficiency and consequently the final AM part [71]. However, the impact of flow behaviour of powder on the properties of sintered part is not fully covered by the previous studies [77]. Attar et al. stated that by improving the flowability of powders, the final density

of the AM product improves [78]. Furthermore, Koo et al. assessed different mixtures of polyamides and reported that poor flowability of powder results into complications in spreading of powders which consequently reduces the quality of sintered part [79]. It has been reported by Sun et al. that homogeneity of layers significantly improves when flowability increases [76]. This suggestion also agreed by Ma et al. that excessive voids in metal powders which is formed by poor flowability creates discontinuities within the final part [80]. Furthermore, it has been stated that packing and flow behaviour of metal powders, are influential factors of powder bed formation that improve the development of melt pools and microscopic homogeneity [81]. Ziegelmeier et al. performed a study regarding the effect of flow behaviour of thermoplastic elastomers powders on resulting parts. The valuation of flowability is conducted through investigation of the Hausner ratio, avalanche angle, Revolution powder analyser and rheometer. It has been gathered that, higher flowability results into higher packing efficiency. This leads to better surface quality, higher ultimate tensile strength, and higher percentage of elongation at break for the final part. Poor flowability adversely affects the arrangement and packing of powders which leads to inhomogeneous pore structure and empty patches within the spread powder layer and this will result in poor sinterability and consequently increases the porosity within the layers and final part [82].

Freeman Technology conducted series of experiment to improve print quality through powder flowability assessment of FT4 powder Rheometer. It has been reported that flow behaviour of the powders has a critical influence to control the process efficiency and quality of final product. Three samples of stainless steel from same supplier is tested to investigate their performance in AM process. It is gathered that sample A and B with lower specific energy exhibit acceptable behaviour compared to sample C with a higher value of specific energy. The higher value of specific energy in sample C implies a higher particle to particle friction hence lower flowability. Sample C with lower flowability caused poor deposition and a lower quality of the final part [83]. In addition, a study by Liu et al. states that better flowability in powders with respect to the value of Hausner ratio, generates parts with increased hardness and ultimate tensile strengths [84]. Furthermore, evaluation of powder layer density on the two samples of stainless steel in the SLM process is studied by Choi et al. It is established that there is no correlation between the values of Hausner Ratio (HR) and Hall flow results. It is also derived that although one of the samples failed the Hall flowmeter test but still showed a successful spread. This implies that testing the flow behaviour of the powders is not adequate to predict

the packing state of deposited layers and consequently the density of final part ,but the quality of packing may varies in different processes conditions [85].

2.3.2 Bulk and Tapped Density

Bulk density, which is also known as apparent density is an important parameter in powder characterisation as it has a substantial impact on flow behaviour of powder during the spreading process. Bulk density is referred to the ratio of the weight of powder to its volume including the voids [86]. Bulk density is related to the size [87], chemical composition [88], moisture content [89], and the magnitude of consolidation stress [62, 90] of the powder. Tapped density on the other hand, is the “ratio of a known weight of a powder to the least volume the powder could occupy upon tapping” [91]. Rate of change in volume through tapping is a good indicator of the flow rate within the powders. The Hausner ratio (HR) and compressibility index (CI) are useful flowability metrics that is obtained through a comparison of the bulk and tapped densities [92, 93].

$$\text{Compressibility Index} = 100 \times \left(\frac{\rho_{\text{Tapped}} - \rho_{\text{Bulkd}}}{\rho_{\text{Tapped}}} \right) \quad \text{Equation 3}$$

and

$$\text{Hausner Ratio} = \left(\frac{\rho_{\text{Tapped}}}{\rho_{\text{Bulk}}} \right) \quad \text{Equation 4}$$

These two measurements can be used as indices of the ability of powder to flow which is influenced by interparticle interactions. Hausner ratio is an indicator to describe the packing behaviour of the powder upon tapping. Hausner ratio close to the value of one indicates a flowable powder while the ratio greater than 1.25 presents powders with unfavourable flow behaviour [61].

Scale of flowability with respect to CI and HR has been presented in Table 4.

Table 4: Scale of flowability based on CI and HR [61].		
Compressibility Index (%)	Scale of flowability	Hausner Ratio
1-10	excellent	1.00-1.11
11-15	Good	1.12-1.18
16-20	Fair	1.19-1.25
21-25	Passable	1.26-1.34
26-31	Poor	1.35-1.45
32-37	Very poor	1.46-1.59
>38	Very, Very poor	>1.60

2.3.2.1 Effect of Bulk and Tapped Density on the Final Part in AM

It has been perceived that utilising powder with high bulk density results into producing parts with enhanced tensile properties. In the presence of inconsistent bulk density of metal powders, poor surface quality and undesirable mechanical properties of final part is predicted. [82]. The density of powders in powder bed fusion process affects the layer bulk density and consequently the sintering process. This will as a result change the surface quality and density of the final part. It is also reported by the same author that utilising recycled powder leads into irregularities of powder density and in return results into non-uniform layer [45]. According to Rausch et al. an increase in the bulk density of metal powders reduces the porosity and surface roughness and increases the relative density of the final part. Moreover, it has been further added that by decreasing the powder bulk density more energy is required to produce dense part which is mainly due to the likelihood of irregular melt pool. This implies that the higher surface roughness is exhibited by using a powder with low bulk density which certainly is a defect in the final part. This can be compensated by using higher energy input, which is cost intensive. Therefore, it is beneficial to make use of powders with high bulk density to create dense parts in a more efficient and economic manner [94]. Schultz et al. reported that defect in mechanical strength of the final part is associated with the use of nylon powder with lower bulk density [95]. A further study of Inconel powders by Nguyen et al. shows that the density of the final part decreases when utilising recycled powders due to the reduction in their bulk density [65]. It has been gathered through examining of different SLS and non-SLS powders that fabrication of weak parts with higher porosity and less dense structures is highly related to the use of less dense material [96]. When the bulk density of the powder decreases, the mean distance between particles tend to increase which results in increase void formation in each layer and consequently cause extrusions and intrusions as well as balling. This will significantly reduce the surface quality and mechanical strength of the final part [94]. Reducing the tapped density of 316L stainless steel powders will results into high porosity and shrinkage during the sintering of the end product [97]. However, according to the study on the 316L stainless steel powders by Spierings et al. generally characterisation of powders based on the tapped density is not a sufficient tool to predict their spreadability and the resulting layer density. This is suggested based on the experiments of three different batches of powders with similar tapped density which exhibit significantly different surface quality and mechanical properties [98].

2.3.3 Particle Size and Size Distribution

Particle size is a key property in powder characterisation as it provides useful information for manufacturing of products and has direct impact on the flowability of the powder. Very fine particles have very high surface area to volume ratio which influence the packing and mechanical properties of the powder [99]. Van der Waals force in fine grains is dominant compared to gravity force, hence agglomeration in fine particles are very common [100]. Two phase interaction of solid/gas in fine particles is a reason of poor flow in bins, hoppers or processing vessels. During powder discharge from the hopper, fine particles are prone to ratholing due to their cohesive nature, which is one major problem of the spreading process. Flooding may also occur by utilising fine particles when rathole collapses or in-feed rate is slower than the discharge rate. Fluidisation (air entrainment) and particle entrainment are two mechanisms which cause segregation in fine particles. The settlement and its duration in fine powders is much more than coarse particles due to air entrapment during the compaction [101]. Nevertheless, utilising fine powders in additive manufacturing is desired since typical layer thickness in EBM and SLM processes are around 50-200 μm . Therefore a thorough understanding for specific design of outlet in AM machines seems to be very beneficial [102]. Tensile strength in smaller particles is larger than coarse particles, since they have larger surface area to volume ratio available for bonding [103, 104]. Larger particle sizes show higher elongations under tensile testing, however they have more tendency to not fully melt due to less laser interaction [98]. Lower specific surface in larger particles leads into greater tapped density. Lower friction between larger particles due to lower specific surface improves the flowability of powders which helps for easier compaction upon tapping and accordingly into a greater value of tapped density [105].

Particle size distribution (PSD) measures the total size of the powder population as a powder property and a suitable graded size distribution that provides a precise scale of coarse and fine particles in a batch of powder is a key factor for better performance of powders [1]. Segregation of powders during the spreading process is a great concern which requires in-depth understanding of PSD in AM applications [106]. However, it is widely accepted that narrow particle size distribution is preferably applied in order to prevent segregation and improve flowability [96, 107]. Sieving and laser diffraction analysis are two common methods which are widely used to measure particle size distribution. However precision in PSD is greatly dependent on the method of measurement, the process and device of use and specifically on the shape of particles. In some measurement techniques such as scanning electron microscopy

(SEM), irregular particles may be assumed to be spherical for ease of measurement which reduces the accuracy of PSD [108, 109].

2.3.3.1 Effect of Particle Size and Size Distribution on the Final Part in AM

Particle size distribution is an important measurement to alter the quality of final part particularly the mechanical resistance, surface quality and porosity of the end product [1, 65]. Sutton et al. found in agreement with Bierwagen and Sanders, Hoffman and Finkers, Zheng et al. and Karapatis and Egger, that finer particles can be advantageous as they exhibit better particle packing that reduces surface roughness on the final part [45, 110-113].

On the other hand, tendency of fine powders to agglomeration is a downsides in PBF process since agglomeration can significantly disturb the flowability of powder through deposition [108, 114-116]. Discontinuous flow behaviour in PBF may result into non-uniform deposition of powders on the build plate and consequently reduction in density and homogeneity within the layers. This hurdle leads to balling effect in different regions and consequently undesired porosity in the final part [116-120]. By utilising larger particles, not only a higher breaking elongation is obtained, but also powder flow is improved hence a homogenous layer is created and consequently balling effect in the final product is reduced. There are several packing defects that directly reduce the packing quality of the layer and consequently quality of final part. For instant “loosening effect” may occur if the mixture predominantly contains larger particles. This defect happens because fine particles are not sufficiently small to fill the voids between larger particles and accordingly the frame of large particles became loosen. In contrast, “wall effect” appears when the PSD is biased to finer particles and wall boundaries created by larger particles interrupts the uniform packing of fine particles. “Wedging effect” is also a particle interaction which occurs when fine particle in a batch are not sufficient enough to fill the voids between larger particles and this happens dominantly for angular particles [121, 122].

Spiering et al. performed a study to compare the density of final part in SLM process by using different grade stainless steel 316L powders. It was stated that, in order to produce parts with the highest possible density in combination with a low surface roughness, it is important to optimise the influential parameters such as PSD. It has been found that although the application of fine particles is necessary to form a thin layer in the spreading process, they reduce the flowability. Therefore, it is essential to generate a suitable PSD to mitigate this issue [123].

According to Bai et al. fabrication of metal parts with mono-sized fine copper powders is a challenge to produce a fully dense part. However, unlike fine particles, coarse particles exhibit better spreading due to higher flowability but they inhibit sintering and densification [15, 124]. However, Simchi stated that decreasing particle size does not necessarily results into higher densification of the final part since reflectivity increases due to agglomeration and laser power is less absorbed when powder size decreases [114]. Nevertheless, using large particles are cost efficient compared to the application of solely fine powders in a powder bed. It is further added that less energy input is required with utilizing bimodal batches of powder as bimodal particles are less sensitive to sintering condition. It is concluded by the author that the use of bimodal powder mixtures in binder jetting improves flowability, packing density and sintered density of final part while reduces the sintering shrinkage [124]. According to Bridgwater, Sommier et al. and Duffy and Puri, when size ratio for free-flowing powders increase, the segregation also increases. However, to minimise segregation, particle properties can be improved through narrowing size distribution biased to smaller particles [107, 125-127]. Vock et al., described that flowability and PSD are directly related such that if the width of PSD decreases, the flowability increases [1, 62, 123]. A further study by Spiering et al. proves that narrower PSD in stainless steel 316L, have a positive impact on the mechanical properties and finishing surface of final part [98]. However, Liu et al. investigated the effect of particle size distribution for two batch of gas atomised stainless steel 316L powders on the process parameters and part quality in SLM and reported that wider particle size distributions increase the powder bed density since smaller particles can fit in the gaps between the larger ones and in return higher part density and smoother side surface for finishing parts is achieved. Additionally, better flowability, high tensile strengths and hardness is attributed to narrow particle size distributions due to less segregation [84]. A further study by Mostafaei et al. stated that utilising narrow PSD in binder jetting method leads to printing defects with high pore coordination while wider PSD results in higher part density [128]. According to Lutter-Gunther, wide PSD improves the powder bed density due to more interlocking. However, it is important to note that this interlocking may reduce the flowability and packing of spread based additive manufacturing, hence wide PSD may be more beneficial for non-spread based methods of AM.

Moreover, increase in packing may improve the powder bed density but not necessarily the density of final part since density of the individual layers does not directly define the final density of the product. The final density is rather influenced by the surface roughness of the individual layers. This is because, inconsistent deposition of layers on top of each other ultimately reduces the density of the final product [1, 129]. The results for powder

characterisation of Inconel powders in PBF by Nguyen revealed that the narrower PSD improves the flowability and accordingly the surface quality while a wide PSD leads to an uneven spread layer, and creates high surface roughness of the printed part [65].

Tang et al. suggested that reusing or recycling powders for a long time may narrow the PSD of metal powders [130]. Moreover, Liu et al. reported that PSD of recycled 316L stainless steel become narrower which in result improves the followability due to less interlocking between the powders [84]. The PSD became narrower since finer particles pass through the gap and spread while larger ones is pushed away with the blade from the build plate. Therefore, a narrower PSD with increased number of large particles and decreased number of fine particles is achieved with recycling powders in PBF method [131]. On the other hand, in some articles such as Yusuf et al. it is suggested that the PSD of recycled 316L SS in SLM method is not noticeably changed compare to the virgin batch [132]. This may be due to the reason that the gap size is large enough to spread the coarse particles along with the finer ones.

2.3.4 Powder Morphology

Powders that are used in actual experimental work are not a perfect sphere and there are always some irregularities within the powders. Therefore, a standard morphological characterisation of powder is imperative. Morphology mainly describes the overall shape of an individual particle such as spherical, dendritic and angular geometries. The powder production method and processes can clearly change the morphological characteristic of the powders. For instance, as it has been mentioned in Section 2.2, powders produced by GA method are more spherical compared to WA process. The necessity of morphological characterisation is mainly due to the significance of shape on the green strength (strength of deposited powders before sintering), flowability, compressibility and bulk density of deposited powders [133].

Sphericity is described by Waddell in 1935 as the ratio of the surface area of an equal-volume sphere to the actual surface area of a particle. The result is quantified between value of 0 and 1, where value of 0 is considered as the most irregular in shape and value of 1 is measured as an absolute spherical shape [134]. Aspect ratio as a shape factor is described as the ratio of minimum to maximum diameter of the particle (i.e. a perfect sphere has an aspect ratio of 1:1). Different shapes of stainless steel powders that is generally categorized as spherical, spongy, rounded, flaky, and cubic have different aspect ratio while the spherical have lower aspect ratio [30, 135]. Convexity is also a shape factor which is described in terms of compactness and is

defined as a ratio between the volume of actual particle to the volume of the smallest convex shape (convex hull). The convexity index equal to 1 is an indicator of smooth outlines and lower than one for rougher shapes [136]. Elongation (also known as eccentricity) and roundness are two other shape factors that has been largely used in different field of studies. Elongation is defined as the ratio of particle diameter to its length, and roundness as a measure of sharpness is the ratio of the average radius curvature of all the convex corners to the circumscribed circle of the particle [137, 138]. Scanning electron microscopy (SEM) is the tools to measure the morphological parameters, however with using of this tool, there is a statistical limitation for the gathered data [2].

2.3.4.1 Effect of Morphology on The Final Part in AM

The shape of stainless steel powders has a substantial influence on different parameters such as sintering, mechanical properties, corrosion resistance and dimensional change of final part. Shape of the particles governs their bonding points, which can directly affect the sintering processes. Therefore, strength, hardness, density and ductility of final part that is related to the sintering processes, highly depends on the shape of particles [30, 133]. It is also reported that shape of the individual powders has a great impact on the flowability, bulk density and packing efficiency of powders that consequently change the quality of the final part [139, 140]. Attar et al. performed a study to investigate the effect of titanium particle morphology on the SLM produced part. It has been recommended that spherical shaped particles increase the homogeneity of layer deposition as well as molten liquid during SLM that results in lower porosities in the end product. It is further concluded that duration of milling processes can significantly change the morphological properties of the powder that results in changes of properties within the final part. Longer milling time leads to more irregularities of the metal particle shape as powders are in collision for a longer period of time and accordingly this may reduce the relevant density, compressive strength and compression strain of the final SLM part [78]. Mussatto et al. carried out a study to address the influence of 316L stainless steel morphology on the powder bed uniformity. It is concluded that the sphericity and surface texture of steel powders affect the quality of deposited layer on the bed. The batch of steel powder with higher sphericity and smoother surface shows higher flowability due to lower mechanical interlocking which ultimately optimise the layer uniformity and consequently influence the density and uniformity of final part [141]. It is important to note that the processes of heat transfer is more effective while using uniformly spherical metal powders that results

into a lower specific heat capacity thus reducing the energy requirements which is cost effective in AM process [142]. It is also reported that the strain hardening of 316L stainless steel powder strongly relates to the morphological factor where irregular shaped powders reduces the ductility of final part [143, 144]. A further study by Olakanmi stated that due to increased inter-particle friction of irregular aluminium particles, the particle packing and bed densities reduces and consequently creates mechanical defects in the final part [145].

As mentioned before, spherical particles with aspect ratio closer to 1 exhibits better flowability during spreading and better bed quality. On the other hand, the surface roughness and packing fraction of the layers increase and decrease respectively, when the aspect ratio of irregular particles increases, particularly at higher translational spreader velocities [146].

It has been agreed by many authors that the morphological properties of the recycled and reused polymer powders may change during the processes and the surface roughness of the final part increases as an ‘orange peel’ texture is appeared on the final part [147-153]. Surface of reused powder may also deform or distort after several cycle of applications. The reused powder became less spherical and gained rougher surface by increasing the reuse time as particles became distorted [76].

However, some researches [154-156] advised that recycling of stainless steel does not have a great impact on the mechanical properties of the final part. It has been stated that “reused powder showed no measurable undesired influence on the AM process and the samples exhibited highly consistent tensile properties through the whole area of the built plate” [130, 157]. Moreover it has been reported that recycled 316L SS powder retain their sphericity and circularity compare to recycled AlSi10Mg powders. It has been further added by the author that the recommended reuse time is up to 30 overall build processes as further reuse may leads to physical and chemical change of the powder [132].

2.3.5 Surface Properties

Porosity is also known as void fraction and is identified as a measure of voids. Porosity is measured as the ratio of void space to the apparent volume of the powder [158]. It is an influential factor that directly changes the physical interaction and chemical reactivity of particles [159]. Small, irregular voids created during manufacturing processes due to differential contraction and larger spherical pores develops from gas entrapments during gas atomisation processes. Powder denudation during the processes of additive manufacturing and

fluctuation of the surface can create spherical pores that may result into even larger spherical pores within the final part [160]. Oxidation and contamination of the powder can also be another reason of pore formation and spatter presence. Metal AM powders are prone to oxidation in aerated conditions, which acts as a major contaminant that increases the rate of porosity within the final manufactured components [161]. It is reported that process-induced porosity can be affected by the characteristic of the powder porosity where sinterability has a direct link to the porosity of the particle [162].

Surface roughness of the powders plays an important role on the flow behaviour of powders such that, rough surfaces of particles decreases the flowability compared to smooth particles and this is mainly due to increased inter-particle friction [78].

Adhesion force between particles during deposition and spreading process is an unfavourable factor which generates an undesirable effect on the flow behaviour of powder, hence, investigation of adhesion force is essential in many manufactural processes and particularly AM industry. Force between particle-to-particle or particle-to-surface which arises from electrostatic forces, capillary forces and the Van der Waals interactions strongly depends on the environmental condition of the workplace and physicochemical properties of powders [163]. Van der Waals force is defined as a distance-dependant interaction between atoms and molecules and is considered as a dominant force of adhesion. Particle size, shape and moisture content are influential factors when evaluating adhesion force. In addition, particle shape is an important parameter when evaluating the adhesion force. Irregular particles induce less adhesive force due to lower contact area while adhesion force in spherical particles increases as effective contact area increases [164, 165].

2.3.5.1 Effect of Surface Properties on the Quality of Final Part

As previously mentioned in Section 2.3.3.1, Lutter-Gunther stated that the density of final part is not necessarily dependent on the layer density but is also influenced by the surface roughness of the individual layers. This implies that porosity and surface roughness are the most important surface properties of particles [129]. The quality of the final part is strongly related to the two types of porosity in AM process, namely powder induced porosity and process induced porosity. It is important to understand that the measure of porosity is entirely dependent on the application of the final AM product, since some products such as aerospace engines need lowest possible porosity whereas biomedical implants requires porosity to some extent for

better integration. In other words, parts that are intended to bear high amount of force requires full density to resist the failure and this necessitates the reduction of porosity [166]. Internal porosity and surface impurities are powder-related defects which degrades the quality of final product. The attached satellites on the surface of the particle which also known as projections are identified as a factor that produces porosity in the final part. This is primarily due to the fact that welded satellites reduce the flowability and uniformity of powder packing [43, 167]. Tang et al. stated that reusing or recycling the metal powders may reduce the satellite projection while the surface of the particle became rougher [130]. Cordova et al. described that internal porosity is due to entrapped gas during the production process which is known as hollow particles. The large number of hollow particles in the batch causes poor flowability and laser interaction which ultimately reduces the density of final part [168]. It is also stated by Sutton et al. that internal porosity of powders increases the amount of voids and subsequently increase the porosity of final part [45]. A further study of Sutton et al. reveals that, increase in internal particle porosity significantly reduces the density and increases the porosity of the final product [140]. It has been reported by Chen et al. that size of internal porosity in the spherical Ti-6Al-4V powders increases with the increase of particle size. This experiment has been applied on three types of powder produced through gas atomisation, plasma rotating electrode process and plasma atomisation process and all three samples show similar result [22].

Adhesion force also contributes an important role on the spreadability of the powder. It is commonly suggested that adhesion is an important element which affects the flow behaviour of metal powders during spreading process. Agglomeration of high adhesive powders tend to be sheared off under the recoater blade in which results to irregular and less dense powder layer. Non-uniform packing fraction due to increased adhesion force, increases the surface roughness of the layer, which substantially reduces the density of final product. It is further added that reducing the particle-to-particle adhesion between fine and cohesive powders and particle-to-blade adhesion improves the layer quality. Layer quality is mainly related to uniform and highly packed spreading of powders without formation of empty patches or jamming within the layer. However, if adhesion between powder and substrate due to surface contamination or oxidation decreases the quality of deposited layer decreases clearly changes the quality of final part in AM [169].

2.4 Effect of Spreading Process on the Quality of Final Part

2.4.1 Gap Size (Layer Thickness)

The height of the layer is an important parameter that controls the quality of spread layer such that reduction of layer thickness result into poor spreading while increasing the thickness of the layers improves uniformity of the spread layer [98, 170, 171]. Although smaller gap size is desirable due to higher absorption of laser energy, but it also results into an increase in shear as particles have less space to pass under the blade (shear zone). Moreover, utilising smaller gap size may increase the formation of empty patches and transient jamming as larger particles or agglomerate powders are not able to pass through the small gap size and may drag other particles on their way.

In some previous researches the effect of layer thickness on the spread layer and accordingly on the final part has been covered. However, the quality of layers is also related to the equipment and other processing parameters that is involved in the test. It is important to note that the effective layer thickness is limited to the energy absorption through the layer. This implies that presence of very coarse particles is not beneficial in layer-based AM process as coarse powders increase the effective layer thickness, which results into less absorption of energy through underlying surfaces. This problem hinders the full melting of particles and accordingly causes inhomogeneity and incomplete fusion. It has been reported that this flaw can end up decreasing ductility in the final part [98]. Therefore, it is expected that reducing the gap size enhances the sinterability, density and surface quality of final part [63, 172]. Typical layer thickness that is currently used in AM is approximately between 20 μm to 150 μm for SLM method [102, 173-175], 50 to 200 μm for EBM method [102, 176] and 40 to 1000 μm for LMD process [102, 173, 177]. In order to have all particles of the batch on the build plate it is expected to have a gap size greater than the maximum particle size. However, in reality other processing conditions such as speed, spreading device and environment may prevent this demand to occur [45, 114]. In order to avoid sintering failure of large particles, it is recommended to used fine powders within the size range of 15 μm to 150 μm . It is important to note that although it is desirable to have a batch of powder with maximum size of 150 but it is also essential to impose a limit for minimum particle size in the PSD to avoid agglomeration and poor flowability [111, 113]. As concluded by Abd-Elghany, increasing the layer thickness, decreases the density within the layers (after sintering) and therefore reduces the density of final steel part. It is further reported that by increasing the layer thickness, surface roughness

of the final part increases as larger particles on the spread layer are not fully melted [178]. Ahmed et al. proposed a simple technique for assessing spreadability of gas-atomised 316 L stainless steel particles in AM. It has been established that the frequency of empty patches increases significantly with smaller gap sizes. In agreement, Nan et al. analysed the transient jamming of irregular stainless steel powders. According to the author, mechanical arching and transient jamming are the output of very thin gap sizes and consequently weakens the bonding between the particles during the sintering phase which significantly reduces the quality of the final part [179-181]. The probability of formation and length of empty patches increases when the gap size decreases. On the other hand, spreading through a large gap size reduces the dimensional accuracy of final part. It is recommended by the author that application of an appropriate gap size with respect to the number based D90 of the batch, can reduce the chance of transient jamming [181]. However, it is suggested by Fayazfar et al. that smaller gap size improves the laser interaction which results into a bounded layer. It is further added; since most of the layered base AM processes require very thin layer of powder, improving the flowability of the powders is a suitable solution to compensate the drawbacks of small gap sizes [7].

2.4.2 Spreading Velocity

Experimental studies regarding the effect of blade velocity on the final AM part is limited. It is described by Abd-Elghany et al. that the interaction between the spreader and 304L stainless steel powders in SLM process has a considerable influence on the solid density of final parts [178]. Zhang et al. conducted a DEM simulation study to investigate the effect of roller-spreading on the powder bed density and it has been concluded that when translational velocity of roller increases powder bed density decreases. This problem results into defects such as inner holes and poor performance of AM parts [182]. According to Haeri et al. [146] and Parteli and Poschel [183], higher transitional velocity of the roller spreader results in larger surface roughness and smaller packing fraction of the layer, hence, lower bed quality. This consequently reduces the surface quality and density of the final part [184]. In an agreement with the previous statements, Parteli and Poschel, also confirmed that increase in blade velocity adversely impacts the powder packing and creates undesirable voids between the deposited powders due to the limited time for particles to fill the voids [183]. Furthermore, Meier et al. stated that mean layer thickness decreases due to the dynamic powder post-flow when the blade velocity increases which ultimately reduce the powder layer quality [171]. Therefore, it is expected that physical and mechanical properties of final part alongside its surface finish reduces when spreading velocity increases.

Increase in blade velocity will also reduce the coordination number mainly because force and pressure of the moving particles in the powder heap increases which increases the chance of collision between the particles. As a result, the packing fraction is negatively affected which reduces the quality of the final part. It is also suggested by the other that the surface quality decreases when spreading speed increases [185]. Furthermore, when the spread velocity increases the probability of vibration also increases that negatively impacts the spread layer [186, 187].

It has been agreed by many authors that low transitional speed results into higher overall packing fraction and authors also confirm that a higher spreader velocity will not only result into a lower packing density but also increase surface roughness on the deposited layer [146, 175, 183, 186]. Although increasing the blade velocity may deteriorate the quality of the final part, it is important to consider that in order to reduce the production time and achieving an efficient throughput, it is necessary to increase the speed of spreading. Thus, it is essential to apply an appropriate blade speed that suits the application and purpose of produced part [175, 188].

2.4.3 Spreader Type and Design

Design, material and type of the spreader can change the powder deposition process and spread behaviour of powders. However, impact of spreading processes is not fully understood through the literature and it is important to note that although some post processing methods such as grinding and polishing may improve the defects that may arise through deposition and spreading processes, but understanding the influential spreading parameters would significantly reduce the cost and time in AM part production [189]. Beitz et al. evaluated the effect of blade geometry on surface roughness of PA12 powder bed in low-cost SLS. The findings show that, shape of the blade has a significant impact on the surface quality and density of the bed. A flat-bottomed blade provides better results compared to sharp and slightly rounded end blades. This is mainly because the compression induced by greater horizontal contact zones between the bed and blade lead to a more uniform and dense powder bed. It is also obtained that direction of deposition also influence the tensile strength and fracture strain of final part; such that the tensile and fracture strain of the specimen that is tested through the deposition direction is considerably higher compared to the values which is obtained within

the perpendicular direction of deposition. According to the author this result is mainly due to more contact of particles through the deposition direction and consequently higher sintering in that direction. But surface quality of the final part did not defer with respect to deposition direction [189]. Furthermore, Haeri designed an optimised blade in his DEM study to achieve the lowest void fraction, which is believed to be a successful substitute compared to complex spreaders. Surprisingly, it has been found that although volume fraction of the bed that is generated by the optimised blade is slightly lower than a roller at low velocities, but by increasing the blade velocity the volume fraction of the layer improves. This could significantly be beneficial since an enhanced final part can be produced in less time [190]. Haeri et al. has done a further study on rod shaped polymers which found that roller type spreader outperforms a blade as the blade has less contact with the bed resulting into particle dragging. This ultimately degrades the bed quality which is generally due to the contact dynamics between the blade and the bed. Evidently, a large area is contacted by the roller that helps a gradual particle rearrangement while for the blade just a single point of the edge is in contact with the bed [146]. Hence, the void fraction of the bed is lower when using the roller rather than blade and this ultimately results into higher density and less porosity of the final part.

Sofia et al. conducted a series of experiments to quantify the effect of powder spreadability on SLS by verifying the effect of powder compression produced by a roller spreading tool on the three batches of different size glass beads. However, it is important to note that this method is not entirely compatible for a blade mechanism as there is no significant compaction on the bed with blade compared to that of a roller mechanism. Results of the test with 3 different mean particle size of 16 μm , 45 μm and 125 μm has been investigated. It has been obtained that rollers which induce compression on the powder bed, has no significant effect on either the resistance or the stiffness for the largest particle size of 125 μm . Conversely, For the smaller particle size (16 μm) there is a significant change in both the stiffness and resistance of final part. Nevertheless, compression force induced by the roller on the average size particles (45 μm) changes the stiffness only, but has no impact on final resistance [191].

However, as stated by Yan et al. the shape of the blade has no negative impact on the packing density when translational speeds of spreading is considerably low [186]. The research of Snow et al. reveals that the material of the blade also has influential impact on the coverage percentage of the bed. It has been found that utilising steel blade results into a better coverage compared to the silicone and ceramic blades [2, 170].

2.4.4 Humidity

Spreading processes in AM industry is commonly conducted in a sealed chamber with an inert environment. However, powder contamination in different phases through production of the powder to the spreading process is an important parameter that requires a precise consideration. Contamination and water adsorption through different steps of powder production and handling may affect the physical and chemical condition of the powder and consequently influence the behaviour of the powder in different processing step of AM production [65, 192]. Humidity rise within the powder, creates liquid bridge inside the bulk powder which can lead to undesirable flow behaviour such as agglomeration [193]. Clearly, relative humidity as an environmental factor plays an important role on density and flowability of the bulk powder. It has been reported that powder can clump together when they are exposed to high humidity and this may reduce the flow and packing behaviour of powders [46]. Creation of liquid bridge within the particles increase the cohesion between particles and consequently results into poor flowability and lower apparent density [194-196]. Moisture content in the metal powder not only decreases the flowability of the powders but also increases the hydrogen porosity through melting processes, which decreases the quality of final part [192, 197]. It is also agreed by Nguyen et al. that the flow behaviour of moist powder can significantly deteriorate during the spreading process which directly decreases the quality of final part [65]. In contrary some studies show that humidity is not necessarily a detrimental factor which negatively influences the packing and flow behaviour of the powder but rather improves the flowability and in return increases the packing density as moisture can act as a lubricant [198]. Moreover moisture content within the electrostatically charged powder provides conductivity that helps to dissipate the charge among the powders [193].

An experimental investigation of AM stainless steel powders conducted by Wu et al. reported that, with increased humidity the powder flow rate decreases [199]. Water vapor adsorption test of three different AlSi7Mg powders by Lerma et al. reveals that water adsorption in the sample with wide PSD biased to higher number of fine particles is higher. It is deduced that fine particles are prone to absorb more moisture due to the higher specific area. High humidity within the sample with greater number of fine particles results into poor flowability and agglomeration and hinder the spreading quality of powder layer, which can create defect in the final part [200]. A similar statement is also approved by Lefebvre et al. which explained that

humidity directly reduces the flowability and apparent density of titanium powders in AM process, specifically if it contains higher ratio of fine particle [201]. Moisture content in the metal powder forms hydrogen porosity during the melting process due to creation of gas bubbles in the melting pool that significantly reduces the homogeneity and density in the aluminium alloy final part in SLM process [197, 202]. It is advised by Li et al. and Weingarten et al. that drying of powders before and during the process considerably reduces the formation of hydrogen pores and subsequently increases the density of final part [203, 204]. A further study by Cordova et al. measures the spreadability of pre-treated and moisturized powders for laser powder bed fusion on metal powders that included, Inconel 718, Ti6Al4V, AlSi10Mg and Scalmalloy. The open and funnel tool that work in a very similar condition of layer spreading in PBF process are proposed by Cordova et al. to measure the spreadability and effect of moisture on flowability. It is stated that the presence of moisture in all samples decreases the flowability and relative density of spread layer. It is also observed that AlSi10Mg which has more roughness and more irregular shape is greatly impacted by humidity compared to other samples and relative density is improved by air drying of Ti6Al4V and AlSi10Mg [192]. However, another study by Bauer et al. showed that even with spherical metal particles, increase in humidity leads to decrease of flowability [205]. It is also gathered by Cordova et al. that existence of satellites and surface roughness on one of the samples allows a higher amount of water to be adsorbed. It is also added that humidity is one of the factors that negatively impacts the repeatability of the spreading [192].

Nevertheless, humidity in EBM method may not be an influential factor as EBM processes takes place in a vacuum environment [206].

2.5 Definition of Spreadability Within the Literature

In many previous researches, spreadability has been addressed as flowability [59, 65, 67, 113, 123, 130, 207-212]. However, accepting flowability as a reliable metric of spreadability is not a promising method, as flow behaviour of powders within the flowability measurement devices is not an exact resemblance of powder flow during spreading in AM machines [1, 3, 192, 213-215]. For instance, Cordova et al. suggested that measure of flowability does not accurately represent the spreading mechanisms. However, due to the necessity of producing thin layers in AM process, the flowability measures has a significant influence and needs to be accounted for [192].

On the other hand, powder spreadability is defined as a flowability measurement by Spierings et al. where they suggest that analysis of powder flowability is a critical requirement in order to predict the quality of spread layer and consequently final part [63].

There are some attempts on defining the term “spreadability” by different authors in both experimental and simulation fields.

Snow et al. established viable powder spreadability metrics with correlating the spread behaviour of powder and characterisation of powder. Spreadability is described as viable metrics related to the percentage of coverage on the built plate, the powder deposition rate and the rate of change of the avalanching angle. Layer thickness, spreading speed, spreader material and powder quality are the main input factors and powder’s angle of repose is considered as an indicative of powder spreadability in this work. It is concluded that increasing the recoating speed results into an increase of deposition rate and the rate of change of the avalanche angle. It also suggested that recoating speed does not have a direct impact on the build plate coverage while blade material has a notable effect. It is noted that the in-depth quantification of packing fraction is missing in this work [2, 170]. Furthermore, a method has been presented by Ahmed et al. which assessed powder spreadability by defining the term as "complex characteristic features of a powder which allows the powder to be spread uniformly as a thin layer of a few multiples of particle size without the formation of any empty patches, presence of agglomerates and rough surfaces." In this paper jamming and empty patches are the measures with respect to the length, area and location of empty patches. It has been gathered that the frequency and size of the empty patches, decreases with increasing gap heights (thickness of spread layer). However, analysis of packing fraction has not been covered in this study [3].

Further experimental investigation by Sophia et al. quantifies the effects of powder spreadability on selective laser sintering process (SLS) by verifying the effect of powder compression produced by a roller spreading tool. It is concluded that with the increase in the particle size, the effect of compression process decreases. It has also been added that resistance of sintered product increases by utilising fine particles to be compressed. However quantification of packing fraction lacks in this study but instead the strength and stiffness is assessed as a measurement of fraction and porosity [191].

The review of Drake et al. suggests that movement of powder has a direct impact on the spread behaviour on the build plate and states that spreadability is the “ability of the powder to spread over itself, its interaction with build plate material, its interaction with the recoater blade or

roller, as well as its interaction with partially built parts within the build chamber". It has been indicated that powders characteristics effects the movement of a particle while spreads over another [216].

Numerical simulation in cooperation with experimental methods is both time and labour efficient to obtain reliable results. For instance, the discrete element method (DEM) as a particle-scale numerical approximation is a solution for simulating the continuous and discontinues behaviour of particles. However, simulation is not precise and may lead to uncertainty as it is generally based on assumptions where an experimental validation is required. Moreover, depending on the model and skills of the modeller it is sometimes very time consuming and expensive [217].

Nan et al. performed a DEM study of jamming during particle spreading in additive manufacturing. The term spreadability is not explicitly defined in this paper but the measure of spreading introduced by this work is in terms of particle dynamics and transient jamming. The jamming is created by the formation of empty patches. It has been found that particles velocity behind the blade decreases when the gap height increases. It is also concluded that by setting a narrower gap height the size of empty patches increases, while the probability of jamming decreases with a greater gap heights [181].

DEM study by Xiang et al. does not directly define the term spreadability, however, packing density and coordination number is calculated in order to evaluate the powder packing. It is gathered that increase in bed height (gap size) results into an increase of packing density and coordination number. Moreover, it is stated that compression on the layer results into an increase in density and coordination number, while it counterbalances the effect of layer thickness. Furthermore, it is shown that utilising mono-sized distribution of powders improves the packing density and coordination number [218].

Parteli and Poschel conducted a DEM study to investigate the spreading behaviour of powders by utilising a cylindrical roller. Results of this study for the spreading of irregular particles indicates that the quality of surface (surface roughness) decreases while velocity of the roller increase [183].

Desai et al. performed a simulation to present a process map that is derived from a physics model-based machine learning. It stated that spreadability of AM powders is quantified through the spread layer properties such as mass of spread layer, spread throughput, porosity of deposited layer and roughness of the spread layer. The spread layer roughness and porosity increases with increased magnitude of the rotational speed [188].

A further DEM powder spreading simulations of rod-shaped polymers is used by Haeri et.al. revealed that utilising roller as a spreader increases the quality of spread layer because compaction of roller reduces the possibility of void creations compared to the spreader blades. The term spreadability is not explicitly defined in this work but rather packing fraction is considered as a measurement of spread layer quality [146]. In addition, a further study is implemented by the same author where a new optimised blade is designed to create a layer with volume fraction close to that of a roller. Surprisingly, in contrast with the majority of the previous studies, it has been found that although packing fraction of the layer in lower spread velocity is slightly lower compared to a normal roller, the optimised blade presents less sensitivity to changes in speed. Increasing the velocity of the optimised blade results into an increase in the volume fraction. This is an innovative achievement as it significantly improves the time efficiency of the processes [190].

Fouda et al. performed a simulation by using the commercial DEM software EDEM[®]. In this work spherical, mono-sized, non-cohesive particle is used for spreading. A vertical blade, powder heap and build plate is modelled as the spreading system in this study while the effect of layer thickness (gap size) and mean normalised velocity in the shear layer is investigated. It is reported that packing fraction of deposited layer is lower than packing fraction of the initial powder heap and this reduction is mainly due to three mechanism. The first mechanism is explained as the shear-induced dilation due to movement of particles by the blade at the initial point. The second mechanism is due to the dilation of powder when it passes through the gap and finally the third mechanism is caused by the movement of particles after passing the blade (at the back of the spreader) due to the inertia. It has been observed that the packing density of the layer is directly influenced by the blade velocity and the gap size. Increase in gap sizes and a decrease in blade velocity results into an increase of packing fraction. However, it is notable that, although mono-sized spheres as a single parameter is used for simplification in this simulation, this would create an uncertainty as it is not a true resemblance of a powder batch in real AM processes. It should be considered that using mono-size sphere powder could potentially lead to a desirable packing fractions that is not necessarily linked with the packing fraction of the actual spreading process [175].

Critical influences of particle size and adhesion on the powder layer uniformity is studied by Meier et al. It has been described that the quality of the spread layer is measured by the packing density and surface uniformity. The results of this simulation show that decrease in packing fraction and non-uniform surface layers occurred by a decrease in particle size and increase in

cohesiveness. It further added that reduction in the adhesive interaction of particles with the recoating blade and substrate will improve the surface uniformity of cohesive powders. Furthermore, increase in nominal layer thickness increases the quality of the layer and mean layer thickness decreases due to the dynamic powder post-flow when the blade velocity increases [171].

Packing quality of stainless steel 316L powder layer during counter-rolling-type powder spreading process has also been studied by Chen et al. It is gathered that the packing layer density decreases when the spreading speed increases and on the other hand the layer surface roughness and the rate of increasing surface roughness rises when the spread velocity increases. Also, when the spread velocity decreases the friction between the particle and build plate increases, which hinders the drag force between particles and the roller. This results in particles to reside on the build plate without any movement, however, increasing the speed has an inverse effect. This means by increasing the spreading speed the drag forces of the roller overcomes the friction forces, and consequently increases the unconfined movement of particles crossing the gap and particles will keep moving before they completely stop, which generates a loose powder layer. It is stated that the packing quality of the layer reduces when the spreading speed increases, and this is mainly due to an increase of particles collision force. It is further added that coordination number of the powder pile decreases when spreading speed increases which causes a looser powder pile and therefore reduces the packing quality of the layer [185].

2.6 Knowledge Gap Regarding the Spreadability of Powders Within the Literature

In summary, cost, labour and time are significant inhibitors of conducting experimental work to measure “spreadability” in AM, hence there is a solid gap of knowledge regarding spreadability in the literature. It has been found that the most common definition of spreadability that is outlined by authors revolves around powder characterisation, packing fraction and the quality of spread layer while a standard technique for predicting the spreadability of powders in the AM process is lacking [2]. Majority of previous studies has separately focused on the powder quality and process parameters while a parallel investigation of both parameter on the spread layer and subsequently the final product is lacking. Although in many of the earlier works, flowability of powder as an important indicator of powder quality is represented as spreadability but there is no direct correlation between these two terms [3]. This is mainly because due to the dynamic nature of powder in the spreading processes; the

static flowability measures such as angle of repose does not necessarily imitate the true flow behaviour of powders during spreading. Moreover, even dynamic measures of flowability such as FT4 powder rheometer does not accurately resemble the spreading process.

Moreover, investigations regarding the effect of process parameters such as gap size, blade speed and process condition on the deposited layer and final product is very limited. Studies that investigate the in-process parameters do not cover the precise physics of powder spreading. For instance, in some researches such as Snow et al.[170] the influence of gap size and spread velocity on the coverage area is reported but the process of measuring the packing density is not specifically covered. Moreover, Ahmed et al.[3] may quantify the jamming and empty patches on the spread layer by utilising different gap sizes but still the measurement of packing density and coverage area are not reported. It is also notable that the effect of environmental condition on the process of spreading is not sufficiently covered in the current literature. Despite the fact that simulation-based studies are more flexible to measure “spreadability” in AM, but experimental validations are crucially essential.

In this work series of experiments is conducted by using an in-house spreading rig to quantitatively and qualitatively evaluate the spreading behaviour of powders in parallel with powder characterisation. The effect of speed and the gap size, between the blade and build plate and humidity has been investigated to achieve reliable results through establishing a standard measurement method for spreadability of powders.

2.7 Summary of Chapter

In this section, the main types of additive manufacturing have been explained in detail that are known as vat photo polymerisation, material extrusion, material jetting, binder jetting, powder bed fusion, direct energy deposition and sheet lamination. Moreover, the different types of powder production and their advantages and disadvantages have been mentioned. As it is derived from Table 1, gas atomisation method is the most suitable type of AM powder production due to excellent metallurgical quality, high powder flow rate due to high sphericity, relatively low cost in high volume production and large supply base. However, satellite presence and wide PSD are the drawbacks of GA method of powder production. Furthermore, powder characterisation and process parameters have been covered in this chapter and their effect on the final product has been gathered from literature. Flowability of the powders, bulk density, size and size distribution, morphology and surface roughness as an individual characteristic are significantly influential in spreading performance of powders while, one can

be impacted from another. For instance, the flowability of powder is highly affected by size, shape and surface of particles. Sphericity significantly improves the flowability, fine powders reduce the flow and particles with rougher surface also reduce the flowability. Moreover, particle size has an impact on tapped and bulk density of powders as larger particles exhibit greater tapped and bulk density due to lower specific surface and easier compaction. In summary, in spread base method of AM, spherical powders, with narrower PSD biased to fine particles and smoother surface can be considered as optimised collection of powders in order to have desirable flow through spreadability and defect free final part. However, it is important to note that a suitable PSD highly depends on the type of manufacturing method and application of final product. For instance, with binder jetting method wider PSD improves the density of final product and with EBM method a range of larger sized particles is required compared to SLM method.

Process parameters during the spreading procedures such as gap size, spread velocity, blade types and environmental conditions are prominent factors that are considerably influential on the spreading behaviour and quality of final part. Although producing a thin layer is desirable in AM processes to increase the laser absorption, spreading of powders through a smaller gap size results into production of layers with lower packing fraction, higher number of empty patches and jamming along the spread layer. Therefore, selecting a suitable gap size is highly related to the application of final product and laser power. However, as previously mentioned in this section increasing the flowability of the feed powder may highly be beneficial to compensate the defects from smaller gap sizes. Speed of spread is also a crucial matter through spreading processes as increasing the spread velocity reduces the packing fraction of the layer and accordingly decreases the density and surface quality of final product. Although increasing the spread velocity degrades the quality of spread layer and final product, production of parts with very low speed is not time and cost efficient as decreasing the speed increases the built and fabrication process time. Therefore, a balance approach for selecting an optimised spread speed is a necessity in AM processes. Spreader material and design may significantly affect the surface quality, uniformity and bulk density of the layer due to variations in powder arrangements and compaction. Moreover, humidity as an environmental factor in powder production, handling and spreading processes significantly impacts the flow and spreading quality of the layers. This is mainly due to moisture bridge within the powder which results into agglomeration and porosity through the layer. However, humidity in EBM method may be of less importance as EBM procedure takes place in a vacuumed condition.

Nevertheless, it is important to note that there is a controversy within the literature that humidity may increase the quality of flow and packing of powders as it has been stated that moisture can act as a lubricant and minimise the static charge among the powders. Therefore, this dispute, forces a demand for further experimental research to draw a conclusion in this regard.

It is necessary to consider that although effect of some factors such as flowability or particle size distributions on the spreading of powders in additive manufacturing may draw more attention within the literature, but all factors are almost equally effective, and they should be assessed in parallel. However, it has been gathered that flowability is an indicator of powder quality since it can be affected by almost all powder properties and processes parameters and accordingly impact the spreading, packing and sinterability of powders in additive manufacturing. It is gathered that for a desirable spreading of powders higher flowability is certainly required but this does not imply that higher degree of flowability necessarily guaranties a desirable spreading as other factors are also influential. However, it is important to note that a desirable degree of flowability for spreading of powders has not been quantitatively defined yet as it is not clear that which measuring device is a definite indicative of flowability in AM process.

CHAPTER THREE

Material and Methodology

3.1 Size and Morphological Properties of Samples

3.2 Measurement of Flowability of Samples

3.3 Mechanical Design of the Rig

3.4 Summary of Chapter

Chapter 3. Material and Methodology

3.1 Size and Morphological Properties of Samples

This project worked on spreading behaviour of two stainless steel samples (SS316L) from the same supplier that have a similar composition but taken from different positions on the phase diagram for powder preparation. They lie on hyper-eutectic and hypo-eutectic points on the phase diagram which has been explained in Section 2.2.5. These powders have been pre-heated at different temperatures up to 1000°C with electron beam powers. However, the beam power was carefully controlled to be low enough to have raw unsintered powders.

The materials have been prepared by researchers from University of Sheffield for the MAPP project. As reported by the supplier both samples are similar in main compositions (FeCrC) but the percentage of minor elements may defer. Both samples are characterised as gas atomised spherical powders with particle size distribution in the range of 15-105µm. Size and morphological characterisation of both samples has been previously measured by Dr Jabbar Gardy at the University of Leeds and is shown in Table 5 and Table 6. Samples are virgin powders, but they have been reused during the spreading process of this project which may deform their surface properties.

Type of Powder	Material	PSD (µm)	D[v,0.9]	Bulk Density (g/cm ³)	Tapped Density (g/cm ³)
Sample 1, Metal Powder	SS316L	15-105	71.88	4.734	5.270
Sample 2, Metal Powder	SS316L	15-105	74.53	4.628	5.147

Table 6: Morphological characteristics of the two samples (v and n denote volume and number based, respectively). (Dr Jabbar Gardy)		
Measurements	Sample 1	Sample 2
CE Diameter D[v,0.05] (μm)	22.097	28.360
CE Diameter D[v,0.1] (μm)	39.599	40.618
CE Diameter D[v,0.5] (μm)	50.739	59.984
CE Diameter D[v,0.9] (μm)	71.878	74.527
CE Diameter D[n,0.05] (μm)	9.832	9.968
CE Diameter D[n,0.1] (μm)	11.66	11.82
CE Diameter D[n,0.5] (μm)	20.00	25.841
CE Diameter D[n,0.9] (μm)	50.739	64.364
HS Circularity D[n,0.05]	0.975	0.975
HS Circularity D[n,0.1]	0.981	0.980
HS Circularity D[n,0.5]	0.989	0.987
HS Circularity D[n,0.9]	0.996	0.994
Convexity D[n,0.05]	0.989	0.989
Convexity D[n,0.1]	0.992	0.992
Convexity D[n,0.5]	0.994	0.995
Convexity D[n,0.9]	0.999	1.000
Aspect Ratio D[n,0.05]	0.926	0.930
Aspect Ratio D[n,0.1]	0.945	0.945
Aspect Ratio D[n,0.5]	0.971	0.970
Aspect Ratio D[n,0.9]	0.994	0.994

Particle size distribution has been carried out by Dr Jabbar Gardy using Morphologi G3 analyser as illustrated in Figure 14 which shows volume-based particle distribution of both samples is similar to some extent. However, some differences have been detected from the graph. For instance, sample 1 has slightly higher fraction of fine particles in the range of 5 to 45 μm while sample two comprises of higher amount of larger particle in the range of 60 to 80 μm . Although PSD of two samples are not significantly different but it is important to note that presence of fine or coarse particle in a given volume could result into differences in the

spreading behaviour of the two batches as shown in Table 6. The results imply that two samples do not have exact similar fraction of particle sizes in their PSD range.

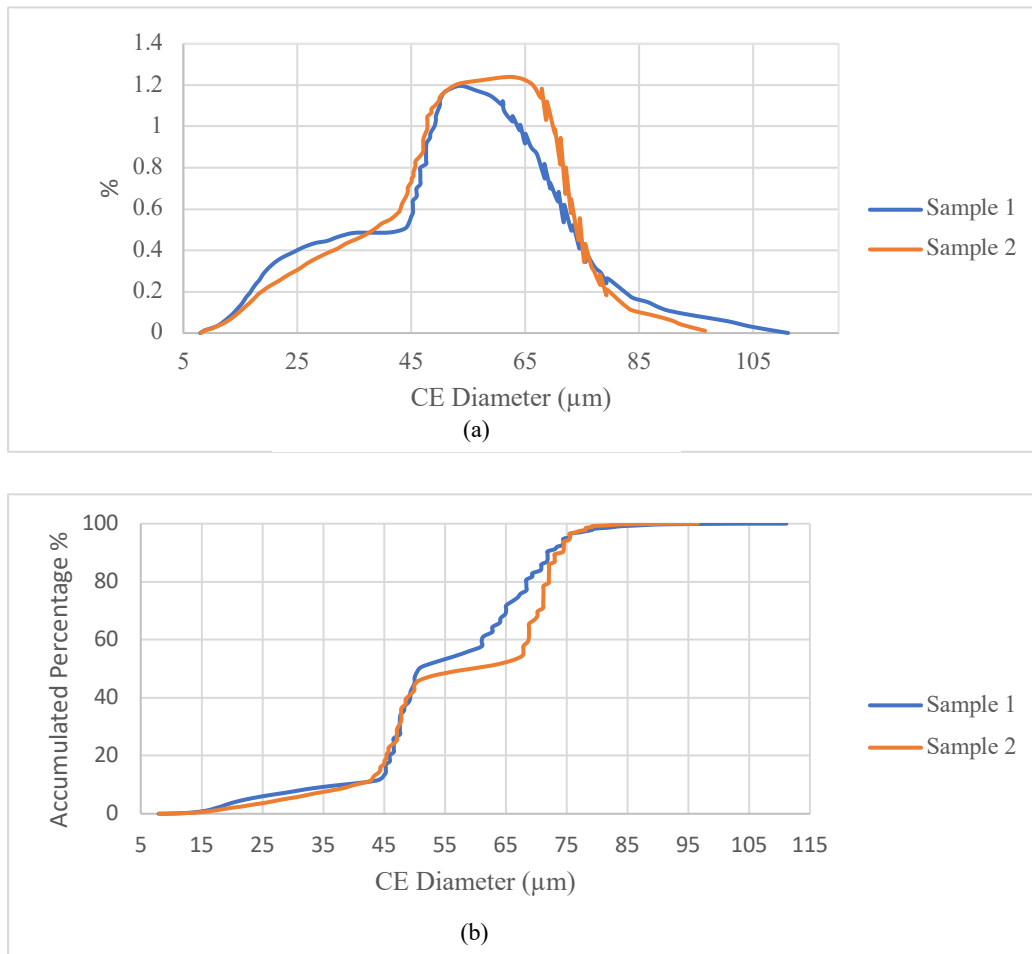


Figure 14: (a) Volume- based particle size distribution and (b) cumulative volume-based particle size distribution.

Shape analysis of two samples has been conducted through Morphologi G3 and scanning electron microscopy (SEM). As it is reported in Table 6 the value of circularity, convexity and aspect ratio for both samples are very close to 1. It has been described in Section 2.3.4 that a perfect sphere has an aspect ratio of 1 and a value of 0 indicates a non-spherical particle. Therefore, both samples can be characterised as spherical particles. This is further approved by qualitative analysis of SEM images taken by Dr Jabbar Gardy that is shown in Figure 15. SEM images of both samples illustrate some cracks, pores and satellite fusion on the surface of the particles. It is also detected that particles are slightly contaminated due to reuse through various experiments. It is important to note that this analysis is performed on few particles among a large number of particles and is not a representation of the whole batch. Therefore, further analysis for greater volume of particle population following adequate sampling selection

methods are necessary to derive a decisive conclusion. Nevertheless, there is no significant differences in the shape characterisation of sample 1 and sample 2.

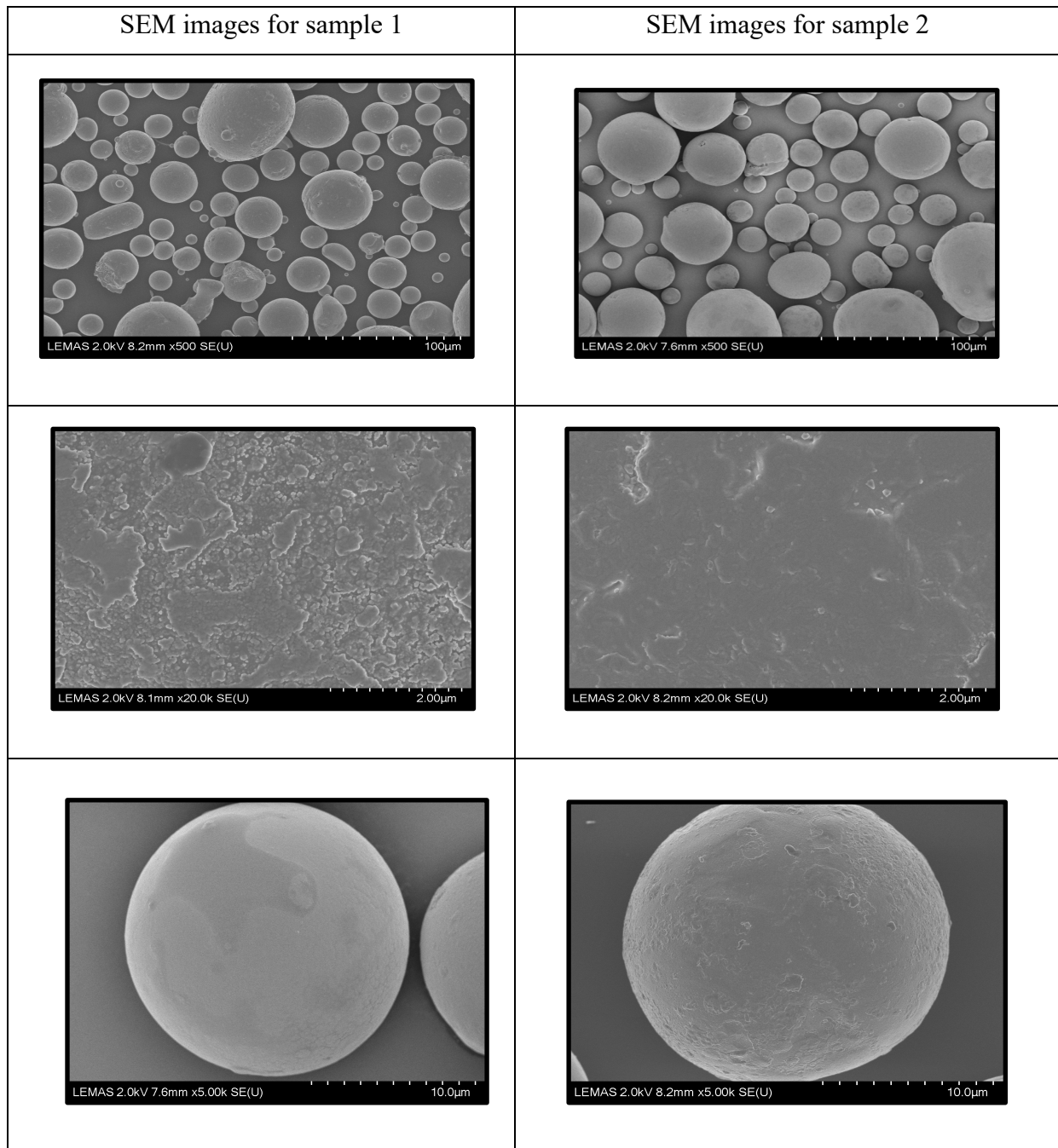


Figure 15: SEM Images of sample 1 and sample 2.

3.2 Measurement of Flowability of Samples

3.2.1 Angle of repose

Angle of repose is a common standard method of static flowability characterisation that is conducted in this work. The process of the measurement is explained in Section 2.3.1.1 and the obtained value of AOR for 200g of both samples has been shown in Table 7. The experiments have been conducted at 48 % relative humidity and 21°C. In order to minimise the error, the experiments are carried out in a stable environmental condition and is repeated by a single user until reaching a minimum variation in iterations. The value of AOR is quite similar for both samples and with respect to the Carr classification in the Table 3, both samples can be considered as very free flowing powders as they both have AOR values lower than 30°. However, sample 1 has a slightly higher value compared to sample 2 which implies that sample 2 is marginally more flowable.

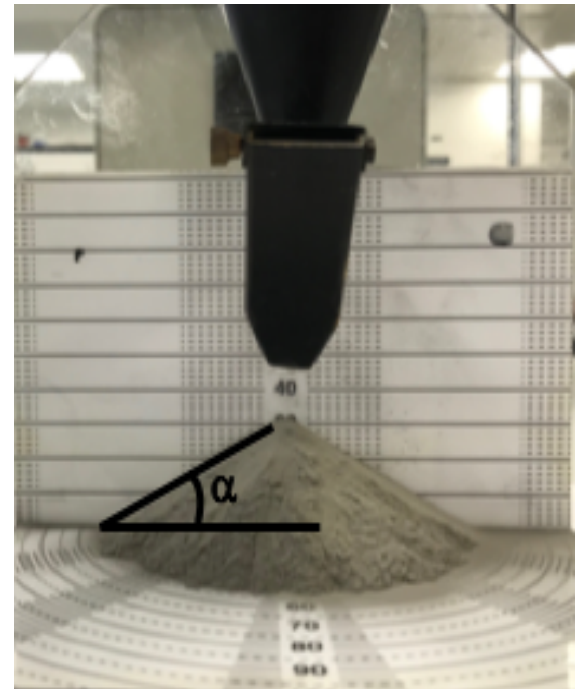


Figure 16: Angle of repose.

3.2.2 Hall flowmeter

Hall flowmeter test is a further flowability test that has been performed in this work. Both samples are examined through different sizes of orifice openings, from 0.5mm to 20 mm diameter while the flow time of the specimen is recorded. The flow time of 100 gram of each sample has been measured several times to eliminate the human error while the flow behaviour of the sample is observed. It has been observed that flow behaviour of sample 1 and sample 2 through the orifice are completely different. Sample 2 smoothly passed through the orifice opening size of 0.5 mm without any external force while sample 1 exhibited no flow through that diameter of the opening. Sample 1 passed through the 5.5 mm opening with tapping force while formation of ratholing is clearly detected and is shown in the Figure 17.

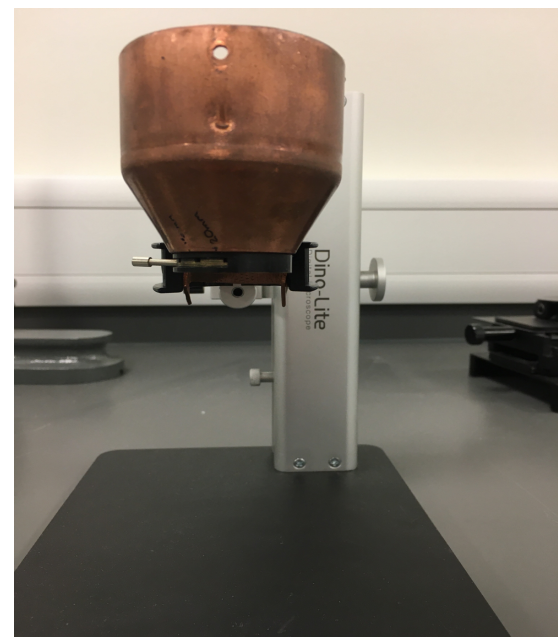
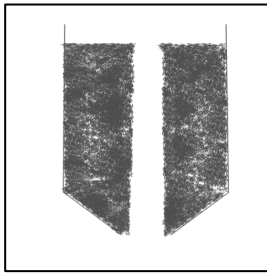


Figure 17: Hall flowmeter.



(a)



(b)



(c)

Figure 18: (a) Side view of ratholing, (b) Ratholing in sample 1, (c) Free flow in Sample 2.

Powder Rheology Metric	Sample 1	Sample 2	Scale of flowability
Tapped Density	5.270	5.147	-
Funnel Test	Rat hole	Free flow	-
Bulk Density	4.734	4.628	-
Angle of Repose (AOR)	29°	27°	Very free flowing
Hausner Ratio (HR)	1.11	1.11	Excellent
Compressibility Index (Carr)	10.17	10.08	Excellent

Table 7 shows the scale of flowability for sample 1 and 2 and it is clearly gathered that both samples have very similar flow patterns except with the Hall flowmeter test. It is noted that based on flowability measures and the classification that has been presented in Table 3 and Table 4, both samples can be categorised as very free flowing powders.

3.2.3 Angle of repose of powder bed

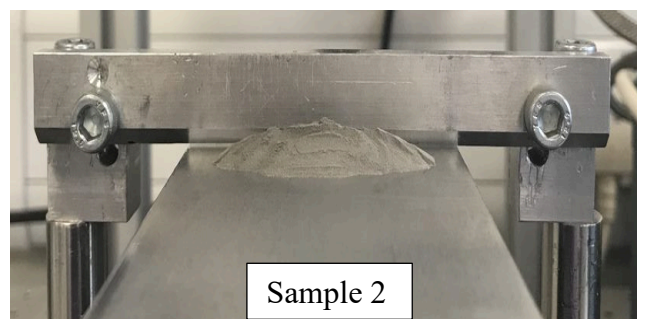
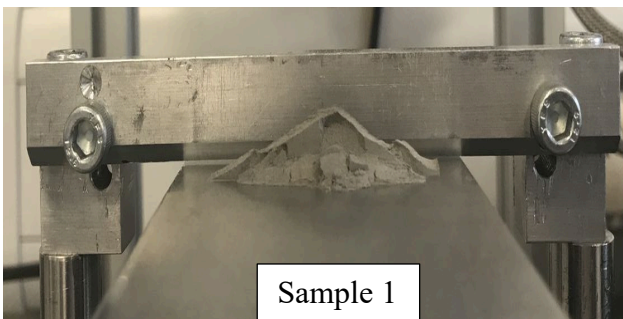


Figure 19: AOR of the powder bed at uncontrolled ambient condition.

The standard test of angle of repose in the laboratory is normally performed with 200g of the sample to form a conical pile. However, due to the size of the rig, the deposited heap on the

build plate is relatively smaller than the heap of 200 g of powder. Therefore, in order to analyse the heap of 7g powder, the captured image of the heap is calibrated through using of ImageJ. The angle of repose for 7g powder is obtained to be compared with the actual AOR angle of 200 g powder and to observe that how angle of repose varies with changing in the mass of powder. Moreover, the form of the heap with 7g powder is qualitatively analysed from the captured images. It is shown in Figure 19 that sample 1 produced a more compacted form of heap while sample 2 looks looser. Slope of both sides of the heap is measured and the average of those values is considered as the final angle of repose for 7g powder bed. AOR values of 7 grams powder bed as shown in Table 8 indicates that sample 2 exhibits lower slope angle, hence it is more flowable compared to sample 1. However, with respect to Carr index in Table 3, AOR of both samples are classified as very free flowing. As previously mentioned in Section 2.3.1, measure of flowability may vary with different testing methods and conditions. Test of AOR is dependent upon the testing process conditions and form of the heap which is created through that method. Hence, although flowability is a good indicator of powder quality but considering flowability as an indicator of spreadability is not conclusive.

Table 8: Angle of repose of 7g powder bed	
Sample1	Sample2
26.3	23.6

3.3 Mechanical design of the rig

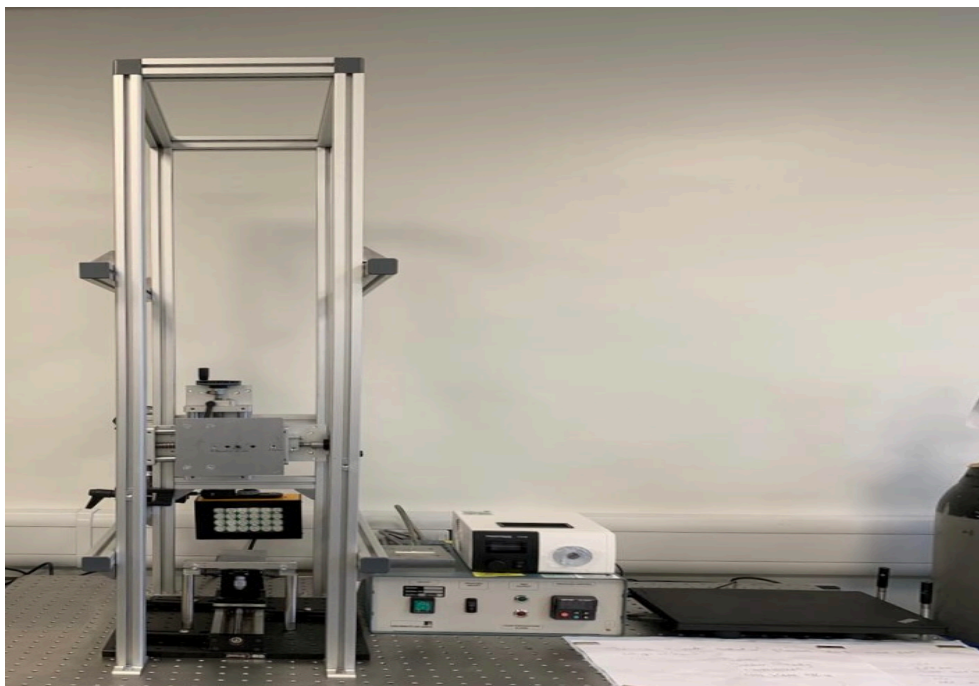
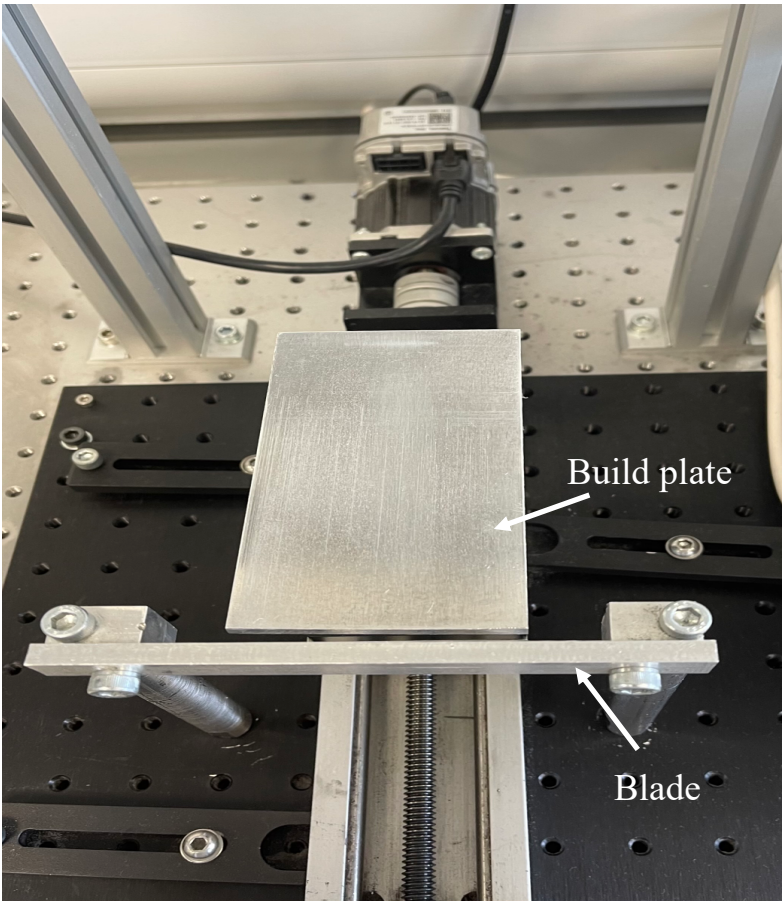


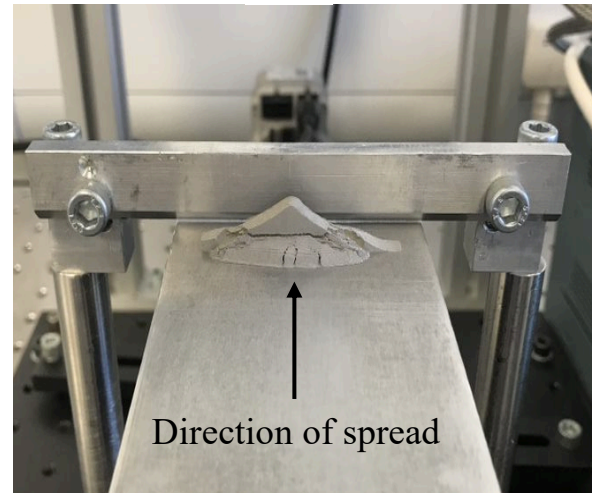
Figure 20: Front view of the rig.



(a)

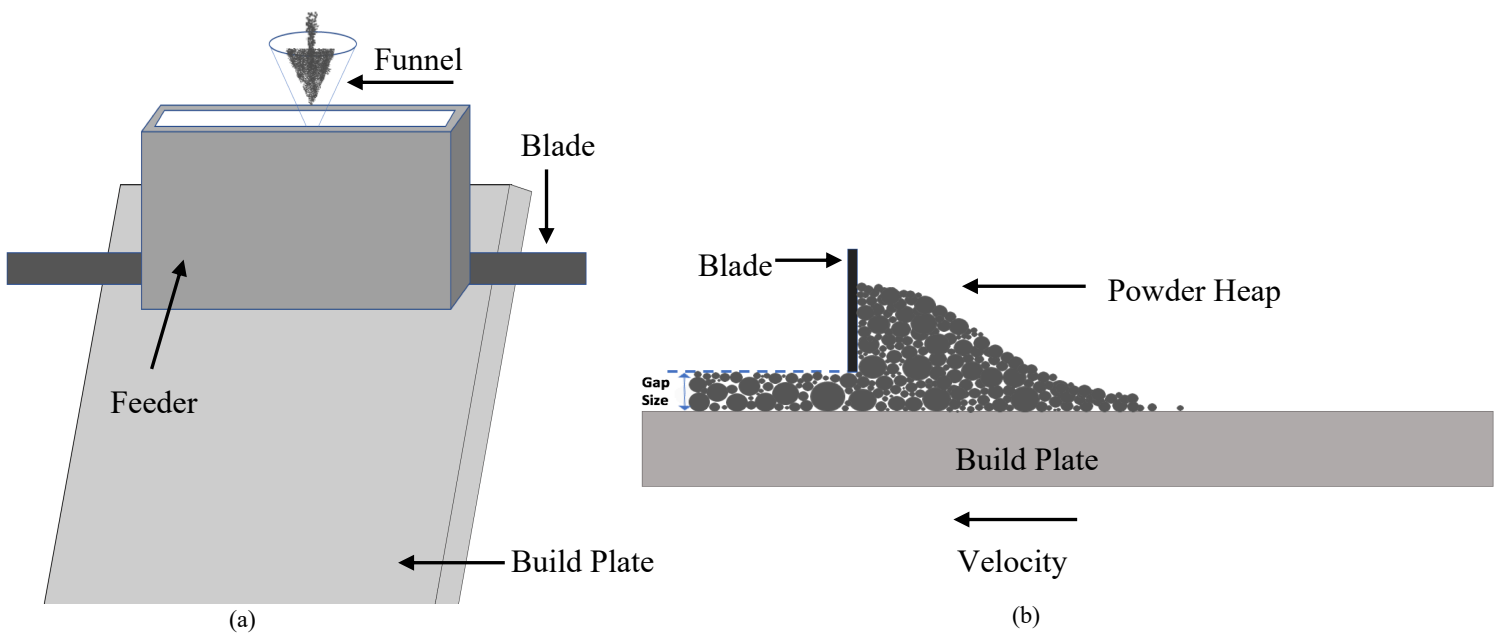


(b)



(c)

Figure 21: (a) Top view of spreading rig, (b) rectangular feeder, (c) Deposited Heap in front of the bevelled blade.



(a)

(b)

Figure 22: (a) Feeding the powder, (b) Initial powder heap- side view.

Figure 20, 21 and 22 illustrates different view of the spreading rig that is subdivided into different sections. The spreading analysis is done through a set of experiments on the rig while different parameters such as spreading speed and gap size are established to observe the spreading behaviour of a single layer of the two samples. The rig consists of a 115mm x 60mm rectangular flat aluminium bed that horizontally moves in the backward and forward motion. The direction and speed of the motion is controlled by the computer that is connected to the motor. The spreading speed of the blade in powder bed AM is commonly up to 150 mm/s [2, 175, 188, 219] hence the spread velocity in this work has been chosen within this range. Four different speed of 50 mm/s, 100 mm/s, 150 mm/s and 200 mm/s are applied in this work. The vertical bevelled blade of the rig is fixed, while the build plate is moving to spread the deposited powder. The gap between the plate and the blade is considered as layer thickness and controlled by a measuring screw under the built plate. The thickness of the gap is measured by different sized thickness gauge assortment. Gap sizes of 51 μm , 102 μm , 191 μm and 318 μm have been chosen based on the D_{90} and the largest particle size of the batch. Gap sizes of 51 μm is smaller than D_{90} and gap size 102 μm is larger than D_{90} but smaller than the largest particle in the batch. Gap sizes 191 μm and 318 μm are both larger than D_{90} and the largest particle in the batch. Each of the samples are experimented under relatively controlled process conditions, where the relative humidity and temperature are recorded. The mass of the powders for each gap size is maintained constant, while speeds has been changed from 50 mm/s to 100 mm/s, 150 mm/s and 200 mm/s.

After fixing the gap size the pre-weighed powder is manually poured through the rectangular feeder to form a conical heap in front of the blade. This process is performed by a single person to minimise the human error. However, it is important to note that a machine-controlled feeding processes certainly improves the accuracy of pouring and heap formation. Due to the design of the rig in this project, collection of the excessive powders from the sides is not possible. Therefore, selection of an adequate mass of powder to create the heap is an important part of the spreading procedure. A suitable mass of powder is selected by trial and error to create a maximum possible coverage on the surface of the plate without powders falling from the sides. The amount of powders that fully cover the built plate without falling from the sides strongly depends on the gap size and speed of spreading and is shown in the Table 9.

After finishing the feeding process, the initial powder heap is settled in front of the blade on the built plate while the feeder is slowly and steadily removed. In this case the powder heap is supported by the built plate from the bottom but is not in contact with the blade at the initial point. In the next step as shown in Figure 21(c) the plate moves backward with a constant

velocity to sweep the powder along the built plate. When the whole length of the built plate passes under the blade, the remained un-spread powder at the end of build plate is collected and weighed to measure the losses. Afterwards, the image of the spread layer profile is captured and saved for further analysis. The quality of the images taken from the digital camera is satisfactory for a visual observation of the spread layer, but a precise assessment of the surface requires high standard imaging techniques. High standard image analysis of the layer is an essential step that can significantly help mitigate the adverse effects of spreading defects and reduces the cost and time of production in additive manufacturing. At the final stage the spread powder is collected from the top of the built plate, weighed and recorded in order to obtain the percentage of spread, mass per area and bulk density of the layer. The amount of collected powder can also be considered as the percentage of spread or percentage of coverage.

3.4 Summary of Chapter

In this chapter the powder characterisation of two samples of stainless steel powders and their spreading processes has been described in detail. It has been gathered that both samples exhibit very similar individual and bulk characteristics such as size distribution, shape, flowability and bulk density. However, the funnel flow test shows a clear variation as sample 1 exhibits ratholing during the measurement while sample 2 easily flows. Initially, it has been assumed that this may be due to cohesion in sample 1. Therefore, many factors such as higher fraction of fine particles, moisture bridge and electrostatic charges may increase the cohesion and be possible factors that cause rathole within sample 1.

The spreading rig has been used for spreading processes of the layers which imitates the industrial powder bed fusion method of AM. An individual layer of powder has been spread on the build plate and for further investigation the layer profile has been captured through use of an overhead camera. Four gap size of 318 μm , 191 μm , 102 μm and 51 μm indicate the thickness of the layer while the experiments has been conducted with different speeds of 50 mm/s, 100 mm/s, 150 mm/s and 200 mm/s. The method in this work has been allocated to measure the combined effect of powder properties and processes parameters on the spreading behaviour of the powders. Furthermore, the percentage of spread, Mass per area and bulk layer density of an individual layer has been obtained to draw a comparison between the spreadability of two different samples that has been explained in detail in next chapters.

CHAPTER FOUR

Effect of Processes Parameters on the Spread Layer of Stainless steel (Velocity, Gap Size, Humidity)

4.1 Spreading Profiles

4.2 Percentage of Spread

4.3 Mass Per Area

4.4 Bulk Layer Density

4.5 Ratio of Layer Bulk Density to Initial Bulk Density

4.6 Dimensionless Shear Rate

4.7 Effect of Humidity on the Spread Layer(conditioning)

4.8 Summary of Chapter

Chapter 4. Effect of Processes Parameters on the Spread Layer of Stainless steel (Velocity, Gap Size, Humidity)

4.1 Spreading Profiles

Mass allocation of feeding powder is the initial issue of the spreading process. By decreasing the gap size, the amount of feeding powder had to be decreased to avoid powder falling from the sides and become contaminated due to limitations of the rig. However, the amount of powder which is going to be poured into the feeder has been obtained by trial and error to ensure that the area and percentage of coverage for all different masses of powders at a specific gap size are fairly close. For instance, the area and percentage of coverage at gap size of 191 μm with 7g of powders are not noticeably different from the values of them with 5g of powders but dropping of powders is prevented with utilising 5g of them.

Nevertheless, it is very important to consider that although decrease of the mass of the powder with decreasing the gap size may not have notable impact on the percentage and coverage of spread but the form of the heap may differ and cause some degree of inaccuracy in results. However, it has been assumed that changes in mass does not considerably impact the formation of the heap.

As previously mentioned, the mass of powder required to be adequate to cover the plate but not fall from the sides. It has been noted by experience through the tests that the highest speed of 200 mm/s is the problematic one, since powders that have been spread at this speed had a higher chance of being scattered or dissipated. Such that a specific amount of powder might effortlessly spread with speed of 50 mm/s or 100 mm/s but scattered with the speed of 200 mm/s. For instance, 8 grams of sample 1 powder with gap size of 318 μm and speed of 200 mm/s, perfectly spreads while with the same amount of mass of sample 2, powders fall from the sides. Nonetheless, for consistency to ensure the accuracy of comparisons, the same amount of mass has been selected for sample 1 and sample 2. The final results of this trial and error is shown in Table 9.

Gap size(μm)	Mass(g)
318	7
191	5
102	3.5
51	3

It is observed through the experiments that spreading profiles for gap size 51 μm exhibits severe jamming and empty patches at all four speeds. This is mainly due to the fact that the D_{90} of both samples are higher than the gap size of 51 μm and as it has been mentioned in Section 2.4.1, in order to have an acceptable spread on the build plate it is expected to have a gap size greater than the D_{90} . Moreover, to have a perfect full spread, it is beneficial to have a gap size larger than the maximum particle size of the PSD. Figure 23 shows the spreading profile of sample 1 with 51 μm gap size at the lowest velocity of 50mm/s. From the profiles of 51 μm it was also observed that at higher speeds of 100mm/s, 150mm/s and 200mm/s, the amount of spread powder on the bed was extremely low to be collected from the surface of the build plate. It is assumed since D_{50} of both samples are higher than 50 μm , 50 percent of particles are not capable of passing through this gap size.

Thus, based on the spreading profile and amount of spread powder on the build plate, the results for gap size of 51 μm is not analysed in this work.



Figure 23 : Spreading profile of gap size 51 μm (sample 1)
Temperature:21-23 $^{\circ}\text{C}$ Humidity:31-38%

The ratio of gap size to D_{90} of both samples has been obtained to demonstrate how many particles are able to pass through the gap above each other at the same time. As shown in Table 10 and Table 11, the ratio is very similar for Sample 1 and 2. As previously mentioned in Section 3.1, the volume based D_{90} of samples 1 and sample 2 are 71.88 μm and 74.53 μm respectively.

Table 10: Ratio of Gap Size to $D[v,0.9]$ for Sample 1.				
Gap size (μm)	318	191	102	51
Gap size/ $D[v,0.9]$	4.42	2.66	1.42	0.71

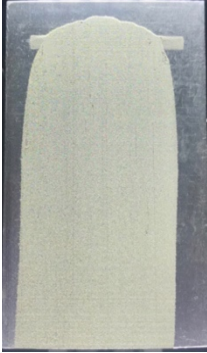
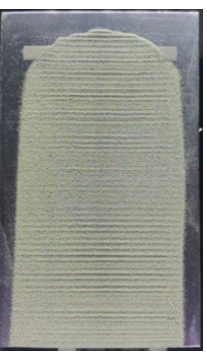
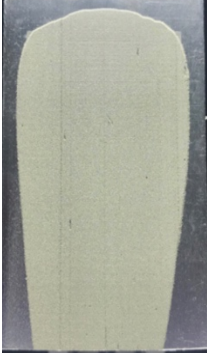
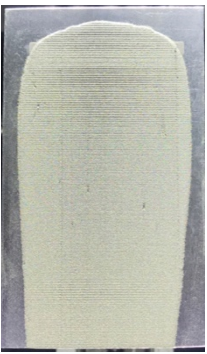
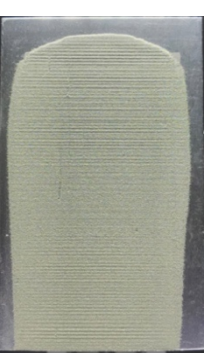
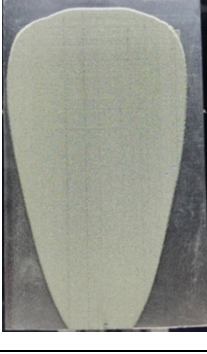
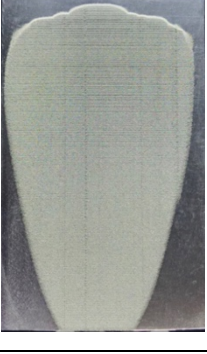
Table 11: Ratio of Gap Size to $D[v,0.9]$ for Sample 2.				
Gap size (μm)	318	191	102	51
Gap size/ $D[v,0.9]$	4.27	2.56	1.37	0.68

Table 12: Spreading profiles of sample 1

Temperature:21-23 °C Humidity:31-38%

	Speed mm/s			
Gap Size (μm)	50	100	150	200
102				NA
191				
318				

Table 13: Spreading profiles of sample 2
 Temperature:21-23 °C Humidity:31-43%

Speed mm/s				
Gap Size (μm)	50	100	150	200
102				
191				
318				

The spreading profile of Sample 1 and sample 2 is shown in the Table 12 and Table 13. The experiments in this work are conducted for a single layer application. It is important to note that the spread quality of a single layer experiment may differ from multi-layer spreading, where the powder is spread on a previously sintered layer. Due to interaction of powders with the previously deposited layer in a multi-layer spreading tests, the new layer might be either uniformly spread or the packing may be disturbed which depends on the surface quality of previous layer. However, in real practice of AM, the new layer is spread on a layer which has been previously sintered. Hence, having more than one layer without sintering the previous layer is not relevant in additive manufacturing. Nevertheless, due to limitation of design of the rig, spreading of multi layers has not been examined in this project.

It is clear that sample 2 exhibits much uniform and homogenous layer in all gap sizes and spread velocities. However, effect of change in gap size and plate speeds is more noticeable in sample 1. It has been gathered that decreasing the gap size in sample 1, significantly reduces the uniformity and continuity of the spread layer but surface layer of sample 2 is less affected by reducing the gap size and speed. It is also observed that the frequency, area and length of empty patches in sample 1 increases by increasing the plate velocity, but this is not been detected for sample 2. At the speed of 200mm/s and gap size of 102 μ m there was no powder of sample 1 collected from the build plate. This can be explained by the fact that with the increase of plate velocity the drag force from the blade increases which leads to empty patches, while with lower spreading speed the friction force between the particles and the build plate may overcome the drag force and consequently particles may stay still after passing under the blade. Increase in the spreading velocity limits the time for particle to pass under the blade, which consequently results into the presence of lower number of spread powders behind the blade. Spreading profiles of sample 1 show that more powders tend to be spread at the sides of the build plate rather than the centre. It is a hypothesis that this may be due to the form of the heap of sample 1. As it can be observed in Figure 21(c) the crown of the heap of Sample 1 is detached from the main body which may possibly collapse and move as a block through the spreading and disturb the packing in the centre of the plate and shifted toward the sides of the plate. However, this assumption requires further analysis with high speed photography.

Furthermore, increase in the speed of the build plate results into increase of waves on the layer of both samples as observed in Table 13. An increase in the speed could results in the vibration

of the bed which can lead to an increase in force and pressure of particles on the moving bed. This could be a potential reason for the wavy surfaces of spread powders at high speeds. This can be however checked in the future work, where the machine vibration could be accurately measured and the wavelength could be compared with that of the spread layer surface.

Interestingly, the area of spread for both samples increases by increasing the gap size, but this is more noticeable with sample 2. The trace of the blade's unevenness on the surface of the layer is also detected on the spreading profile of sample 1, while for sample 2 it is negligible. The probability of this defect may increase when a larger particle or agglomerates of fine and cohesive powders in front of the blade sweep other particles on their way of spreading along the layer. However, as stated by previous researches, this defect may be prevented by using a roller, since roller induces more compaction rather than dragging the particles [146]. It is also assumed that the occurrence of empty patches in the spreading profiles of sample 1 is mainly due to jamming of particles in front of the blade. Since the frequency of empty patches increases by reducing the gap size, this may imply that powders of sample 1 are more prone to agglomerate or clumped together and are not able to pass through the smaller gaps. It is important to note that this may also lead to segregation of particles in the area behind and in front of the blade.

It has been gathered that although powder characteristics of both samples are similar, the spreading behaviour of them are significantly different. As it is explained in Section 3.1 and Section 3.2 measurement of size, shape and flowability of both samples is conducted in this work but there was no specific differentiation to explain the disparity in their spreading profiles. Triboelectric charging test of sample 1 also suggests that there is no difference in charging of the sample during 5 runs of the test. Surprisingly, through the experiments on sample 1 it has been found that increasing the relative humidity from 38% to 54%, the percentage of spread decreases from 79% to 60% while the occurrence of empty patches also increases. Therefore, it drew a conclusion that rise of humidity may explain the disparity in spreading behaviour of sample 1 and sample 2. Hence, spreading behaviour of both samples at gap size of 318 μm and four different speeds of 50 mm/s, 100mm/s, 150 mm/s and 200mm/s at high humidity of 73% has been tested. Several batches of powder with the mass of 7g is contained in the desiccator for more than 24 hours to absorb 73% of humidity and is removed one by one through the tests so that the batch contains a constant humidity in all tests.

Table 14: Spreading profiles of sample 1&2 stored under 73%humidity

Temperature:20-21 °C Stored under 73 % humidity

	Speed mm/s			
	50	100	150	200
Sample 1				
Sample 2				

Comparison of the spreading profiles shows that surface quality of spread layer for sample 1 considerably deteriorated after conditioning the sample with 73% of humidity. But notably, sample 2 exhibits much lower impact when 73% relative humidity is applied to the batch. Spreading profiles of sample 2 with higher humidity also show that when velocity of the build plate reduces, the effect of humidity also reduces. Such that with the velocity of 50mm/s the spreading profile of sample 2 with 73% humidity is almost the same as the profile of sample 2 at uncontrolled ambient condition (i.e. gap size 318 μm and speed of 50 mm/s). Therefore, it has been derived that effect of humidity increases when spreading velocity increases. Throughout the feeding processes of sample 1 at higher humidity, it is observed that tapping is required in order to help the powders pass through the funnel while sample 2 freely flowed. As it has been explained in Section 2.4.4, humidity creates cohesion within the powder batch due

to liquid bridge and powders can clump together. This implies that powders of sample 1 may be more prone to cohesion compared to sample 2. Referring to Section 2.2.5 this may occur due to chemical composition of the sample 1, which is taken from different position on the phase diagram. Moreover, humidity can create agglomeration when finer particles exist in the batch and in an agreement with this fact, it is reported in Section 3.1 that PSD of sample1 contains slightly larger amount of fine particle. Furthermore, reusing of powders for longer periods seems to increase the adverse effect of humidity as powders can absorb moisture for a longer period of time. This is proven through the experiments of all four velocities, when humidity increases the repeatability of the tests decreases and the surface of the spreading profiles deteriorates by repeating the processes.

4.2 Percentage of Spread

The percentage of spread and losses through spreading of both samples has been recorded and shown in Table 15 and Table 16. Percentage of losses has been obtained by measuring the dropped powders after spreading. This value is recorded to detect how much of the powders may scatter or dissipate due to human or machine error. This confirms that the error in measurement of spread percentage is very negligible.

Gap size(μm)	318				191				102			
Velocity(mm/s)	50	100	150	200	50	100	150	200	50	100	150	200
Spread (%)	79.9	72.1	60.9	50.9	43.3	22.3	18.6	12.5	11.06	11.6	7.6	NA
Losses (%)	20.1	27.1	39.1	49.1	56.7	77.7	81.3	87.7	88.9	88.4	92.3	NA

Gap size(μm)	318				191				102			
Velocity(mm/s)	50	100	150	200	50	100	150	200	50	100	150	200
Spread (%)	98.5	97.5	93.1	83.2	82.9	73.9	66.1	61.8	54.9	43.6	36.9	32.5
Losses (%)	1.5	2.5	6.9	16.8	17.1	26.1	33.9	38.2	45.1	56.4	63.1	67.5

Tables above proves that with all gap sizes and speeds, the percentage of spread on the build plate for sample 1 is notably lower than sample 2. However, for both samples, increasing the gap size leads to an increase of percentage of spread while increasing the velocity results into a decrease of this measure. In other words, percentage of spread decreases when the spread velocity increases and decreasing the gap size intensifies this deficiency. Percentage of spread of sample 1 at the lowest gap size of 102 μm and the highest speed of 200 mm/s is zero as there was no powder for collection in this set of process parameters.

Surprisingly, sample 2 exhibits much higher percentage of spread even with the least optimised set of spreading parameter (smallest gap size and highest speed).

However, percentage of spread is not a definite measure of spreadability mainly because in real AM practice, the built plate is fully covered by the powder while the excessive powder would fall off from the base plate after spreading, hence the percentage of spread may not provide beneficial information. Nevertheless, since the design of the rig is not facilitated to be fully covered by the powder, the percentage of spread has been looked and analysed in this project to investigate the spread flux. Therefore, percentage of spread is a useful indicator to assess the effect of different variables such as speed and gap size on the spreading processes in this project.

4.3 Mass Per Area(g/cm^2)

The mass per area (g/cm^2) of each layer is established as an indicator of packing behaviour and is obtained by measuring the mass of spread powder within the area of spread profile that is calculated through ImageJ. As portrayed in Figure 24, after calibrating the image of spread layer the area is calculated and recorded.

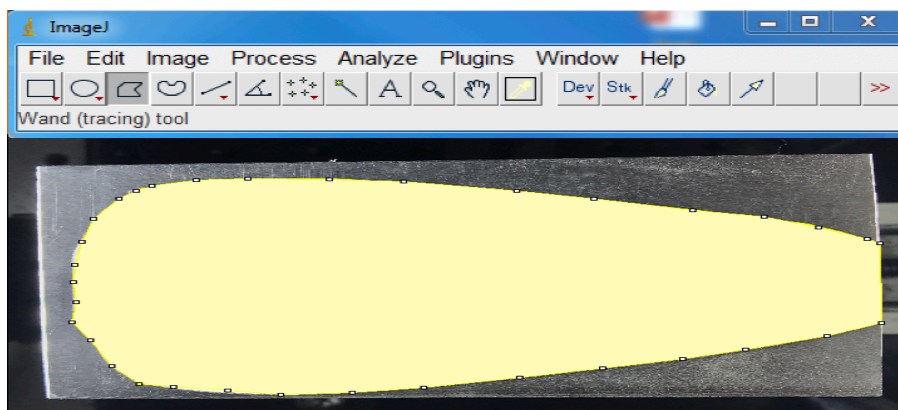


Figure 24: Area of Spread layer through ImageJ.

Figure 25, 26 and 27 portray the graphs of mass per area (g/cm^2) for all gap sizes and velocities. For all gap sizes and velocities mass per area of sample 2 are notably higher compared to sample 1. Moreover, increasing the gap size for both samples increases the amount of powder that passes through the blade and consequently the value of mass per area, while increasing the speed decreases this value.

It is clearly observed that the error bars of sample 2 decreases as the gap sizes increase and at the lowest gap size of $102\ \mu\text{m}$, error bars are much larger. This implies that with sample 2, decreasing the gap size reduces the repeatability through different iterations. Surprisingly, this is not the case for sample 1, as a decrease in the gap size results into a decrease within the error bars. This may be explained by the amount of larger number of fine particles in sample 1, which may indicate better repeatability of powders under smaller gap sizes. However, it is very important to note that although repeatability is an important factor of spreading, other factors such as powder arrangement and surface quality have a higher influence on the quality of the spread layer and are the main indicators of spread quality.

Thus, comparing the values of mass per area for both samples proves that sample 2 is a suitable batch for powder spreading regardless of the repeatability.

It is also obtained that mass per area of both samples are closer together at larger gap size of $318\ \mu\text{m}$ while the distance between the two graphs incrementally increases as the gap size decreases. This implies that decreasing the gap size magnifies the difference of mass per area between the two samples.

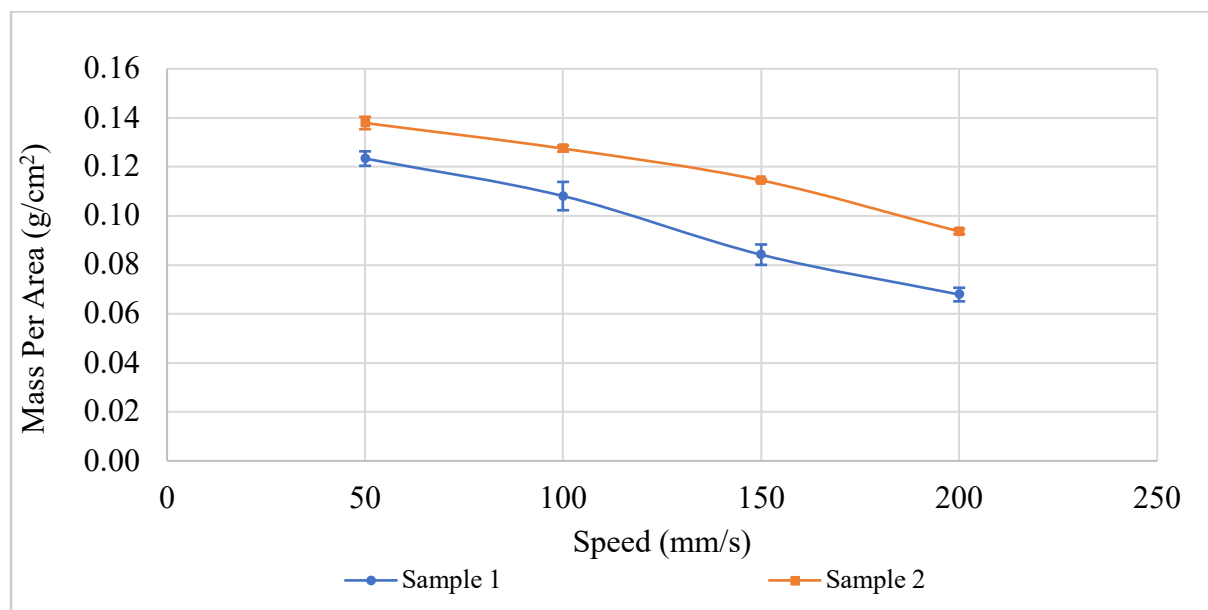


Figure 25: Graph of Speed (mm/s) Against Mass Per Area for Gap size $318\ \mu\text{m}$.

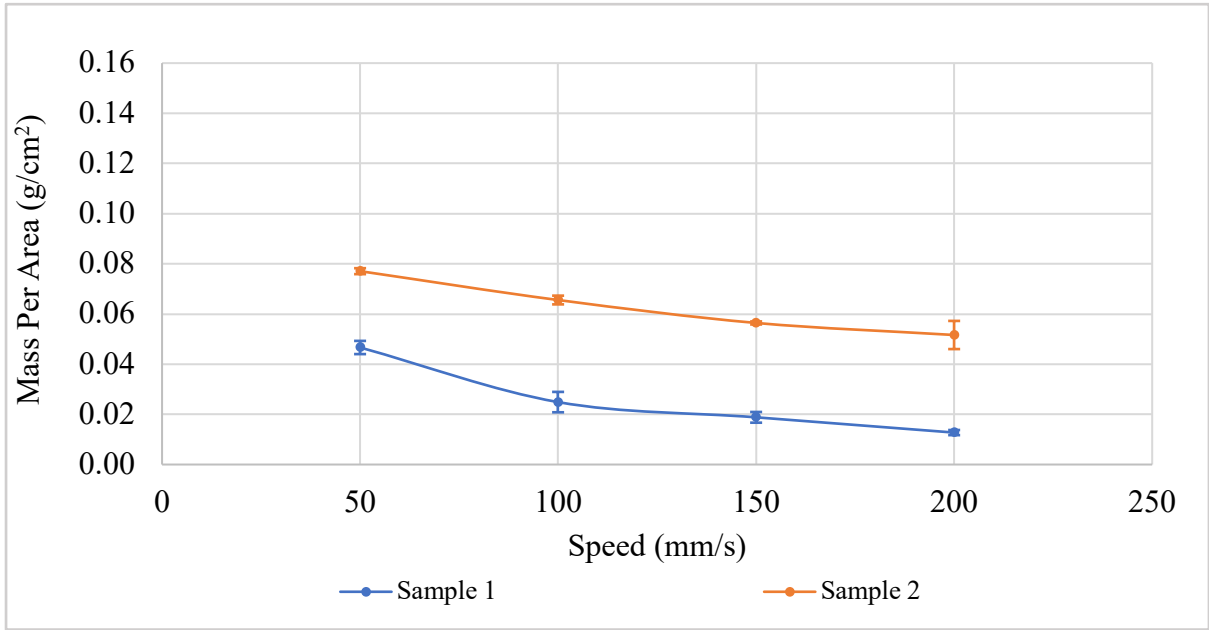


Figure 26: Graph of Speed (mm/s) Against Mass Per Area for Gap size 191 μm .

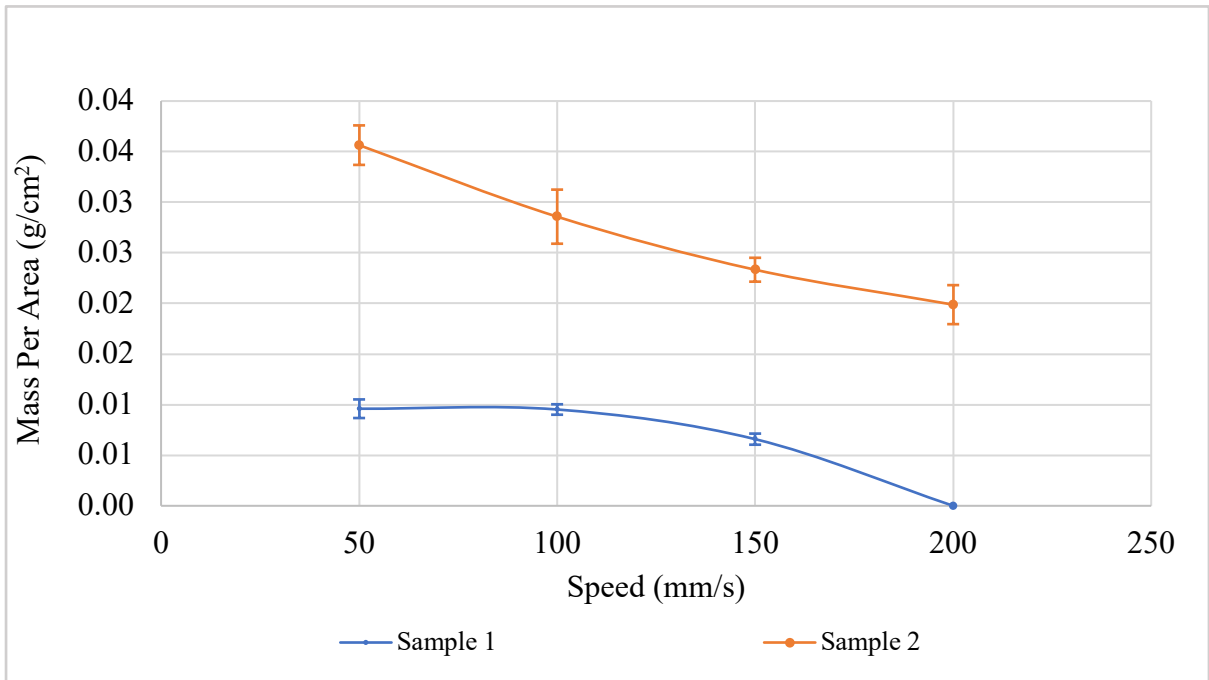


Figure 27: Graph of Speed (mm/s) Against Mass Per Area for Gap size 102 μm .

4.4 Bulk Layer Density

Bulk layer density is a quantitative measure that is established as a metric of spreadability in this project. The effect of speed and gap size between the blade and build plate has been investigated through calculating the bulk layer density in order to evaluate and compare to the initial bulk and tapped density of powders. In order to calculate the bulk layer density, the volume of the spreading profile is obtained through the use of ImageJ software, while the respective gap size is considered as the depth of the layer. Subsequently, the mass of the spread layer gathered from the collected spread powder is divided by the volume to provide the value of bulk layer density. It is important to note that considering the gap size as the thickness of the layer is not very accurate as thickness of the layer may vary along the layer. This requires further consideration in future works to precisely obtain the thickness of the layer. Considering the gap size as the depth of the layer is not truly applicable as the precision of the rig is not sufficient to create an absolute even layer along the whole area of the build plate. Therefore, to eliminate this uncertainty the measure of mass per area (g/cm^2) from the previous section, which is completely independent from the thickness of the layer, is a useful metric that can be used in parallel with the analysis of bulk layer density.

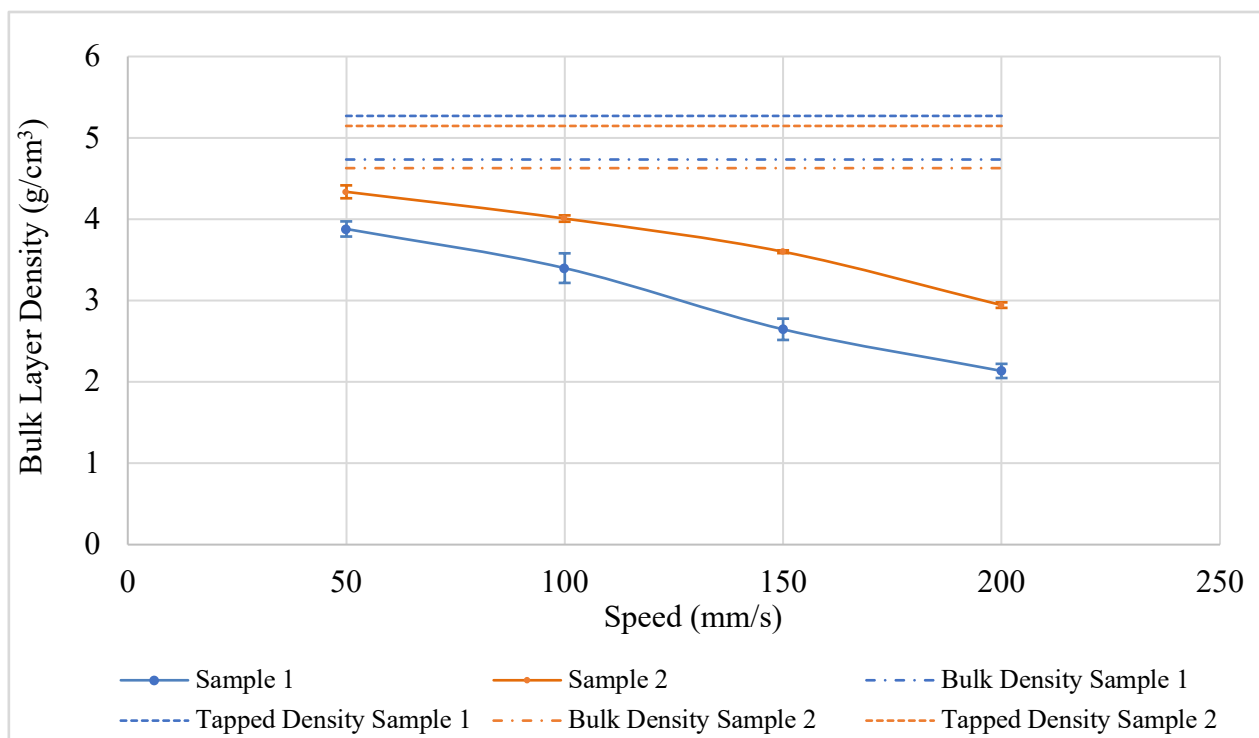


Figure 28: Graph of Speed (mm/s) Against Layer Density for Gap size 318 μm .

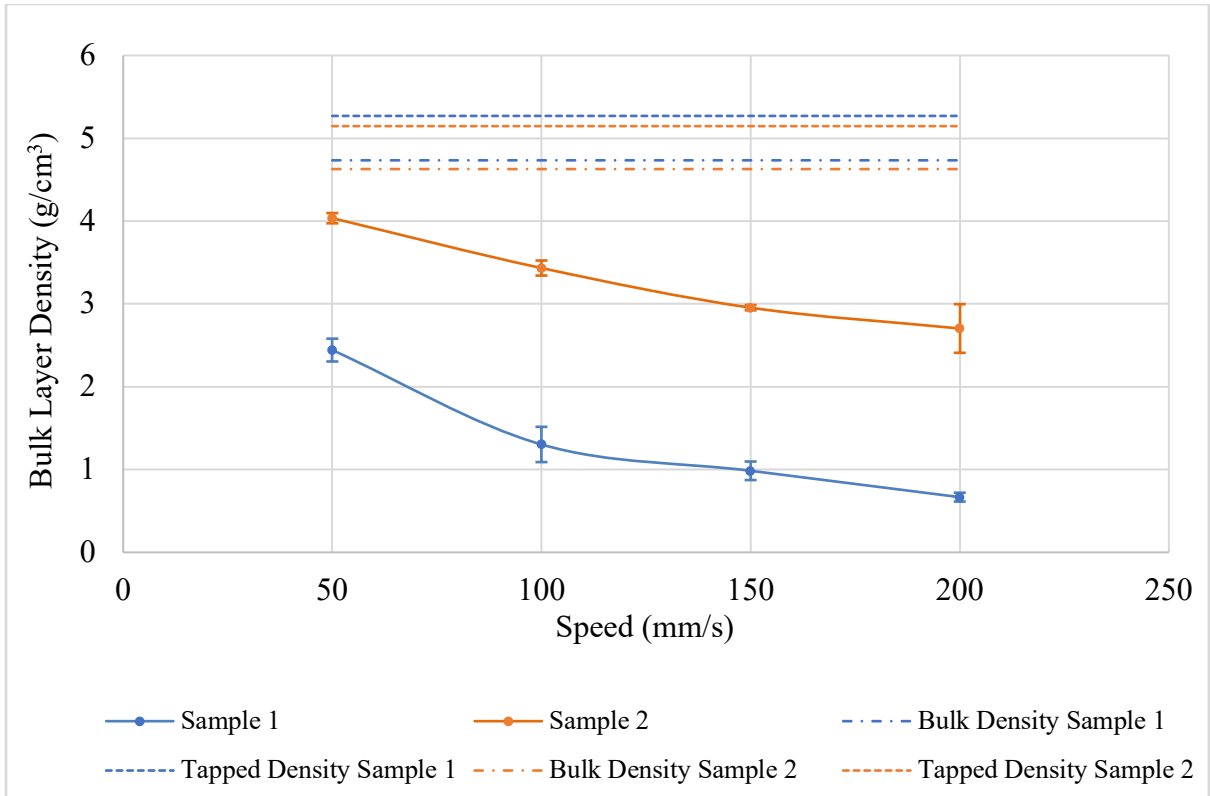


Figure 29: Graph of Speed (mm/s) Against Layer Density for Gap size 191 μm.

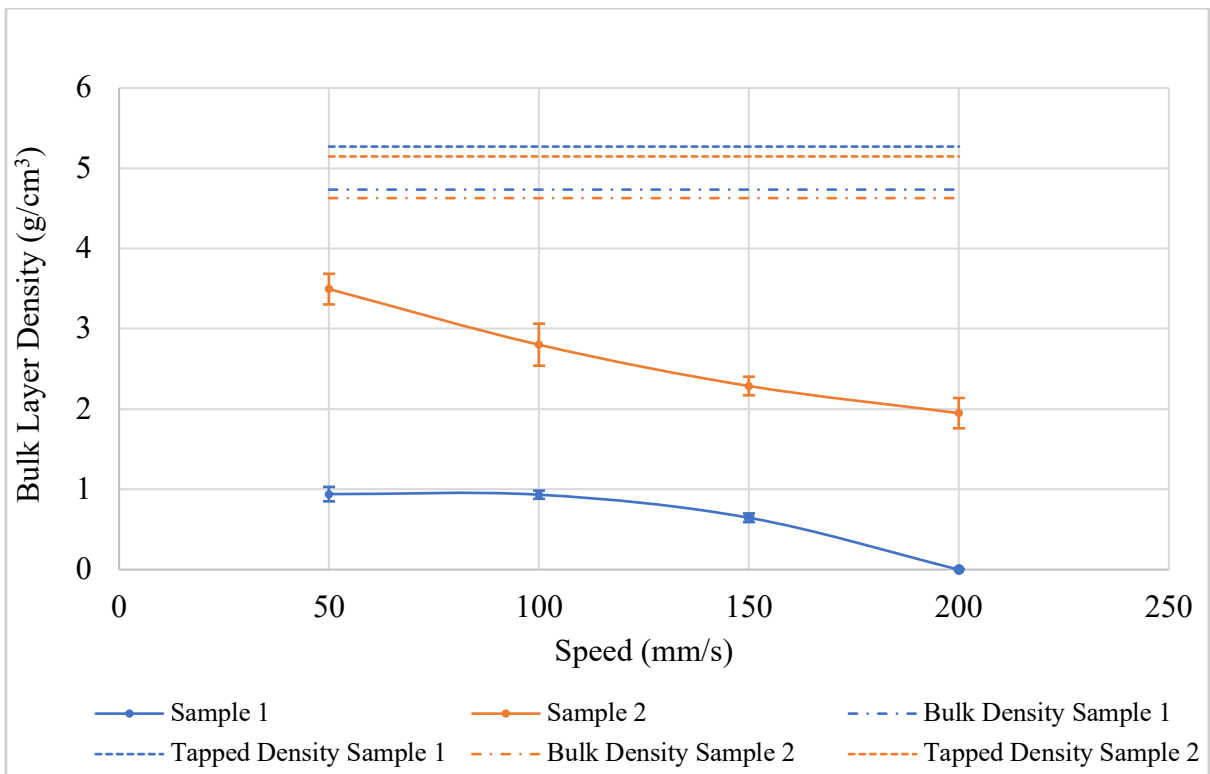


Figure 30: Graph of Speed (mm/s) Against Layer Density for Gap size 102 μm.

Figure 28 illustrates the graph of spreading velocity against bulk layer density for both samples at a constant gap size of 318 μm . As it is shown in the graph, sample 2 clearly has higher bulk layer density at all four velocities compared to sample 1. However, for both samples bulk layer density decreases when the spreading velocity increases. Surprisingly, although both samples have very similar sizes, shapes and flowability characterisation, they achieved very different values of bulk layer density under similar conditions. For sample 2, it is observed that at gap size 318 μm at the lowest velocity of 50 mm/s, the value of bulk layer density is very close to the initial bulk density of the sample. The initial bulk density of sample 2 is 4.628 g/cm³ and the bulk layer density that is achieved after spreading is 4.337 g/cm³.

On the other hand, bulk layer density of sample 1 is not suitable because even at the gap size of 318 μm , which is more than 5 times larger than the D_{90} of the sample along with the lowest speed of 50 mm/s, the bulk layer density is far from the value of initial bulk density of the sample. Bulk layer density of 3.88 g/cm³ has been obtained by spreading sample 1 at the speed of 50 mm/s and gap size 318 μm while the initial density is 4.734 g/cm³. Error bars of sample 1 at gap size 318 μm are larger compared to sample 2, which means the repeatability of the tests for sample 2 is higher than sample 1.

The initial bulk density of the two samples is considered as a benchmark for comparison. In this work the values of the bulk layer density of the two samples are very close, hence they can be directly compared together. The difference between the bulk layer densities of the two samples at gap size of 318 μm decreases when velocity decreases such that at the lowest speed of 50mm/s, the graph of both samples converges together while with increased velocity they gradually diverge. Nevertheless, it has been proven that for both samples at gap size of 318 μm , increasing the speed degrades the bulk layer density.

Graph of gap size 191 μm for both samples is shown in Figure 29 and illustrates; when velocity of spread increases the bulk layer, density decreases. The layer thickness with this gap size is more than 2 times larger than the D_{90} of sample 2 and at the lowest speed of 50 mm/s, the bulk layer density of 4.04 g/cm³ is achieved which is still in a satisfactory range with respect to the initial bulk density of the sample. It is important to note that, the difference of bulk layer densities of the two samples at gap size 191 μm are not dependent to the spread velocity as the distance between them on the graph are rather similar at all four velocities.

For speed of 50 mm/s, 100 mm/s and 150 mm/s the error bars for sample 2 are smaller compared to sample 1 but contrarily, at the highest speed of 200 mm/s, error bars of sample 2 is larger than sample 1. This suggests that repeatability of sample 2 reduces with the highest velocity of 200 mm/s. It is also observed that error bars of sample 1 decreases when the gap size decreases

while for sample 2, the error bars decrease when gap size increases and as mentioned in the previous section this may be due to presence of larger fraction of fine particles in the sample 1.

Figure 30 presents the values of bulk layer density of sample 1 drastically reduces with gap size of 102 μm and it is further impaired when velocity increases. At the speed of 200 mm/s there was no powder collected from the surface of the build plate and accordingly bulk layer density reaches to the value of zero. But the reduction of the bulk layer density of sample 2 by reducing the gap size is not as significant as sample 1.

However, it can be derived that for both samples a packing close to the respective tapped density of them has not been achieved which means none of the samples achieved a fully compacted packing.

In sum, it has been gathered that the optimised bulk layer density is obtained through spreading of sample 2 at the largest gap size of 318 μm and lowest velocity of 50 mm/s while bulk layer densities of sample 1 through all different gap sizes and velocities are not suitable to use.

This means that the most desirable layer density is only achievable at the lowest velocity and largest gap size which certainly is not efficient in terms of cost and time. Thickness of the layer should be carefully selected as absorption of laser energy reduces when the thickness of the layer is not desirably small which significantly reduces the quality of final part. Moreover, since speed is an important factor in additive manufacturing industry, it is essential to understand the application of the end product and establish a balanced approach to choose an optimised spreading velocity and accordingly prioritise the properties that is desired from the final part.

4.5 Ratio of Layer Bulk Density to Initial Bulk Density

The percentage of spread and mass per area may not be a certain indication of spread quality as the quality of the bed is dependent on the packing of it rather than the coverage. As previously mentioned in Section 4.2, in reality there is enough powder to cover the whole area of the bed and the full area of the bed would be covered with the powder. Therefore, packing of powders rather than the percentage or area of coverage is the most accurate indicator of the spread quality. Therefore, a layer packing close to the initial bulk density of the powder is a potential feasible measure of spreadability. Since shape, size and the value of bulk density of sample 1 and sample 2 are very similar (i.e. spherical shape, PSD in the range of 15 μm to

105 μm and bulk density is 4.734 g/cm³ and 4.628 g/cm³ respectively for sample 1 and sample 2), the comparison of them on a same graph would be reasonably reliable.

However, it is important to consider that, if the value of initial bulk density of different samples is not the same, comparing them on a single graph would not be an accurate comparison since each sample has a separate benchmark. This means a sample may show a higher bulk density to other samples on the graph, while it is not close to its initial bulk density as the other sample is. Hence, the ratio of bulk layer density to the initial bulk density would give the most reliable result for this comparison.

Therefore, spreadability index in this work is defined as the ratio of bulk layer density to the initial bulk density of the powder. This implies that the spreadability index should be a value between 0 to 1 where, the value of 1 indicates the maximum packing and 0 indicates no packing. The value over 1 indicates that the layer is over packed and compacted.

It has been reported in the literature, when powders are very compacted in SLS method the depth of sintering reduces as there is not sufficient space for laser to penetrate which may affect the productivity of multi-layered product. Moreover, when powders are over packed the sintered layer under the top layer, may be interacted again by laser and this may damage the layer. It has been stated by the author that in SLS method use of freely poured layer of powders are common rather than compacted layer[220]. However, the degree of compaction in EBM method is not as important as SLS and SLM method, since EBM method takes place in vacuum environment and also the EBM method operates with larger or deeper diffuse spot which can freely penetrated to a compacted layer [221, 222].

Figure 31, 32 and 33 presents the ratio of layer bulk density to initial bulk density of sample 1 and sample 2. It has been obtained that the ratio of layer bulk density to initial bulk density of sample 2 at all gap sizes and velocities are higher than the respective value of sample 1. This value for sample 2 at gap size 318 μm and 191 μm at lowest spread velocity of 50 mm/s is close to 1 which indicates a good packing of this sample while sample 1 exhibits poor packing compare to sample 2. It is shown in the Figures of 31, 32 and 33 that with increasing of speed the distance of this ratio (layer bulk density to initial bulk density) to the value of 1 gradually increases and tends toward zero. This implies that at all gap sizes, the quality of spread decreases when velocity increases.

It is clear that this ratio for sample 1 is considerably low enough to state that the quality of spread for sample 1 at all different gap sizes and spread velocities are not in a satisfactory range.

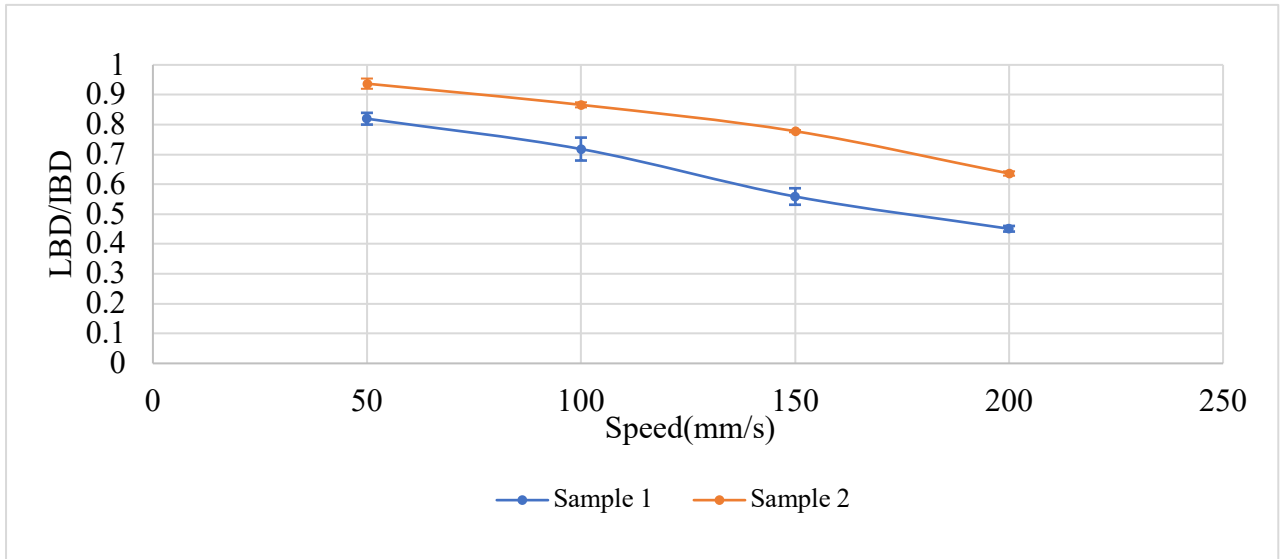


Figure 31: Graph of Layer Bulk Density/Initial Bulk Density against speed for Gap size 318µm.

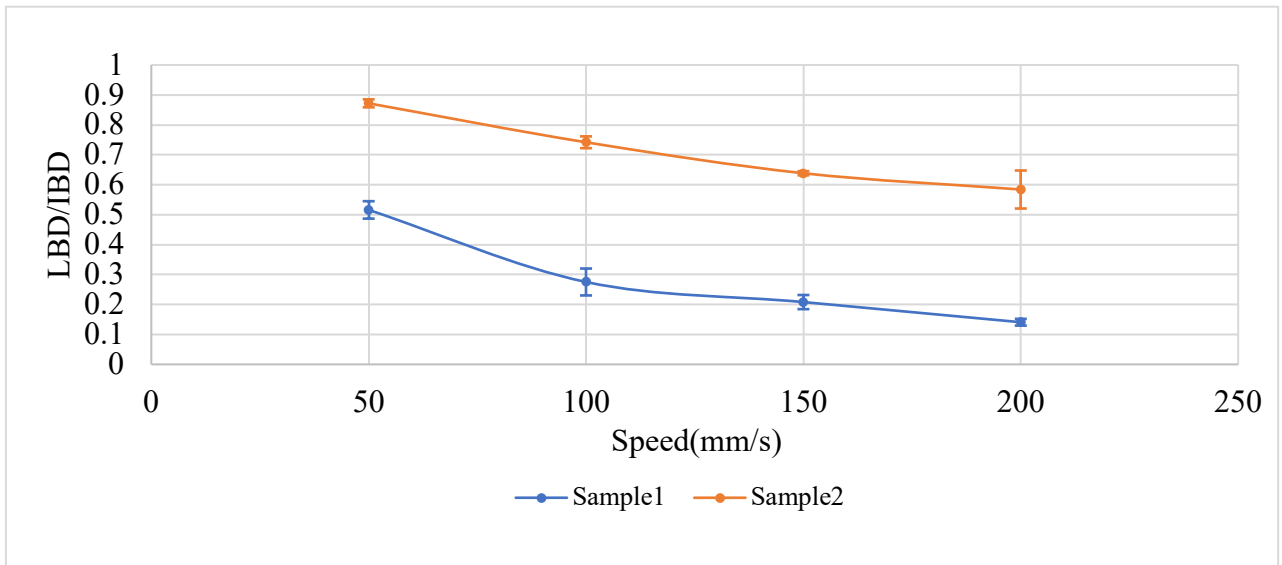


Figure 32: Graph of Layer Bulk Density/Initial Bulk Density against Speed for Gap size 191 µm.

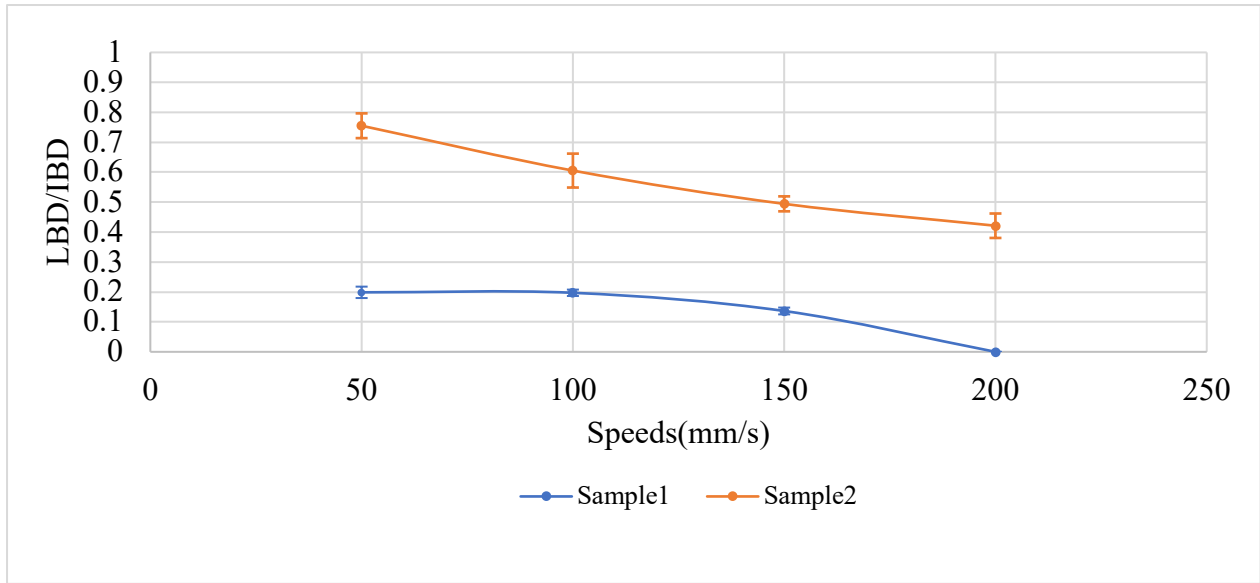


Figure 33: Graph of Layer Bulk Density /Initial Bulk Density against Speed for Gap size 102 μm .

4.6 Dimensionless shear rate

The proposed equation of dimensionless shear rate by Tardos has been used in this work to perform a comparison in terms of the shear strain rate (γ°) as a different representation of previous results in this work. Shear strain rate is defined as a parameter that combines two variables of spread velocity and specific shear zone depth (gap size). Therefore, referring to Section 2.3.1.5 the equation of Tardos has been performed in the form of:

$$\gamma^{\circ*} = \left(\frac{\text{Velocity } (v)}{\text{Gap size } (h)} \right) [D_{50} / g]^{1/2} \quad \text{Equation 5}$$

where all different gap size of 318 μm , 191 μm and 102 μm and different velocity of 50 mm/s, 100 mm/s, 150 mm/s and 200 mm/s has been assessed in the equation while the average particle size (D_{50}) and acceleration of gravity (g) is also used to calculate the dimensionless shear rate of each specific set of data. The obtained value of $\gamma^{\circ*}$ revealed that for all of the spreading sets the flow regimes of both samples lies in the rapid flow region ($\gamma^{\circ*} > 0.3$) due to collisions between the particles. It is clear that dimensionless shear rates of both samples are not located in the quasi-static and intermediate flow region as in these regions the frictional force is an influential factor and may affect the movement of the particle which means there is no possibility for spreading of powders in these two regions.

Table 17: Dimensionless shear rate for sample 1.		
Gap Size (μm)	Speed (mm/s)	γ^{0*} $=\gamma^0(D_{50}/g)^{1/2}$
318	50	0.358
	100	0.715
	150	1.073
	200	1.430
191	50	0.595
	100	1.191
	150	1.786
	200	2.381
102	50	1.115
	100	2.230
	150	3.344
	200	4.459

Table 18: Dimensionless shear rate for Sample 2.		
Gap Size (μm)	Speed (mm/s)	γ^{0*} $=\gamma^0(D_{50}/g)^{1/2}$
318	50	0.389
	100	0.778
	150	1.166
	200	1.555
191	50	0.647
	100	1.295
	150	1.942
	200	2.589
102	50	1.212
	100	2.424
	150	3.636
	200	4.849

It has been shown in the Figure 34 and Figure 35 that although each individual value of γ^{0*} in sample 1 and sample 2 are not significantly different, the bulk layer density at different gap sizes in sample 2 are closer together compared to sample 1. Hence the three lines of sample 2 in the Figure 35 are unified while Figure 34 shows that sample 1 exhibits less unification. It has been detected that sample 2 shows a significant correlation in different gap sizes, while the graph of dimensionless shear rate against bulk layer density for sample 1 displays a convergence with larger gap size at 318 μm . This implies that sample 2 is more reliable for spreading compared to sample 1 as shear rate of the powders in sample 2 is not significantly affected by change in gap sizes.

The values of dimensionless shear rate for each individual gap size and spread velocity has been calculated and presented in Table 17 and Table 18 which revealed that an increase in gap size (depth of shear zone) decreases the value of dimensionless shear rate while an increase in spread velocity increases the possibility of collisions between the particles and consequently increases the value of dimensionless shear rate. These findings are also in line with the results of bulk layer density and mass per area.

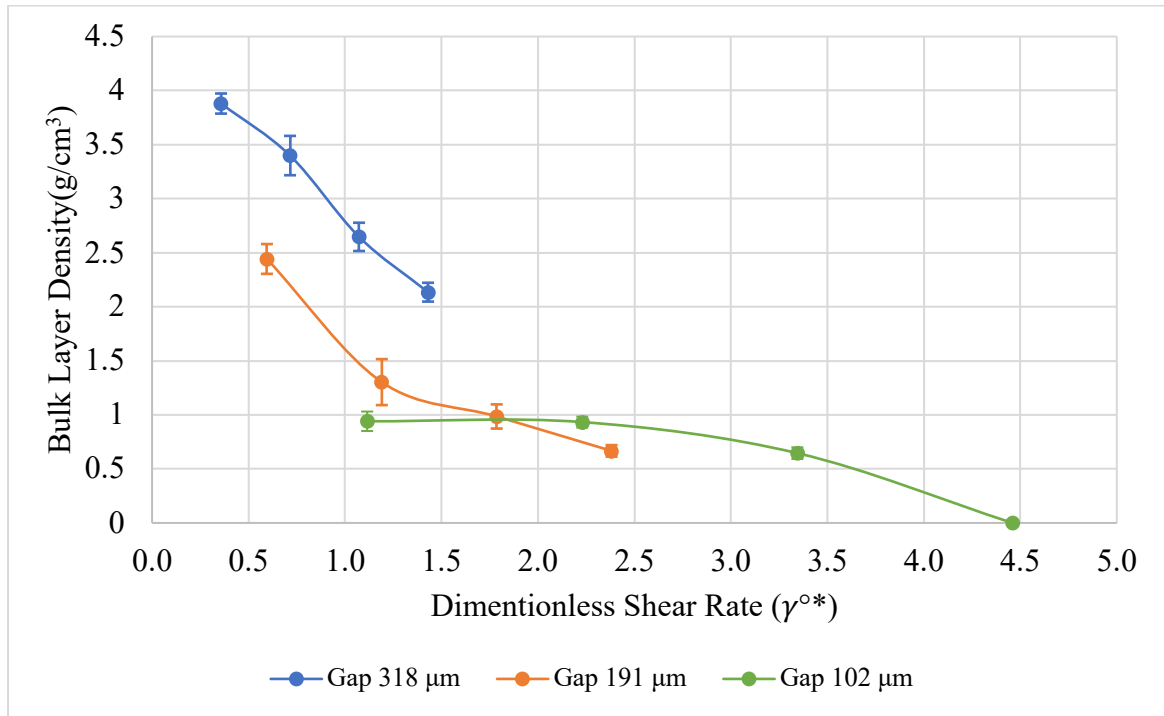


Figure 34: Dimensionless shear rate against bulk layer density of Sample1.

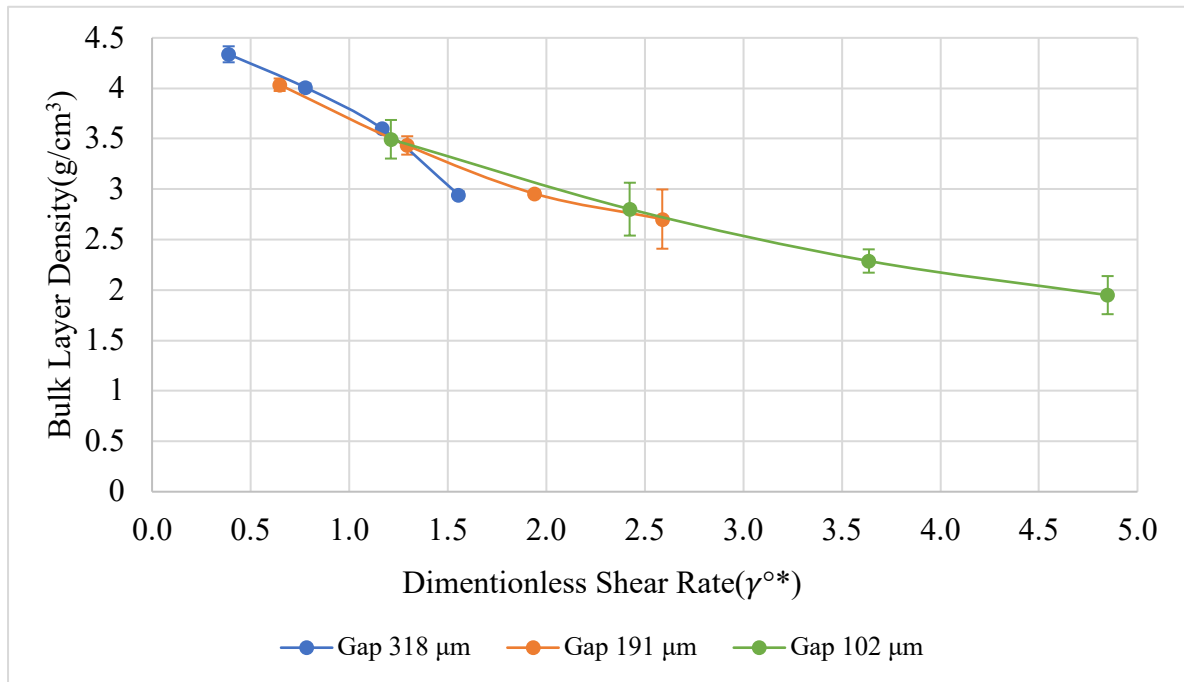


Figure 35: Dimensionless shear rate against bulk layer density of Sample 2.

4.7 Effect of Humidity on the Spread Layer (Conditioning)

It is shown in the previous sections, despite the fact that both samples have very similar powder characterisation scales, but their spreading behaviour is significantly different. Afterwards, through testing the samples, it has been recognised that humidity is a potential factor since powders behave different at high humidity conditions. The bulk layer density of both samples with gap size 318 μm has been obtained through conditioning at an average relative humidity of 73%. As it can be found from Figure 36, regardless of the speed, the bulk layer density of sample 1 drastically reduces when the humidity rises, however this change particularly at the lower velocities was not observed for sample 2. The bulk layer density of sample 2 at the speed of 50 mm/s at uncontrolled ambient conditions and 73% relative humidity is 4.19 g/cm^3 and 4.34 g/cm^3 respectively, which is close to the initial bulk density of the powder (4.628 g/cm^3).

It is also gathered that with sample 2, increase of velocity signifies the effect of humidity as at speed of 150 mm/s and 200 mm/s the reduction of bulk layer density is more obvious with this sample. The difference between the bulk layer densities of sample 2 at different humidity condition increases while the spread velocity increases which means spread velocity intensifies the effect of humidity in sample 2.

It is also noted that the error bars of the graphs with higher humidity for both samples are larger than the uncontrolled ambient condition. This implies that increase in humidity reduces the repeatability of spreading tests. However, it has been detected that error bars of sample 2 with gap size 318 μm at both high humidity and uncontrolled ambient conditions are much lower than that of sample 1.

Moreover, the graph of Layer bulk density over initial density against speed at 73% humidity shows that with the increase of humidity, particularly at lower speeds, there is no remarkable changes in the ratio of layer bulk density over initial density of sample 2 while this difference for sample 1 is highly noticeable. This suggests that increase in humidity has a major impact on spread quality of sample 1. However, it is concluded that regardless of the environmental condition, bulk layer density of both samples decreases when spreading velocity increases.

Therefore, with respect to the findings of this section it is assumed that humidity is a potential reason of difference in spreading behaviour of sample 1 compare to sample 2.

The difference in spreading behaviour of two samples could be related to different assumptions. Firstly, the larger number of fine particles in sample 1 may result into agglomerations of particles or low flowability, which consequently results into jamming and empty patches of the layers. As stated in Section 2.4.4, when size of the powders decreases to fine particles, they become more sensitive to moisture and this led to undesirable flow behaviour such as agglomeration and clumping of powders. This can be detected in this work as sample 1 with larger fraction of fine particles are very sensitive to humidity.

The presence of rathole in Hall flow meter test in Section 3.2.2 may also confirms that sample1 is more sensitive to humidity.

Secondly, they lie on different positions on phase diagram as one sample is placed on hyper-eutectic side and other sample is positioned on hypo-eutectic side of the diagram. Referring to Selection 2.2.5, this may be due to the difference of some minor elements in chemical composition of two samples, which may also result to changes in their microstructure and corrosion resistance. However, information regarding the cooling and heating rate during the powder production, which can strongly impact the microstructure and surface quality of particles is unavailable.

Therefore, further investigation is required to understand the exact difference in microstructure and internal characterisation of two samples.

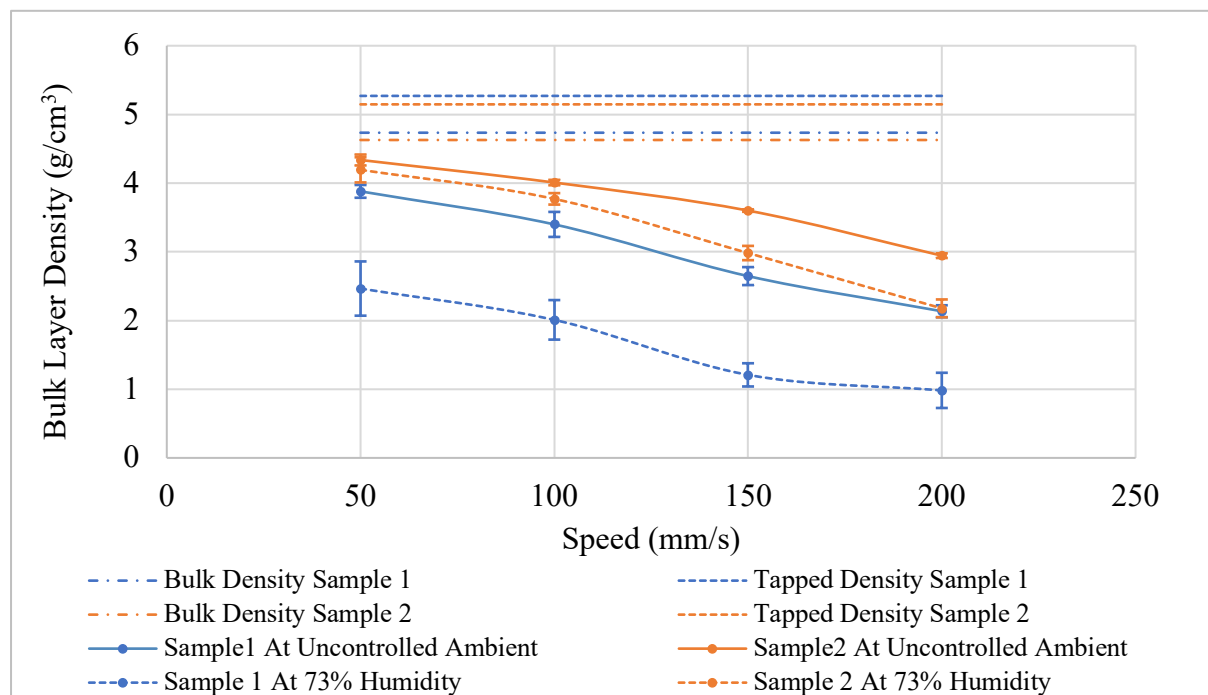


Figure 36: Comparison of Bulk Layer Density for Gap Size 318µm With Change in Humidity.

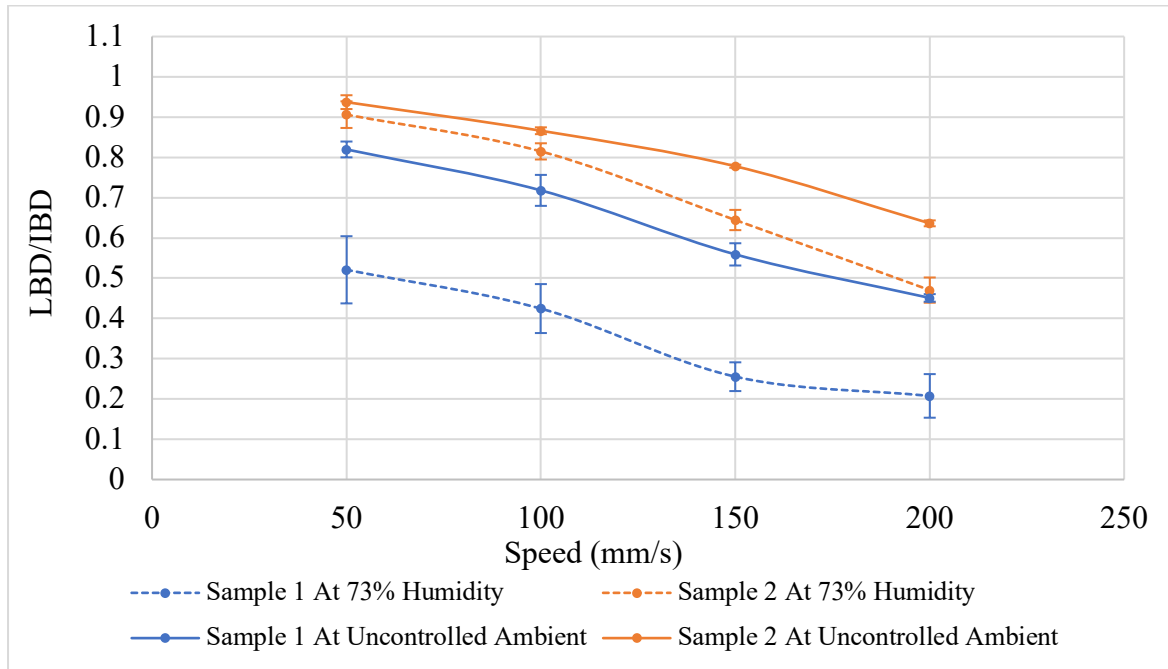


Figure 37: Comparison of Bulk Layer Density/Initial Density for Gap Size 318 μ m With Change in Humidity.

4.8 Summary of Chapter

The qualitative and quantitative analysis of spread profiles has been performed to form a comparison in this section.

Qualitative observation through image analysis of layer profiles for both samples indicates that by reducing the gap size from 318 μ m to 51 μ m, the surface quality of the layer drastically decreases which results into the elimination of the 51 μ m. This was clearly predictable as the gap size should be larger than the D_{90} and preferably greater than the largest particle in the batch. However, sample 1 exhibits a significantly poor layer profile regardless of the gap size and spread velocity. The quality of surface using sample 1 is severely lower than the respective layer created with sample 2.

Quantitative measures have been established to define spreadability metrics through investigation of individual spread layers that is created with a spreadability rig. Percentage of spread, mass per area, layer bulk density, ratio of layer bulk density to the initial density of the powder and dimensionless shear rate, are established in this work to achieve a viable measure for spread quality of stainless steel in AM. Since each method had its own limitation through different phase of spreading processes, a correlation between the results has been formed which

shows an exceptional agreement between them. However, it has been finally gathered that the ratio of layer bulk density to the initial density is the potential measure which can be defined as the spread quality to predict the spreading performance of the layers.

Interestingly, the result of different metrics in this project follows a single pattern which confirms that increasing the gap size for both samples improves the spreading quality, while increasing the speed degrades the spreadability measures. The quantitative values obtained from the defined metric (the ratio of bulk layer density over the initial bulk density of the powder) indicates that sample 2 exhibits optimised spreadability compared to sample 1. Sample 2 is more repetitive through the experiments while sample 1 seems to be an unreliable feeding material to be spread on the build plate.

Sample 2 exhibits an optimised spread quality at gap size 318 μm and speed of 50 mm/s. Moreover, at gap size 191 μm and speed of 50 mm/s the spread quality is still desirable. However, since gap size of 318 μm is out of range of the recommended layer thickness for PBF method (20-200 μm), hence gap size of 191 μm which is larger than the largest particle and also the D_{90} of the batch is preferably recommended.

As previously mentioned, the recommended spread velocity in AM is generally less than 150 mm/s. However, it is beneficial to achieve the best quality of spread at highest speeds without decrease of spreadability, which may be achievable by utilising narrower PSD or flow agent to improve flowability that requires further investigation.

Furthermore, the effect of humidity on the spread performance of the two batches has been studied and it has been found that sample 1 is highly sensitive to humidity. This could be a hypothesis to explain that the difference in spreading behaviour of these two samples could be due to the negative impact of humidity on sample 1.

CHAPTER FIVE

Conclusions

Chapter 5. Conclusions

The results of experiments in terms of effect of speed and gap size on the layer density have been summarised in the provided matrices and the guidelines of colour codes is available at the end of this page which explains the presented colour based on the value of bulk layer density.

- **Matrices of experiments at uncontrolled ambient conditions**

SS316L: Sample 1												
Gap Size (μm)	318				191				102			
Speed (mm/s)	50	100	150	200	50	100	150	200	50	100	150	200
Mass/Area (g/cm^2)	0.12	0.11	0.08	0.07	0.05	0.03	0.02	0.01	0.01	0.01	0.01	NA
Density (g/cm^3)	3.88	3.40	2.65	2.13	2.44	1.30	0.99	0.67	0.94	0.93	0.65	NA
LBD/ID	0.82	0.72	0.56	0.45	0.52	0.28	0.21	0.14	0.20	0.20	0.14	NA

SS316L: Sample 2												
Gap Size (μm)	318				191				102			
Speed (mm/s)	50	100	150	200	50	100	150	200	50	100	150	200
Mass/Area (g/cm^2)	0.14	0.13	0.11	0.09	0.08	0.07	0.06	0.05	0.04	0.03	0.02	0.02
Density (g/cm^3)	4.34	4.01	3.60	2.94	4.04	3.43	2.95	2.70	3.49	2.80	2.29	1.95
LBD/ID	0.94	0.87	0.78	0.64	0.87	0.74	0.64	0.58	0.76	0.61	0.49	0.42

- **Matrix of experiments at high relative humidity (73%)**

SS316L: HIGH HUMIDITY 73%								
	Sample 1, Gap size 318 μm				Sample 2, Gap size 318 μm			
Speed (mm/s)	50	100	150	200	50	100	150	200
Mass/Area (g/cm^2)	0.08	0.06	0.04	0.03	0.13	0.12	0.09	0.07
Density (g/cm^3)	2.47	2.01	1.21	0.98	4.19	3.77	2.98	2.18
LBD/ID	0.52	0.42	0.26	0.21	0.91	0.81	0.64	0.47

- Table of colour code guideline

Density (g/cm^3)		
	5-4	Excellent
	4-3	Good
	3-0	Poor

The quality of the final part in AM depends on both the powder quality and process parameters. To date, no agreement is found regarding the term “spreadability” in additive manufacturing. Therefore, defining a standard spreadability metric with respect to processes parameters is essential in additive manufacturing. This necessity calls for new researches in this field to perform qualitative and quantitative analysis of spreadability. Despite the fact that quality of the final part is directly related to the spreading behaviour of the powders, there is a considerable gap in the knowledge regarding the correlation of powder characterisation and spreadability. Furthermore, since quality of the layers is an influential factor in quality control of the final part, the spreading behaviour of the powders needs to be thoroughly investigated. The method of this project has been developed through collecting relevant ideas within available literature regarding spreadability of powders in additive manufacturing. Conceptual guidelines have been provided through review of some studies such as Snow et al. [170], Ahmed et al. [3], Fouda et al. [175] and Chen et al. [185] while gap of these researches has also been considered. However, there are some differences in the results of this project compared to previous studies. For instance, it is concluded by Snow et al. that angle of repose of powder is an indicative of its spreadability, while in this work two powders with almost the same measure of angle of repose exhibit very different spreading behaviour. This implies that scale of flowability with a specific method of assessment such as AOR is not a definitive measure for spreadability since this flow property is not an intrinsic property of powder and it may differ upon the condition of measurement.

It is assumed that the effect of environmental condition on the spread behaviour of powder within the sample 1 may be the reason for this disparity. Hypothetical effect of humidity on the surface chemistry at nanoscopic scale could adversely affect the flow behaviour of this sample compared to sample 2.

This project is conducted to focus on the process variables and identify a set of quantitative metrics along with qualitative assessments to predict a correlation between powder characterisation, processes parameters and spreadability in additive manufacturing.

Therefore, a quantitative analysis of bulk layer density has been employed in this project. Through establishing different metrics and mitigating the drawbacks of each metric, it has been gathered that the ratio of bulk layer density over initial density of the powder is a possible metric to measure the quality of spread.

To draw a conclusion, the presented matrices is provided which shows a summary of the results that have been obtained through the experimental tests. The colour code on the matrices has been selected based on the proximity of the bulk layer density to the initial density of the

batches. The green colour represents a value of bulk layer density that is very close to the initial bulk density, colour orange denotes the value that is not very high but still is in an acceptable range and colour red indicates that the obtained bulk layer density is very far from the initial bulk density of the batch. Therefore, the closer the value of this ratio to 1 the higher the spread quality and a ratio close to 0 is an indicator of poor spread quality. As explained in previous sections, bulk layer density of sample 1 in all different gap sizes and speeds is notably lower than sample 2, which is possibly due to higher moisture adsorption of sample 1. It has been detected that sample 1 is significantly affected when 73% relative humidity is applied to the batch, while sample 2 has a considerably low impact from the changes in humidity. However, for both samples the bulk layer density decreases when spread velocity increases. Furthermore, increasing the spread velocity signifies the influence of humidity on sample 2 as with speed of 50 mm/s at 73% humidity condition, the bulk layer density is still in the green category while increasing the velocity, the bulk layer density decreases compared to its value at uncontrolled ambient conditions.

Correlation of the powder properties and process parameters is not fully covered within literature and findings of this project conform that the spread quality of powders not only depends on the characteristics of powders but also conditions of application are highly influential.

Investigation through this project reveals that spreadability of two gas atomised spherical batches of stainless-steel 316L with similar size distribution, particle shape, morphology, and bulk density are considerably different, and this disparity directly depends on the process parameters such as gap size, spread velocity and particularly environmental conditions. It has been obtained that sample 1 is not a suitable choice of powder to be used in uncontrolled environments, but it may fit with non-spread based AM methods and requires further investigation in future works. However, although highest spread quality is achieved with sample 2 at largest gap size of 318 μm and lowest speed of 50 mm/s, but both of these processes parameter options are not very cost and time effective as higher layer thickness reduces the laser absorption and lower speed reduce the production rate. Therefore, depending on the application of the final product these parameters can be chosen and also by altering the PSD, improving the flowability or improving the design of the spreader blade, the spread quality may improve with lower gap size and higher speed.

However, due to the pandemic and time restriction, thorough understanding regarding the nature of these two samples and their spread behaviour in different processes conditions is limited in this project which necessitates further experimental and simulation investigations.

CHAPTER SIX

Future Work

Chapter 6. Future Work

This project focused on two samples of stainless steel to generate a viable measure for spreadability. However, it is very important to note that in order to establish a spreadability map regime, investigation on different powders and powder characterisation along with different processes parameters is essential. Similar to majority of the spreadability studies within the literature, this work is also limited to investigation of only one single layer while impact of spreading behaviour of individual layers upon each other is neglected. The surface quality of previous layers may have a significant influence on the spreading behaviour of the new deposited layer. Therefore, investigation of spreadability in multi-layer experiments gives more accurate information.

Furthermore, the current rig is not facilitated with laser to sinter the deposited layer before spreading of the next layer. Hence, the spreading processes is not very close to the actual spreading of powders in powder bed fusion machines, as particle arrangements and interactions may vary when deposited on the previously sintered layer. Therefore, application of laser is recommended for the future work.

Particle size distribution of both samples used in this project is 15-105 μm that is a desirable broad PSD but spreading of a narrower PSD would certainly give different results, which may be useful for future works. Narrow PSD biased to fine particles may be a suitable choice for future work as this would lead to a thin and uniform packing of the layer with smoother surface. However, it is important to note that a powder batch with excessive fine particles is prone to agglomeration, so it is important to have enough large particles to help the flow.

Moreover, effect of surrounding environment on the spreading behaviour of the powders also is an influential factor affecting spreadability. Hence, it is recommended to conduct the experiments in a well-controlled and isolated environment. As it has been explained before humidity had a significant impact on the spreading behaviour of sample 1, therefore, further investigation to gather all information regarding the flowability, internal structure, microstructure, surface analysis and surface oxidation is crucial at different environmental conditions. To fully understand the effects of humidity on both the flowability and spreading performance, flowability of the humid powders are required to be analysed.

Focused ion beam (FIB) and x-ray tomography (XRT) may be used for further analyse of the internal structure of both samples. Furthermore, x-ray photoelectron spectroscopy (XPS) technique is also a useful application to identify elemental composition and surface analysis of these powders.

Furthermore, utilising high-speed camera within the spreading processes would be very useful since effects of different parameters can be captured with high level precision.

Spreadability of powders is greatly affected by different types of the spreaders and this can be detected when roller or different types of blades with different angles are used. It has been explained within the literature review of this work that optimisation of the spreader tool compensates the negative impact of speed and gap size. Rounded, bevelled and flat end blade are different options that can be used in the future experiments.

More importantly redesigning the rig to a more practical version would be significantly beneficial. The current rig is not capable of collecting the excessive powders after spreading processes, which limits the variety and combination of the variety of experimental choice regarding mass of powders, speeds and gap sizes. Moreover, currently gap size is measured through utilising plastic gauges that is not an accurate measurement, therefore a precise motor to control the depth of the gap size would give considerably more accurate result. Measuring the depth of the layers through all points of the build plate is a limitation of this project and gap size has been considered as the thickness of the layer which is not the case in real spreading of powders in AM. Therefore, methods such as X-ray imaging can be conducted to measure the thickness of the layer.

Surface quality of the layers is also an influential factor that directly affects the quality of final product. Optical measuring methods may be performed to evaluate the surface quality of the layer.

CHAPTER SEVEN

References

Chapter 7. References

- [1] S. Vock, B. Klöden, A. Kirchner, T. Weißgärber, and B. Kieback, "Powders for powder bed fusion: a review," *Progress in Additive Manufacturing*, pp. 1-15, 2019.
- [2] Z. K. Snow, "Understanding Powder Spreadability in Powder Bed Fusion Additive Manufacturing," 2018.
- [3] M. Ahmed, M. Pasha, W. Nan, and M. Ghadiri, "A simple method for assessing powder spreadability for additive manufacturing," *Powder Technology*, vol. 367, pp. 671-679, 2020/05/01/ 2020, doi: <https://doi.org/10.1016/j.powtec.2020.04.033>.
- [4] A. Standard, "F2792-12a: standard terminology for additive manufacturing technologies (ASTM International, West Conshohocken, PA, 2012)," *Procedia Eng*, vol. 63, pp. 4-11, 2013.
- [5] L. University. "About Additive Manufacturing." Loughboyough University. <https://www.lboro.ac.uk/research/amrg/about/the7categoriesofadditivemanufacturing/> (accessed 15/03/2021, 2021).
- [6] M. S. Alqahtani, A. Al-Tamimi, H. Almeida, G. Cooper, and P. Bartolo, "A review on the use of additive manufacturing to produce lower limb orthoses," *Progress in Additive Manufacturing*, vol. 5, no. 2, pp. 85-94, 2020.
- [7] H. Fayazfar *et al.*, "A critical review of powder-based additive manufacturing of ferrous alloys: Process parameters, microstructure and mechanical properties," *Materials & Design*, vol. 144, pp. 98-128, 2018.
- [8] T. D. Ngo, A. Kashani, G. Imbalzano, K. T. Nguyen, and D. Hui, "Additive manufacturing (3D printing): A review of materials, methods, applications and challenges," *Composites Part B: Engineering*, vol. 143, pp. 172-196, 2018.
- [9] S. Romano, P. Nezhadfar, N. Shamsaei, M. Seifi, and S. Beretta, "High cycle fatigue behavior and life prediction for additively manufactured 17-4 PH stainless steel: Effect of sub-surface porosity and surface roughness," *Theoretical and Applied Fracture Mechanics*, vol. 106, p. 102477, 2020.
- [10] D. Chen, H. Daoud, F. Scherm, B. Klötzer, C. Hauck, and U. Glatzel, "Stainless steel powder produced by a novel arc spray process," *Journal of Materials Research and Technology*, vol. 9, no. 4, pp. 8314-8322, 2020.
- [11] V. Bhavar, P. Kattire, V. Patil, S. Khot, K. Gujar, and R. Singh, "A review on powder bed fusion technology of metal additive manufacturing," *Additive manufacturing handbook*, pp. 251-253, 2017.
- [12] J. A. Slotwinski and E. J. Garboczi, "Porosity of additive manufacturing parts for process monitoring," in *AIP conference proceedings*, 2014, vol. 1581, no. 1: American Institute of Physics, pp. 1197-1204.
- [13] R. Peter, I. Saric, I. K. Piltaver, I. J. Badovinac, and M. Petravic, "Oxide formation on chromium metal surfaces by low-energy oxygen implantation at room temperature," *Thin Solid Films*, vol. 636, pp. 225-231, 2017.
- [14] S. M. Allen and E. M. Sachs, "Three-dimensional printing of metal parts for tooling and other applications," *Metals and Materials*, vol. 6, no. 6, pp. 589-594, 2000.
- [15] Y. Bai, G. Wagner, and C. B. Williams, "Effect of bimodal powder mixture on powder packing density and sintered density in binder jetting of metals," in *2015 Annual International Solid Freeform Fabrication Symposium*, 2015, vol. 62, pp. 758-771.

- [16] A. Bailey, A. Merriman, A. Elliott, and M. Basti, "Preliminary testing of nanoparticle effectiveness in binder jetting applications," in *27th Annual International Solid Freeform Fabrication Symposium*, 2016, pp. 1069-1077.
- [17] D. D. Kopeliovich. "Powder preparation." SubsTech. http://www.substech.com/dokuwiki/doku.php?id=powder_preparation (accessed 22/03/2021, 2021).
- [18] J. Dawes, R. Bowerman, and R. Trepleton, "Introduction to the additive manufacturing powder metallurgy supply chain," *Johnson Matthey Technology Review*, vol. 59, no. 3, pp. 243-256, 2015.
- [19] S. Grenier and F. Allaire, "Plasma Atomization gives unique spherical Powders," *Metal Powder Report*, vol. 52, no. 11, p. 34, 1997.
- [20] A. Alagheband and C. Brown, "Plasma Atomization goes commercial," *Metal Powder Report*, vol. 53, no. 11, pp. 26-28, 1998.
- [21] L. V. Antony and R. G. Reddy, "Processes for production of high-purity metal powders," *Jom*, vol. 55, no. 3, pp. 14-18, 2003.
- [22] G. Chen, S. Y. Zhao, P. Tan, J. Wang, C. S. Xiang, and H. P. Tang, "A comparative study of Ti-6Al-4V powders for additive manufacturing by gas atomization, plasma rotating electrode process and plasma atomization," *Powder Technology*, vol. 333, pp. 38-46, 2018/06/15/ 2018, doi: <https://doi.org/10.1016/j.powtec.2018.04.013>.
- [23] I. M. A. Manufacturing. "why is powder feedstock for metal AM so expensive?" <https://www.insidemetaladditivemanufacturing.com/blog/why-is-powder-feedstock-for-metal-am-so-expensive> (accessed 25/03/2021, 2021).
- [24] I. C. Ltd. "Metal AM." Inovar Communications Ltd. <https://www.metal-am.com/articles/metal-powders-for-3d-printing-manufacturing-processes-and-properties/> (accessed 25/03/2021, 2021).
- [25] T. S. a. H. K. D. H. Bhadeshia. "Stainless Steels." University of Cambridge. http://www.phase-trans.msm.cam.ac.uk/2005/Stainless_steels/stainless.html (accessed 13/04/2021, 2021).
- [26] Amarine, "Ferrite content in stainless steel and embrittlement," in *Amarineblog*, ed, 2021.
- [27] F. Edler, Y. Kim, G. Machin, J. Pearce, and D. White, *Guide on secondary thermometry: specialised fixed points above 0°C*. 2017.
- [28] T. Materia, "Microstructures in Austenitic Stainless Steels." [Online]. Available: <https://www.totalmateria.com/page.aspx?ID=CheckArticle&site=kts&NM=268>
- [29] M. AM. "Additive Manufacturing at World PM2016: Opportunities for the use of water atomised metal powders." Metal AM. <https://www.metal-am.com/articles/additive-manufacturing-3d-printing-water-atomised-metal-powders/> (accessed 21/5/2021, 2021).
- [30] B. Al-Mangour, "Powder metallurgy of stainless steel: state-of-the art, challenges, and development," *Stainless Steel: Microstructure, Mechanical Properties and Methods of Application: Nova Science Publishers*, pp. 37-80, 2015.
- [31] N. Ciftci, N. Ellendt, R. von Bargen, H. Henein, L. Mädler, and V. Uhlenwinkel, "Atomization and characterization of a glass forming alloy $\{(Fe_{0.6}Co_{0.4})_{0.75}B_{0.2}Si_{0.05}\}_{96}Nb_4$," *Journal of Non-Crystalline Solids*, vol. 394-395, pp. 36-42, 2014/07/01/ 2014, doi: <https://doi.org/10.1016/j.jnoncrysol.2014.03.023>.

- [32] J. Wiskel, H. Henein, and E. Maire, "Solidification study of aluminum alloys using impulse atomization: Part I: Heat transfer analysis of an atomized droplet," *Canadian metallurgical quarterly*, vol. 41, no. 1, pp. 97-110, 2002.
- [33] C. Schade and J. J. Dunkley, "Atomization[1]," in *Powder Metallurgy*, vol. 7, P. Samal and J. Newkirk Eds.: ASM International, 2015, p. 0.
- [34] A. Zwiren, C. Schade, G. Hoeganaes, and S. Hoeges, "Economic Additive Manufacturing using Water Atomized Stainless Steel Powder."
- [35] D. A. Porter and K. E. Easterling, *Phase transformations in metals and alloys (revised reprint)*. CRC press, 2009.
- [36] N. Ciftci, N. Ellendt, G. Coulthard, E. Soares Barreto, L. Mädler, and V. Uhlenwinkel, "Novel Cooling Rate Correlations in Molten Metal Gas Atomization," *Metallurgical and Materials Transactions B*, vol. 50, no. 2, pp. 666-677, 2019/04/01 2019, doi: 10.1007/s11663-019-01508-0.
- [37] T. M. Abu-Lebdeh, G. P.-d. Leon, S. A. Hamoush, R. D. Seals, and V. E. Lamberti, "Gas atomization of molten metal: part II. Applications," *American Journal of Engineering and Applied Sciences*, vol. 9, no. 2, 2016.
- [38] M. Tului *et al.*, "Amorphous steel coatings deposited by cold-gas spraying," *Metals*, vol. 9, no. 6, p. 678, 2019.
- [39] G. Bae, Y. Xiong, S. Kumar, K. Kang, and C. Lee, "General aspects of interface bonding in kinetic sprayed coatings," *Acta Materialia*, vol. 56, no. 17, pp. 4858-4868, 2008/10/01/ 2008, doi: <https://doi.org/10.1016/j.actamat.2008.06.003>.
- [40] S. Yin, C. Chen, and R. Lupoi, "Chapter 3 - Nanostructured Metal Coatings via Cold Spray," in *Advanced Nanomaterials and Coatings by Thermal Spray*, G.-J. Yang and X. Suo Eds.: Elsevier, 2019, pp. 27-60.
- [41] T. Pettersson, "Characterization of metal powders produced by two gas atomizing methods for thermal spraying applications," ed, 2015.
- [42] M. R. Raza, F. Ahmad, M. A. Omar, and R. M. German, "Effects of cooling rate on mechanical properties and corrosion resistance of vacuum sintered powder injection molded 316L stainless steel," *Journal of Materials Processing Technology*, vol. 212, no. 1, pp. 164-170, 2012/01/01/ 2012, doi: <https://doi.org/10.1016/j.jmatprotec.2011.08.019>.
- [43] I. E. Anderson, E. M. White, and R. Dehoff, "Feedstock powder processing research needs for additive manufacturing development," *Current Opinion in Solid State and Materials Science*, vol. 22, no. 1, pp. 8-15, 2018.
- [44] J. A. Slotwinski, E. J. Garboczi, P. E. Stutzman, C. F. Ferraris, S. S. Watson, and M. A. Peltz, "Characterization of metal powders used for additive manufacturing," *Journal of research of the National Institute of Standards and Technology*, vol. 119, p. 460, 2014.
- [45] A. T. Sutton, C. S. Kriewall, M. C. Leu, and J. W. Newkirk, "Powders for additive manufacturing processes: Characterization techniques and effects on part properties," *Solid Freeform Fabrication*, vol. 1, pp. 1004-1030, 2016.
- [46] J. A. Slotwinski and E. J. Garboczi, "Metrology needs for metal additive manufacturing powders," *Jom*, vol. 67, no. 3, pp. 538-543, 2015.
- [47] P. Kiani, U. Scipioni Bertoli, A. D. Dupuy, K. Ma, and J. M. Schoenung, "A statistical analysis of powder flowability in metal additive manufacturing," *Advanced Engineering Materials*, vol. 22, no. 10, p. 2000022, 2020.

- [48] J. K. Prescott and R. A. Barnum, "On powder flowability," *Pharmaceutical technology*, vol. 24, no. 10, pp. 60-85, 2000.
- [49] A. W. Jenike, "Storage and flow of solids. Bulletin No. 123 of the Utah Engineering Experiment Station; Vol. 53, No. 26, November 1964," Utah Univ., Salt Lake City (United States), 1976.
- [50] J. Zegzulka, "The angle of internal friction as a measure of work loss in granular material flow," *Powder Technology*, vol. 233, pp. 347-353, 2013/01/01/ 2013, doi: <https://doi.org/10.1016/j.powtec.2012.06.047>.
- [51] J. Zegzulka, D. Gelnar, L. Jezerska, A. Ramirez-Gomez, J. Necas, and J. Rozbroj, "Internal friction angle of metal powders," *Metals*, vol. 8, no. 4, p. 255, 2018.
- [52] K. Shinohara, M. Oida, and B. Golman, "Effect of particle shape on angle of internal friction by triaxial compression test," *Powder technology*, vol. 107, no. 1-2, pp. 131-136, 2000.
- [53] T. W. Lambe and W. A. Marr, "Stress path method," *Journal of the geotechnical engineering division*, vol. 105, no. 6, pp. 727-738, 1979.
- [54] M. Yousuff and N. Page, "Particle material, morphology and load effects on internal friction in powders," *Powder technology*, vol. 76, no. 2, pp. 155-164, 1993.
- [55] L. C. Chan and N. W. Page, "Particle fractal and load effects on internal friction in powders," *Powder Technology*, vol. 90, no. 3, pp. 259-266, 1997.
- [56] O. D. Neikov, S. S. Naboychenko, and N. A. Yefimov, *Handbook of Non-Ferrous Metal Powders: Technologies and Applications*, Second Edition ed. Elsevier (in English), 2019.
- [57] I. S. Organisation. "ISO 4490:2014—Metallic powders—Determination of flow rate by means of a calibrated funnel (Hall flowmeter)." ISO 4490. <https://www.iso.org/standard/65132.html> (accessed 22/03/2021, 2021).
- [58] A. International. "ASTM B213 - 13 Standard Test Methods for Flow Rate of Metal Powders Using the Hall Flowmeter Funnel." ASTM. <https://www.astm.org/> (accessed 22/03/2021, 2021).
- [59] A. B. Spierings, M. Voegtlin, T. u. Bauer, and K. Wegener, "Powder flowability characterisation methodology for powder-bed-based metal additive manufacturing," *Progress in Additive Manufacturing*, vol. 1, no. 1, pp. 9-20, 2016.
- [60] D. Geldart, E. Abdullah, A. Hassanpour, L. Nwoke, and I. Wouters, "Characterization of powder flowability using measurement of angle of repose," *China Particuology*, vol. 4, no. 3-4, pp. 104-107, 2006.
- [61] R.L.Carr, "Evaluating Flow Properties of Solids," *Chemical Engineering Journal*, vol. 72, pp. 163-168, 1965.
- [62] D. Schulze, "Powders and bulk solids," *Behaviour, characterization, storage and flow*. Springer, vol. 22, 2008.
- [63] A. B. Spierings, *Powder Spreadability and Characterization of Sc-and Zr-modified Aluminium Alloys Processed by Selective Laser Melting: Quality Management System for Additive Manufacturing*. ETH Zurich, 2018.
- [64] Metallurgist. <https://www.911metallurgist.com/how-to-keep-bins-flowing/> (accessed 26/05/2021, 2021).
- [65] Q. B. Nguyen, M. L. S. Nai, Z. Zhu, C.-N. Sun, J. Wei, and W. Zhou, "Characteristics of inconel powders for powder-bed additive manufacturing," *Engineering*, vol. 3, no. 5, pp. 695-700, 2017.
- [66] F. Technology. "ABOUT THE FT4 POWDER RHEOMETER®"

- Powder Flow Testing with the FT4 Powder Rheometer." Freeman Technology and Powder Rheometer are registered trademarks of Freeman Technology Ltd
https://www.freemantech.co.uk/powder-testing/ft4-powder-rheometer-powder-flow-tester?gclid=Cj0KCQjw9YWDBhDyARIsADt6sGbGD5TnID83T8GFAWt3F4taKeFp6T24vc59zS1BSIVz11rQ0ClK1ZsaAg-7EALw_wcB (accessed 20/03/2021, 2021).
- [67] J. Clayton, "Optimising metal powders for additive manufacturing," *Metal Powder Report*, vol. 69, no. 5, pp. 14-17, 2014.
- [68] L. Markusson, "Powder Characterization for Additive Manufacturing Processes," ed, 2017.
- [69] R. Freeman, "Measuring the flow properties of consolidated, conditioned and aerated powders—a comparative study using a powder rheometer and a rotational shear cell," *Powder Technology*, vol. 174, no. 1-2, pp. 25-33, 2007.
- [70] C. Hare, U. Zafar, M. Ghadiri, T. Freeman, J. Clayton, and M. Murtagh, "Analysis of the dynamics of the FT4 powder rheometer," *Powder Technology*, vol. 285, pp. 123-127, 2015.
- [71] A. B. Spierings, M. Voegtlin, T. Bauer, and K. Wegener, "Powder flowability characterisation methodology for powder-bed-based metal additive manufacturing," *Progress in Additive Manufacturing*, vol. 1, no. 1, pp. 9-20, 2016.
- [72] W. B. James. "Mercury Scientific Revolution ASTM Paper
 ASTM COMMITTEE B09 WORKSHOP ON POWDER CHARACTERISATION." Meritics Ltd.
<https://www.meritics.com/mercury-scientific-revolution-astm-paper/> (accessed 30/03/2021, 2021).
- [73] M. Pasha, C. Hare, A. Hassanpour, and M. Ghadiri, "Numerical analysis of strain rate sensitivity in ball indentation on cohesive powder Beds," *Chemical Engineering Science*, vol. 123, pp. 92-98, 2015.
- [74] U. Zafar, C. Hare, A. Hassanpour, and M. Ghadiri, "Effect of strain rate on powder flow behaviour using ball indentation method," *Powder Technology*, vol. 380, pp. 567-573, 2021/03/01/ 2021, doi: <https://doi.org/10.1016/j.powtec.2020.11.057>.
- [75] G. I. Tardos, S. McNamara, and I. Talu, "Slow and intermediate flow of a frictional bulk powder in the Couette geometry," *Powder Technology*, vol. 131, no. 1, pp. 23-39, 2003/03/03/ 2003, doi: [https://doi.org/10.1016/S0032-5910\(02\)00315-7](https://doi.org/10.1016/S0032-5910(02)00315-7).
- [76] Y. Sun, S. Gulizia, C. Oh, C. Doblin, Y. Yang, and M. Qian, "Manipulation and characterization of a novel titanium powder precursor for additive manufacturing applications," *Jom*, vol. 67, no. 3, pp. 564-572, 2015.
- [77] A. Amado, M. Schmid, G. Levy, and K. Wegener, "Advances in SLS powder characterization," *Group*, vol. 7, no. 10, p. 12, 2011.
- [78] H. Attar *et al.*, "Effect of powder particle shape on the properties of in situ Ti–TiB composite materials produced by selective laser melting," *Journal of Materials Science & Technology*, vol. 31, no. 10, pp. 1001-1005, 2015.
- [79] J. Koo *et al.*, "Polyamide nanocomposites for selective laser sintering," in *2006 International Solid Freeform Fabrication Symposium*, 2006.
- [80] Y. Ma, T. M. Evans, N. Philips, and N. Cunningham, "Numerical simulation of the effect of fine fraction on the flowability of powders in additive manufacturing," *Powder Technology*, vol. 360, pp. 608-621, 2020.
- [81] M. Qian, "Metal powder for additive manufacturing," *Jom*, vol. 67, no. 3, pp. 536-537, 2015.

- [82] S. Ziegelmeier *et al.*, "An experimental study into the effects of bulk and flow behaviour of laser sintering polymer powders on resulting part properties," *Journal of Materials Processing Technology*, vol. 215, pp. 239-250, 2015.
- [83] F. Technology. "Additive Manufacturing – Improve Print Quality and Reuse with Powder Rheometry." AZoM. <https://www.azom.com/article.aspx?ArticleID=13391> (accessed 23/03/2021, 2021).
- [84] B. Liu, R. Wildman, C. Tuck, I. Ashcroft, and R. Hague, "Investigation the effect of particle size distribution on processing parameters optimisation in selective laser melting process," *Additive manufacturing research group, Loughborough University*, pp. 227-238, 2011.
- [85] J.-P. Choi *et al.*, "Evaluation of powder layer density for the selective laser melting (SLM) process," *Materials transactions*, vol. 58, no. 2, pp. 294-297, 2017.
- [86] D. V. Rosato, *Plastics engineered product design*. Elsevier, 2003.
- [87] J. Johanson, "Flow indices in the prediction of powder behavior," *Pharm. Manuf. Int.*, pp. 159-164, 1995.
- [88] K. A. Rosentrater, "Some physical properties of distillers dried grains with solubles (DDGS)," *Applied Engineering in Agriculture*, vol. 22, no. 4, pp. 589-595, 2006.
- [89] V. Ganesan, K. A. Rosentrater, and K. Muthukumarappan, "Flowability and handling characteristics of bulk solids and powders—A review," in *2005 ASAE Annual Meeting, 2005: American Society of Agricultural and Biological Engineers*, p. 1.
- [90] A. Santomaso, P. Lazzaro, and P. Canu, "Powder flowability and density ratios: the impact of granules packing," *Chemical Engineering Science*, vol. 58, no. 13, pp. 2857-2874, 2003.
- [91] A. C.-Y. Wong, "Characterisation of the flowability of glass beads by bulk densities ratio," *Chemical Engineering Science*, vol. 55, no. 18, pp. 3855-3859, 2000.
- [92] R. O. Grey and J. K. Beddow, "On the Hausner Ratio and its relationship to some properties of metal powders," *Powder Technology*, vol. 2, no. 6, pp. 323-326, 1969/09/01/ 1969, doi: [https://doi.org/10.1016/0032-5910\(69\)80024-0](https://doi.org/10.1016/0032-5910(69)80024-0).
- [93] R. B. Shah, M. A. Tawakkul, and M. A. Khan, "Comparative Evaluation of Flow for Pharmaceutical Powders and Granules," *AAPS PharmSciTech*, vol. 9, no. 1, pp. 250-258, 2008/03/01 2008, doi: 10.1208/s12249-008-9046-8.
- [94] A. M. Rausch, V. E. Küng, C. Pobel, M. Markl, and C. Körner, "Predictive simulation of process windows for powder bed fusion additive manufacturing: influence of the powder bulk density," *Materials*, vol. 10, no. 10, p. 1117, 2017.
- [95] J. P. Schultz, J. P. Martin, R. G. Kander, and C. T. Suchicital, "Selective laser sintering of nylon 12-PEEK blends formed by cryogenic mechanical alloying," in *2000 International Solid Freeform Fabrication Symposium, 2000*.
- [96] S. Berretta, O. Ghita, K. E. Evans, A. Anderson, and C. Newman, "Size, shape and flow of powders for use in Selective Laser Sintering (SLS)," *High Value Manufacturing: Advanced Research in Virtual and Rapid Prototyping*, p. 49, 2013.
- [97] R. Frykholm, Y. Takeda, B.-G. Andersson, and R. Carlström, "Solid State Sintered 3-D Printing Component by Using Inkjet (Binder) Method," *Journal of the Japan Society of Powder and Powder Metallurgy*, vol. 63, no. 7, pp. 421-426, 2016, doi: 10.2497/jjspm.63.421.
- [98] A. B. Spierings, N. Herres, and G. Levy, "Influence of the particle size distribution on surface quality and mechanical properties in AM steel parts," *Rapid Prototyping Journal*, 2011.

- [99] T. Ö. Oğurtanı, ed: ResearchGate, 2017.
- [100] M. Sobhani, ed, 2017.
- [101] T. A. Royal and J. W. Carson, "Fine powder flow phenomena in bins, hoppers and processing vessels," in *Conference: Bulk*, 2000.
- [102] D. Herzog, V. Seyda, E. Wycisk, and C. Emmelmann, "Additive manufacturing of metals," *Acta Materialia*, vol. 117, pp. 371-392, 2016/09/15/ 2016, doi: <https://doi.org/10.1016/j.actamat.2016.07.019>.
- [103] S. Abdel-Hamid, F. Alshihabi, and G. Betz, "Investigating the effect of particle size and shape on high speed tableting through radial die-wall pressure monitoring," *International journal of pharmaceuticals*, vol. 413, no. 1-2, pp. 29-35, 2011.
- [104] A. Hart, "Effect of particle size on detergent powders flowability and tableability," *J Chem Eng Process Technol*, vol. 6, no. 1, 2015.
- [105] A. B. "What happen to tapped density when increasing particle size of the powder?" ResearchGate. https://www.researchgate.net/post/What_happen_to_tapped_density_when_increasing_particle_size_of_the_powder/59aaa73893553ba41929cbef/citation/download (accessed 31/03/2021, 2021).
- [106] P. Tang and V. M. Puri, "Methods for Minimizing Segregation: A Review," *Particulate Science and Technology*, vol. 22, no. 4, pp. 321-337, 2004/10/01 2004, doi: 10.1080/02726350490501420.
- [107] P. Tang and V. Puri, "Methods for minimizing segregation: a review," *Particulate Science and Technology*, vol. 22, no. 4, pp. 321-337, 2004.
- [108] R. M. German, *Powder metallurgy and particulate materials processing: the processes, materials, products, properties and applications*. Metal powder industries federation Princeton, 2005.
- [109] A. Jillavenkatesa, S. Dapkunas, and L. Lum, "NIST Recommended Practice Guide: Particle Size Characterization, Special Publication 960-1," ed, 2001.
- [110] G. Bierwagen and T. Sanders, "Studies of the effects of particle size distribution on the packing efficiency of particles," *Powder technology*, vol. 10, no. 3, pp. 111-119, 1974.
- [111] A. Hoffmann and H. Finkers, "A relation for the void fraction of randomly packed particle beds," *Powder Technology*, vol. 82, no. 2, pp. 197-203, 1995.
- [112] J. Zheng, W. B. Carlson, and J. S. Reed, "The packing density of binary powder mixtures," *Journal of the European Ceramic Society*, vol. 15, no. 5, pp. 479-483, 1995.
- [113] N. Karapatis, G. Egger, P. Gyax, and R. Glardon, "Optimization of powder layer density in selective laser sintering," in *1999 International Solid Freeform Fabrication Symposium*, 1999.
- [114] A. Simchi, "The role of particle size on the laser sintering of iron powder," *Metallurgical and Materials Transactions B*, vol. 35, no. 5, pp. 937-948, 2004.
- [115] G. Nichols *et al.*, "A review of the terms agglomerate and aggregate with a recommendation for nomenclature used in powder and particle characterization," *Journal of pharmaceutical sciences*, vol. 91, no. 10, pp. 2103-2109, 2002.
- [116] Y. Shi, Z. Li, H. Sun, S. Huang, and F. Zeng, "Effect of the properties of the polymer materials on the quality of selective laser sintering parts," *Proceedings of the Institution of Mechanical Engineers, Part L: Journal of Materials: Design and Applications*, vol. 218, no. 3, pp. 247-252, 2004.

- [117] X. Zhou, X. Liu, D. Zhang, Z. Shen, and W. Liu, "Balling phenomena in selective laser melted tungsten," *Journal of Materials Processing Technology*, vol. 222, pp. 33-42, 2015.
- [118] N. K. Tolochko *et al.*, "Balling processes during selective laser treatment of powders," *Rapid Prototyping Journal*, 2004.
- [119] J.-P. Kruth, L. Froyen, J. Van Vaerenbergh, P. Mercelis, M. Rombouts, and B. Lauwers, "Selective laser melting of iron-based powder," *Journal of materials processing technology*, vol. 149, no. 1-3, pp. 616-622, 2004.
- [120] Y. Lee and W. Zhang, "Mesoscopic simulation of heat transfer and fluid flow in laser powder bed additive manufacturing," in *International solid free form fabrication symposium, Austin*, 2015, pp. 1154-1165.
- [121] F. De Larrard, *Concrete mixture proportioning: a scientific approach*. CRC Press, 1999.
- [122] I. Mehdipour and K. Khayat, "Understanding the role of particle packing characteristics in rheo-physical properties of cementitious suspensions: A literature review," *Construction and Building Materials*, vol. 161, pp. 340-353, 02/10 2018, doi: 10.1016/j.conbuildmat.2017.11.147.
- [123] A. B. Spierings and G. Levy, "Comparison of density of stainless steel 316L parts produced with selective laser melting using different powder grades," in *Proceedings of the Annual International Solid Freeform Fabrication Symposium*, 2009: Austin, TX, pp. 342-353.
- [124] Y. Bai, G. Wagner, and C. B. Williams, "Effect of Particle Size Distribution on Powder Packing and Sintering in Binder Jetting Additive Manufacturing of Metals," *Journal of Manufacturing Science and Engineering*, vol. 139, no. 8, 2017, doi: 10.1115/1.4036640.
- [125] J. Bridgwater, "Mixing and segregation mechanisms in particle flow," in *Granular matter*: Springer, 1994, pp. 161-193.
- [126] N. Sommier, P. Porion, P. Evesque, B. Leclerc, P. Tchoreloff, and G. Couarraze, "Magnetic resonance imaging investigation of the mixing-segregation process in a pharmaceutical blender," *International journal of pharmaceutics*, vol. 222, no. 2, pp. 243-258, 2001.
- [127] S. P. Duffy and V. M. Puri, "Primary segregation shear cell for size-segregation analysis of binary mixtures," *KONA Powder and Particle Journal*, vol. 20, pp. 196-207, 2002.
- [128] A. Mostafaei, P. Rodriguez De Vecchis, I. Nettleship, and M. Chmielus, "Effect of powder size distribution on densification and microstructural evolution of binder-jet 3D-printed alloy 625," *Materials & Design*, vol. 162, pp. 375-383, 2019/01/15/ 2019, doi: <https://doi.org/10.1016/j.matdes.2018.11.051>.
- [129] M. Lutter-Günther, M. Horn, C. Seidel, and G. Reinhart, "Influence of particle size distribution on powder flowability and part properties in laser beam melting," in *Rapid. Tech—international trade show and conference for additive manufacturing*, 2017, pp. 297-311.
- [130] H. Tang, M. Qian, N. Liu, X. Zhang, G. Yang, and J. Wang, "Effect of powder reuse times on additive manufacturing of Ti-6Al-4V by selective electron beam melting," *Jom*, vol. 67, no. 3, pp. 555-563, 2015.
- [131] P. D. Nezhadfar, A. Soltani-Tehrani, A. Sterling, N. Tsolas, and N. Shamsaei, "The effects of powder recycling on the mechanical properties of additively manufactured

- 17-4 PH stainless steel," *Solid Freeform Fab. Proceed. 29th Ann. International*, pp. 1292-1300, 2018.
- [132] S. Mohd Yusuf, E. Choo, and N. Gao, "Comparison between Virgin and Recycled 316L SS and AlSi10Mg Powders Used for Laser Powder Bed Fusion Additive Manufacturing," *Metals*, vol. 10, no. 12, p. 1625, 2020.
- [133] Z. Brytan, M. A. Grande, M. Rosso, R. Bidulský, and L. Dobrzański, "Stainless steels sintered from the mixture of prealloyed stainless steel and alloying element powders," in *Materials Science Forum*, 2011, vol. 672: Trans Tech Publ, pp. 165-170.
- [134] D. Wang and L. S. Fan, "2 - Particle characterization and behavior relevant to fluidized bed combustion and gasification systems," in *Fluidized Bed Technologies for Near-Zero Emission Combustion and Gasification*, F. Scala Ed.: Woodhead Publishing, 2013, pp. 42-76.
- [135] E. Klar and P. K. Samal, *Powder metallurgy stainless steels: processing, microstructures, and properties*. ASM international, 2007.
- [136] B. Suhr, W. A. Skipper, R. Lewis, and K. Six, "Shape analysis of railway ballast stones: curvature-based calculation of particle angularity," *Scientific reports*, vol. 10, no. 1, pp. 1-14, 2020.
- [137] I. Cruz-Matías *et al.*, "Sphericity and roundness computation for particles using the extreme vertices model," *Journal of Computational Science*, vol. 30, pp. 28-40, 2019/01/01/ 2019, doi: <https://doi.org/10.1016/j.jocs.2018.11.005>.
- [138] Sympatec. "Particle shape analysis." Sympatec GmbH. <https://www.sympatec.com/en/particle-measurement/glossary/particle-shape/> (accessed 31/5/2021).
- [139] V. Mikli, H. Kaerdi, P. Kulu, and M. Besterci, "Characterization of powder particle morphology," *Proceedings of the Estonian Academy of Sciences: Engineering(Estonia)*, vol. 7, no. 1, pp. 22-34, 2001.
- [140] A. T. Sutton, C. S. Kriewall, M. C. Leu, and J. W. Newkirk, "Powder characterisation techniques and effects of powder characteristics on part properties in powder-bed fusion processes," *Virtual and physical prototyping*, vol. 12, no. 1, pp. 3-29, 2017.
- [141] A. Mussatto, R. Groarke, A. O'Neill, M. A. Obeidi, Y. Delaure, and D. Brabazon, "Influences of powder morphology and spreading parameters on the powder bed topography uniformity in powder bed fusion metal additive manufacturing," *Additive Manufacturing*, vol. 38, p. 101807, 2021/02/01/ 2021, doi: <https://doi.org/10.1016/j.addma.2020.101807>.
- [142] S. Angayarkanni, V. Sunny, and J. Philip, "Effect of nanoparticle size, morphology and concentration on specific heat capacity and thermal conductivity of nanofluids," *Journal of Nanofluids*, vol. 4, no. 3, pp. 302-309, 2015.
- [143] M. Shamsujjoha, S. R. Agnew, J. M. Fitz-Gerald, W. R. Moore, and T. A. Newman, "High strength and ductility of additively manufactured 316L stainless steel explained," *Metallurgical and Materials Transactions A*, vol. 49, no. 7, pp. 3011-3027, 2018.
- [144] P. Bajaj, A. Hariharan, A. Kini, P. Kürnsteiner, D. Raabe, and E. A. Jäggle, "Steels in additive manufacturing: A review of their microstructure and properties," *Materials Science and Engineering: A*, vol. 772, p. 138633, 2020.
- [145] E. Olakanmi, "Selective laser sintering/melting (SLS/SLM) of pure Al, Al-Mg, and Al-Si powders: Effect of processing conditions and powder properties," *Journal of Materials Processing Technology*, vol. 213, no. 8, pp. 1387-1405, 2013.

- [146] S. Haeri, Y. Wang, O. Ghita, and J. Sun, "Discrete element simulation and experimental study of powder spreading process in additive manufacturing," *Powder Technology*, vol. 306, pp. 45-54, 2017.
- [147] D. T. Pham, K. Dotchev, and W. Yusoff, "Deterioration of polyamide powder properties in the laser sintering process," *Proceedings of the Institution of Mechanical Engineers, Part C: Journal of Mechanical Engineering Science*, vol. 222, no. 11, pp. 2163-2176, 2008.
- [148] T. Gornet, K. Davis, T. Starr, and K. Mulloy, "Characterization of Selective Laser Sintering™ Materials to Determine Process Stability," in *2002 International Solid Freeform Fabrication Symposium*, 2002.
- [149] J.-P. Kruth, G. Levy, F. Klocke, and T. Childs, "Consolidation phenomena in laser and powder-bed based layered manufacturing," *CIRP annals*, vol. 56, no. 2, pp. 730-759, 2007.
- [150] K. Dotchev and W. Yusoff, "Recycling of polyamide 12 based powders in the laser sintering process," *Rapid Prototyping Journal*, 2009.
- [151] R. Goodridge, C. Tuck, and R. Hague, "Laser sintering of polyamides and other polymers," *Progress in Materials science*, vol. 57, no. 2, pp. 229-267, 2012.
- [152] D. L. Bourell, T. J. Watt, D. K. Leigh, and B. Fulcher, "Performance limitations in polymer laser sintering," *Physics Procedia*, vol. 56, pp. 147-156, 2014.
- [153] M. Schmid, A. Amado, and K. Wegener, "Materials perspective of polymers for additive manufacturing with selective laser sintering," *Journal of Materials Research*, vol. 29, no. 17, pp. 1824-1832, 2014.
- [154] S. Mirzababaei, B. K. Paul, and S. Pasebani, "Metal powder recyclability in binder jet additive manufacturing," *Jom*, vol. 72, no. 9, pp. 3070-3079, 2020.
- [155] G. Jacob, G. Jacob, C. U. Brown, M. A. Donmez, S. S. Watson, and J. Slotwinski, *Effects of powder recycling on stainless steel powder and built material properties in metal powder bed fusion processes*. US Department of Commerce, National Institute of Standards and Technology ..., 2017.
- [156] P. Nandwana *et al.*, "Recyclability study on Inconel 718 and Ti-6Al-4V powders for use in electron beam melting," *Metallurgical and Materials Transactions B*, vol. 47, no. 1, pp. 754-762, 2016.
- [157] M. Yan, W. Xu, M. Dargusch, H. Tang, M. Brandt, and M. Qian, "Review of effect of oxygen on room temperature ductility of titanium and titanium alloys," *Powder metallurgy*, vol. 57, no. 4, pp. 251-257, 2014.
- [158] D. Salamon, "Chapter 6 - Advanced Ceramics," in *Advanced Ceramics for Dentistry*, J. Z. Shen and T. Kosmač Eds. Oxford: Butterworth-Heinemann, 2014, pp. 103-122.
- [159] L. Espinal, "Porosity and its measurement," *Characterization of Materials*, pp. 1-10, 2002.
- [160] M. Iebba *et al.*, "Influence of powder characteristics on formation of porosity in additive manufacturing of Ti-6Al-4V components," *Journal of Materials Engineering and Performance*, vol. 26, no. 8, pp. 4138-4147, 2017.
- [161] A. Sola and A. Nouri, "Microstructural porosity in additive manufacturing: The formation and detection of pores in metal parts fabricated by powder bed fusion," *Journal of Advanced Manufacturing and Processing*, vol. 1, no. 3, p. e10021, 2019.
- [162] J. M. Benson and E. Snyders, "The need for powder characterisation in the additive manufacturing industry and the establishment of a national facility," *South African Journal of Industrial Engineering*, vol. 26, no. 2, pp. 104-114, 2015.

- [163] F. Podczec, *Particle-particle adhesion in pharmaceutical powder handling*. World Scientific, 1998.
- [164] Y. Shimada, Y. Yonezawa, H. Sunada, R. Nonaka, K. Katou, and H. Morishita, "Development of an Apparatus for Measuring Adhesive Force between Fine Particles [Translated]," *KONA Powder and Particle Journal*, vol. 20, no. 0, pp. 223-230, 2002.
- [165] G. Salazar-Banda, M. Felicetti, J. Gonçalves, J. Coury, and M. Aguiar, "Determination of the adhesion force between particles and a flat surface, using the centrifuge technique," *Powder technology*, vol. 173, no. 2, pp. 107-117, 2007.
- [166] J. A. Slotwinski and E. J. Garboczi, "Porosity of Additive Manufacturing Parts for Process Monitoring," *AIP Conference Proceedings*, vol. 1581, 01/31 2014, doi: 10.1063/1.4864957.
- [167] P. Delroisse, P. J. Jacques, E. Maire, O. Rigo, and A. Simar, "Effect of strut orientation on the microstructure heterogeneities in AlSi10Mg lattices processed by selective laser melting," *Scripta Materialia*, vol. 141, pp. 32-35, 2017.
- [168] L. Cordova *et al.*, "Powder characterization and optimization for additive manufacturing," *Tribol. Int.*, vol. 128, p. 926872, 2017.
- [169] C. Meier, R. Weissbach, J. Weinberg, W. Wall, and A. Hart, "Critical Influences of Particle Size and Adhesion on the Powder Layer Uniformity in Metal Additive Manufacturing," *Journal of Materials Processing Technology*, vol. 266, 04/18 2018, doi: 10.1016/j.jmatprotec.2018.10.037.
- [170] Z. Snow, R. Martukanitz, and S. Joshi, "On the development of powder spreadability metrics and feedstock requirements for powder bed fusion additive manufacturing," *Additive Manufacturing*, vol. 28, pp. 78-86, 2019/08/01/ 2019, doi: <https://doi.org/10.1016/j.addma.2019.04.017>.
- [171] C. Meier, R. Weissbach, J. Weinberg, W. A. Wall, and A. J. Hart, "Critical influences of particle size and adhesion on the powder layer uniformity in metal additive manufacturing," *Journal of Materials Processing Technology*, vol. 266, pp. 484-501, 2019/04/01/ 2019, doi: <https://doi.org/10.1016/j.jmatprotec.2018.10.037>.
- [172] G. Yablokova *et al.*, "Rheological behavior of β -Ti and NiTi powders produced by atomization for SLM production of open porous orthopedic implants," *Powder Technology*, vol. 283, pp. 199-209, 2015.
- [173] M. Yan and P. Yu, "An Overview of densification, microstructure and mechanical property of additively manufactured Ti-6Al-4V—Comparison among selective laser melting, electron beam melting, laser metal deposition and selective laser sintering, and with conventional powder," *Sintering techniques of materials*, 2015.
- [174] R. Poprawe, C. Hinke, W. Meiners, J. Schrage, S. Bremen, and S. Merkt, "SLM production systems: recent developments in process development, machine concepts and component design," *Advances in Production Technology*, pp. 49-65, 2015.
- [175] Y. M. Fouda and A. E. Bayly, "A DEM study of powder spreading in additive layer manufacturing," *Granular Matter*, vol. 22, no. 1, pp. 1-18, 2020.
- [176] X. Gong, T. Anderson, and K. Chou, "Review on powder-based electron beam additive manufacturing technology," in *International Symposium on Flexible Automation*, 2012, vol. 45110: American Society of Mechanical Engineers, pp. 507-515.

- [177] X. Tan *et al.*, "Graded microstructure and mechanical properties of additive manufactured Ti–6Al–4V via electron beam melting," *Acta Materialia*, vol. 97, pp. 1-16, 2015.
- [178] K. Abd-Elghany and D. Bourell, "Property evaluation of 304L stainless steel fabricated by selective laser melting," *Rapid Prototyping Journal*, 2012.
- [179] A. Townsend, N. Senin, L. Blunt, R. K. Leach, and J. S. Taylor, "Surface texture metrology for metal additive manufacturing: a review," *Precision Engineering*, vol. 46, pp. 34-47, 2016/10/01/ 2016, doi: <https://doi.org/10.1016/j.precisioneng.2016.06.001>.
- [180] S. A. Khairallah, A. T. Anderson, A. Rubenchik, and W. E. King, "Laser powder-bed fusion additive manufacturing: Physics of complex melt flow and formation mechanisms of pores, spatter, and denudation zones," *Acta Materialia*, vol. 108, pp. 36-45, 2016/04/15/ 2016, doi: <https://doi.org/10.1016/j.actamat.2016.02.014>.
- [181] W. Nan *et al.*, "Jamming during particle spreading in additive manufacturing," *Powder Technology*, vol. 338, pp. 253-262, 2018/10/01/ 2018, doi: <https://doi.org/10.1016/j.powtec.2018.07.030>.
- [182] J. Zhang, Y. Tan, T. Bao, Y. Xu, X. Xiao, and S. Jiang, "Discrete Element Simulation of the Effect of Roller-Spreading Parameters on Powder-Bed Density in Additive Manufacturing," *Materials*, vol. 13, no. 10, p. 2285, 2020.
- [183] E. J. Parteli and T. Pöschel, "Particle-based simulation of powder application in additive manufacturing," *Powder Technology*, vol. 288, pp. 96-102, 2016.
- [184] W. Nan and M. Ghadiri, "Numerical simulation of powder flow during spreading in additive manufacturing," *Powder technology*, vol. 342, pp. 801-807, 2019.
- [185] H. Chen, Y. Chen, Y. Liu, Q. Wei, Y. Shi, and W. Yan, "Packing quality of powder layer during counter-rolling-type powder spreading process in additive manufacturing," *International Journal of Machine Tools and Manufacture*, vol. 153, p. 103553, 2020.
- [186] W. Yan, Y. Qian, W. Ma, B. Zhou, Y. Shen, and F. Lin, "Modeling and experimental validation of the electron beam selective melting process," *Engineering*, vol. 3, no. 5, pp. 701-707, 2017.
- [187] C. Guo, W. Ge, and F. Lin, "Dual-material electron beam selective melting: hardware development and validation studies," *Engineering*, vol. 1, no. 1, pp. 124-130, 2015.
- [188] P. S. Desai and C. F. Higgs, "Spreading process maps for powder-bed additive manufacturing derived from physics model-based machine learning," *Metals*, vol. 9, no. 11, p. 1176, 2019.
- [189] S. Beitz, R. Uerlich, T. Bokelmann, A. Diener, T. Vietor, and A. Kwade, "Influence of powder deposition on powder bed and specimen properties," *Materials*, vol. 12, no. 2, p. 297, 2019.
- [190] S. Haeri, "Optimisation of blade type spreaders for powder bed preparation in Additive Manufacturing using DEM simulations," *Powder Technology*, vol. 321, pp. 94-104, 2017.
- [191] D. Sofia, M. Lupo, D. Barletta, and M. Poletto, "Validation of an Experimental Procedure to Quantify The Effects of Powder Spreadability on Selective Laser Sintering Process," *CHEMICAL ENGINEERING*, vol. 74, 2019.
- [192] L. Cordova, T. Bor, M. de Smit, M. Campos, and T. Tinga, "Measuring the spreadability of pre-treated and moisturized powders for laser powder bed fusion," *Additive manufacturing*, vol. 32, p. 101082, 2020.

- [193] B. Armstrong, K. Brockbank, and J. Clayton, "Understand the effects of moisture on powder behavior," *Chem. Eng. Prog.*, vol. 110, pp. 25-30, 2014.
- [194] J. Fiscina, G. Lumay, F. Ludewig, and N. Vandewalle, "Compaction dynamics of wet granular assemblies," *Physical review letters*, vol. 105, no. 4, p. 048001, 2010.
- [195] A. Rescaglio, J. Schockmel, N. Vandewalle, and G. Lumay, "Combined effect of moisture and electrostatic charges on powder flow," in *EPJ Web of Conferences*, 2017, vol. 140: EDP Sciences, p. 13009.
- [196] L. Bocquet, E. Charlaix, S. Ciliberto, and J. Crassous, "Moisture-induced ageing in granular media and the kinetics of capillary condensation," *Nature*, vol. 396, no. 6713, pp. 735-737, 1998.
- [197] C. Galy, E. Le Guen, E. Lacoste, and C. Arvieu, "Main defects observed in aluminum alloy parts produced by SLM: from causes to consequences," *Additive manufacturing*, vol. 22, pp. 165-175, 2018.
- [198] B. Amstrong and J. Clayton, "Quantifying the impact of humidity on powder properties," in *ACHEMA 2012: Frankfurt Germany*, 2012.
- [199] H. Wu, D. Pritchett, S. Wolff, J. Cao, K. Ehmann, and P. Zou, "A vibration-assisted powder delivery system for additive manufacturing-an experimental investigation," *Additive Manufacturing*, vol. 34, p. 101170, 2020.
- [200] J. A. Muñiz-Lerma, A. Nommeots-Nomm, K. E. Waters, and M. Brochu, "A comprehensive approach to powder feedstock characterization for powder bed fusion additive manufacturing: A case study on AlSi7Mg," *Materials*, vol. 11, no. 12, p. 2386, 2018.
- [201] L. P. Lefebvre, J. Dai, Y. Thomas, and Y. Martinez-Rubi, "Metal powder flowability: effect of humidity and impact on the reproducibility of the measurements," presented at the Proceeding of the Additive Manufacturing with Powder Metallurgy Conference 2019, 2019/06, 2019.
- [202] N. T. Aboulkhair, N. M. Everitt, I. Ashcroft, and C. Tuck, "Reducing porosity in AlSi10Mg parts processed by selective laser melting," *Additive manufacturing*, vol. 1, pp. 77-86, 2014.
- [203] X. Li, K. O'donnell, and T. B. Sercombe, "Selective laser melting of Al-12Si alloy: Enhanced densification via powder drying," *Additive Manufacturing*, vol. 10, pp. 10-14, 2016.
- [204] C. Weingarten, D. Buchbinder, N. Pirch, W. Meiners, K. Wissenbach, and R. Poprawe, "Formation and reduction of hydrogen porosity during selective laser melting of AlSi10Mg," *Journal of Materials Processing Technology*, vol. 221, pp. 112-120, 2015.
- [205] D. M. Bauer, E. Schwarzenböck, I. Ludwig, N. Schupp, F. Palm, and G. Witt, "Investigations of aging behaviour for aluminium powders during an atmosphere simulation of the LBM process," *Powder Metallurgy*, vol. 60, no. 3, pp. 175-183, 2017.
- [206] L. C. Zhang, Y. Liu, S. Li, and Y. Hao, "Additive manufacturing of titanium alloys by electron beam melting: a review," *Advanced Engineering Materials*, vol. 20, no. 5, p. 1700842, 2018.
- [207] J. Clayton, D. Millington-Smith, and B. Armstrong, "The application of powder rheology in additive manufacturing," *Jom*, vol. 67, no. 3, pp. 544-548, 2015.
- [208] M. Seifi, A. Salem, J. Beuth, O. Harrysson, and J. J. Lewandowski, "Overview of materials qualification needs for metal additive manufacturing," *Jom*, vol. 68, no. 3, pp. 747-764, 2016.

- [209] L. Ardila *et al.*, "Effect of IN718 recycled powder reuse on properties of parts manufactured by means of selective laser melting," *Physics Procedia*, vol. 56, pp. 99-107, 2014.
- [210] A. Strondl, O. Lyckfeldt, H. k. Brodin, and U. Ackelid, "Characterization and control of powder properties for additive manufacturing," *Jom*, vol. 67, no. 3, pp. 549-554, 2015.
- [211] M. Sadowski, L. Ladani, W. Brindley, and J. Romano, "Optimizing quality of additively manufactured Inconel 718 using powder bed laser melting process," *Additive Manufacturing*, vol. 11, pp. 60-70, 2016.
- [212] Q. Jia and D. Gu, "Selective laser melting additive manufacturing of Inconel 718 superalloy parts: Densification, microstructure and properties," *Journal of Alloys and Compounds*, vol. 585, pp. 713-721, 2014.
- [213] Y. He, A. Hassanpour, and A. E. Bayly, "Linking particle properties to layer characteristics: Discrete element modelling of cohesive fine powder spreading in additive manufacturing," *Additive Manufacturing*, vol. 36, p. 101685, 2020/12/01/ 2020, doi: <https://doi.org/10.1016/j.addma.2020.101685>.
- [214] M. Van den Eynde, L. Verbelen, and P. Van Puyvelde, "Assessing polymer powder flow for the application of laser sintering," *Powder Technology*, vol. 286, pp. 151-155, 2015.
- [215] Y. Sun, S. Gulizia, C. Oh, C. Doblin, Y. F. Yang, and M. Qian, "Manipulation and characterization of a novel titanium powder precursor for additive manufacturing applications," *Jom*, vol. 67, no. 3, pp. 564-572, 2015.
- [216] D. Drake, "An approach for defining the key quality characteristics of metal powder for powder bed fusion and directed energy deposition," *Colorado school of mines*, 2018.
- [217] J. C. Steuben, A. P. Iliopoulos, and J. G. Michopoulos, "Discrete element modeling of particle-based additive manufacturing processes," *Computer Methods in Applied Mechanics and Engineering*, vol. 305, pp. 537-561, 2016/06/15/ 2016, doi: <https://doi.org/10.1016/j.cma.2016.02.023>.
- [218] Z. Xiang, M. Yin, Z. Deng, X. Mei, and G. Yin, "Simulation of forming process of powder bed for additive manufacturing," *Journal of Manufacturing Science and Engineering*, vol. 138, no. 8, 2016.
- [219] D. Oropeza, R. Roberts, and A. Hart, "A modular testbed for mechanized spreading of powder layers for additive manufacturing," *Review of Scientific Instruments*, vol. 92, no. 1, p. 015114, 2021.
- [220] E. Hernández-Nava, P. Mahoney, C. Smith, J. Donoghue, I. Todd, and S. Tammas-Williams, "Additive manufacturing titanium components with isotropic or graded properties by hybrid electron beam melting/hot isostatic pressing powder processing," *Scientific reports*, vol. 9, no. 1, pp. 1-11, 2019.
- [221] H. Gong, K. Rafi, H. Gu, T. Starr, and B. Stucker, "Analysis of defect generation in Ti-6Al-4V parts made using powder bed fusion additive manufacturing processes," *Additive Manufacturing*, vol. 1-4, pp. 87-98, 2014/10/01/ 2014, doi: <https://doi.org/10.1016/j.addma.2014.08.002>.
- [222] J. Hiemenz, "Electron beam melting," *Advanced Materials & Processes*, vol. 165, no. 3, pp. 45-46, 2007.

Appendix

Angle of Repose of 7g powder heap on the bed for sample 1

Iteration	H(left),mm	B(Left), mm	AoR (Left), Radians	AoR (Left), Degrees	H (Right), mm	B (Right), mm	AoR (Right), Radians	AoR (Right), Degrees	AoR (Average), Degrees	
1	11.485	27.778	0.392053	22.46298	13.087	26.159	0.463877	26.57819	24.52058	
2	15.256	25.541	0.538442	30.85047	11.639	31.194	0.357118	20.46138	25.65592	
3	13.797	28.79	0.446893	25.60509	11.996	27.59	0.410138	23.49917	24.55213	
4	15.163	26.244	0.523914	30.01804	13.458	28.113	0.446472	25.58095	27.79949	
5	15.972	24.427	0.579089	33.17933	13.152	28.186	0.436584	25.01445	29.09689	
									Average	26.325
									STDEV	1.827794

Angle of Repose of 7g powder heap on the bed for sample 2

Iteration	H(left),mm	B(Left), mm	AoR (Left), Radians	AoR (Left), Degrees	H (Right), mm	B (Right), mm	AoR (Right), Radians	AoR (Right), Degrees	AoR (Average), Degrees	
1	12.442	25.226	0.45821	26.2535	12.955	27.791	0.436209	24.99296	25.62323	
2	13.299	29.111	0.428526	24.5527	11.563	29.689	0.371397	21.27946	22.91608	
3	12.704	25.584	0.460892	26.40717	10.587	29.11	0.348818	19.98579	23.19648	
4	13.595	26.79	0.469602	26.90622	10.798	24.792	0.410767	23.53523	25.22073	
5	11.274	29.473	0.365347	20.93283	10.287	26.504	0.370232	21.21273	21.07278	
									Average	23.60586
									STDEV	1.657555

Angle of repose of sample 1 for 200 g

Weight of the empty container: 2.4803 g

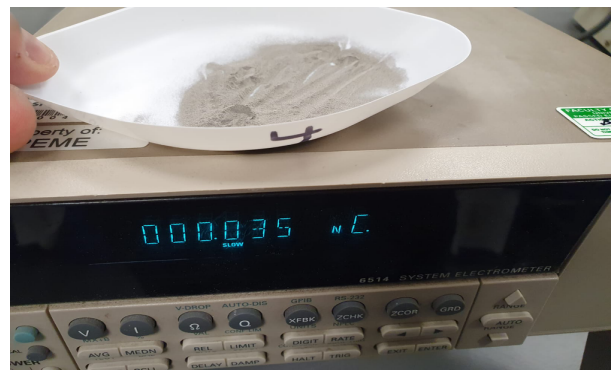
Iterations	Net weight (g)	R1	R2	R3	R4	R5	R(avg)	Height (mm)	AoR	Aor (Degrees)
1	200.27	55	55	55	54	52	54.2	32	0.533	30.558
2	200.05	55	55	58	59	56	56.6	30	0.487	27.925
3	200.01	55	55	54	56	52	54.4	31	0.518	29.677
4	200.06	55	55	58	52	54	54.8	30	0.501	28.698
5	200.04	54	52	55	57	55	54.6	31	0.516	29.586
6	200.05	55	52	51	55	52	53	30	0.515	29.511
7	200.04	55	58	52	51	54	54	30	0.507	29.055
Average	200.0411									29.28723
										Standard Deviation
										0.771104

Angle of repose of sample 2 for 200 g

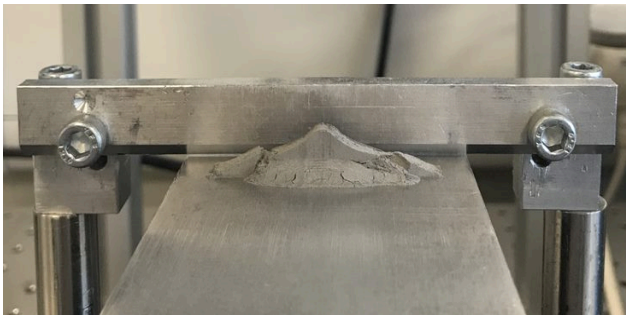
Weight of the empty container: 2.4803 g

Iterations	Net weight (g)	R1	R2	R3	R4	R5	R(avg)	Height (mm)	AoR	Aor (Degrees)
1	200.08	53	54	57	56	55	55	28	0.471	26.980
2	200.13	58	54	56	59	59	57.2	30	0.483	27.676
3	200.07	53	55	55	58	59	56	29	0.478	27.378
4	200.01	57	54	55	58	58	56.4	29	0.475	27.212
5	200.10	55	57	55	55	55	55.4	29	0.482	27.631
6	200.01	58	55	54	59	53	55.8	28	0.465	26.647
7	200.02	55	55	55	59	56	56	29	0.478	27.378
Average	200.0552									27.27153
										Standard Deviation
										0.336635

Triboelectric Charging Test of Sample 1 by Dr Jabbar Gardy



Run 5	Run 4	Run 3	Run 2	Run 1
5.000	0.035	0.041	0.051	0.032
0.040	0.030	0.033	0.028	0.040
0.031	0.034	0.028	0.044	0.024
0.04	0.026	0.038	0.035	0.03
0.035	0.037	0.034	0.038	0.038
0.146	0.127	0.133	0.145	0.132
0.0365	0.032	0.033	0.0363	0.033
Page 2				
0.0203	0.04	0.0202	0.03	0.0197
0.03	0.0201	0.04	0.0196	0.03
1.0000	1.7980	1.0000	1.5749	1.0000
			1.6913	1.0000
			1.8008	1.0000
				1.6871



Powder heap in 73% relative humidity

Composition of Austenitic Stainless Steels[25]

AISI grade	C max.	Si max.	Mn max.	Cr	Ni	Mo	Ti	Nb	Al	V
301	0.15	1.00	2.00	16-18	6-8					
302	0.15	1.00	2.00	17-19	8-10					
304	0.08	1.00	2.00	17.5-20	8-10.5					
310	0.25	1.50	2.00	24-26	19-22					
316	0.08	1.00	2.00	16-18	10-14	2.0-3.0				
321	0.08	1.00	2.00	17-19	9-12		5 x %C min.			
347	0.08	1.00	2.00	17-19	9-13			10 x %C min.		
E 1250	0.1	0.5	6.0	15.0	10.0					0.25
20/25-Nb	0.05	1.0	1.0	20.0	25.0			0.7		
A 286	0.05	1.0	1.0	15.0	26.0	1.2	~1.9	~0.18	~0.25	
254SMO	0.02	0.8	1.0	18.5-20.5	17.5-18.5	6-6.5	~1.9	~0.18	~0.25	
AL-6XN	0.03	1.0	2.0	20-22	23.5-25.5	6-7				

Records of temperature and humidity through the experiments:

	Gap(μm)	Speed(mm/s)	Temp $^{\circ}\text{C}$	Humidity%
Sample1	318	50	23	31
		100	23	31
		150	23	31
		200	24	33
	191	50	21	36
		100	22	35
		150	21	36
		200	21	36
	102	50	21	37
		100	21	37
		150	21	38
		200	-	-

	Gap(μm)	Speed(mm/s)	Temp $^{\circ}\text{C}$	Humidity%
Sample2	318	50	21	33
		100	21	38
		150	22	43
		200	22	43
	191	50	22	31
		100	23	31
		150	23	31
		200	22	35
	318	50	22	28
		100	22	34
		150	22	34
		200	23	35

	Gap(μm)	Speed(mm/s)	Temp $^{\circ}\text{C}$	Humidity%
Sample1 73%RH	318	50	21	73
		100	21	73
		150	20	73
		200	20	72

	Gap(μm)	Speed(mm/s)	Temp $^{\circ}\text{C}$	Humidity%
Sample2 73%RH	318	50	20	74
		100	20	73
		150	21	73
		200	21	73